

Exact solution of the $p + ip$ pairing Hamiltonian and a hierarchy of integrable models.

Clare Dunning⁽¹⁾, Miguel Ibañez⁽²⁾, Jon Links⁽³⁾,
Germán Sierra⁽²⁾ and Shao-You Zhao⁽³⁾

⁽¹⁾School of Mathematics, Statistics and Actuarial Science,
The University of Kent, CT2 7NZ, UK,

⁽²⁾Instituto de Física Teórica, UAM-CSIC,
Cantoblanco, 28049 Madrid, Spain

⁽³⁾Centre for Mathematical Physics, School of Mathematics and Physics,
The University of Queensland 4072, Australia,

November 1, 2018

Abstract

Using the well-known trigonometric six-vertex solution of the Yang-Baxter equation we derive an integrable pairing Hamiltonian with anyonic degrees of freedom. The exact algebraic Bethe ansatz solution is obtained using standard techniques. From this model we obtain several limiting models, including the pairing Hamiltonian with $p + ip$ -wave symmetry. An in-depth study of the $p + ip$ model is then undertaken, including a mean-field analysis, analytic and numerical solution of the Bethe ansatz equations, and an investigation of the topological properties of the ground-state wavefunction. Our main result is that the ground-state phase diagram of the $p + ip$ model consists of three phases. There is the known boundary line with gapless excitations that occurs for vanishing chemical potential, separating the topologically trivial strong pairing phase and the topologically non-trivial weak pairing phase. We argue that a second boundary line exists separating the weak pairing phase from a topologically trivial weak coupling BCS phase, which includes the Fermi sea in the limit of zero coupling. The ground state on this second boundary line is the Moore-Read state.

Contents

| | | |
|----------|---|-----------|
| 1 | Introduction | 3 |
| 2 | Construction of an integrable anyonic pairing model | 5 |
| 2.1 | The Yang–Baxter equation | 5 |
| 2.2 | Transfer matrix, Hamiltonian, and exact solution | 7 |
| 3 | Limiting cases | 11 |
| 3.1 | Russian doll and s -wave BCS models | 11 |
| 3.2 | The $p + ip$ -wave BCS model | 12 |
| 3.3 | The Gaudin models | 15 |
| 4 | Analysis of the $p + ip$ model | 16 |
| 4.1 | Ground-state phase diagram from BCS mean-field theory | 16 |
| 4.1.1 | The Moore-Read and Read-Green lines | 17 |
| 4.1.2 | The Volovik line | 21 |
| 4.1.3 | Fidelity susceptibility | 22 |
| 4.2 | Analysis of the Bethe ansatz equations in the continuum limit | 24 |
| 4.2.1 | The electrostatic analogy | 24 |
| 4.2.2 | Weak coupling BCS phase | 26 |
| 4.2.3 | Moore–Read line | 28 |
| 4.2.4 | Weak pairing phase | 30 |
| 4.2.5 | Read–Green line | 31 |
| 4.2.6 | Strong pairing phase | 31 |
| 4.3 | Topological properties of the ground state | 31 |
| 4.3.1 | Dressing and duality | 31 |
| 4.3.2 | Numerical solution of the Bethe ansatz equations for finite systems | 34 |
| 4.3.3 | A zeroth-order quantum phase transition | 37 |
| 4.3.4 | Winding number of wavefunctions | 38 |
| 4.4 | Vortex wavefunctions | 41 |
| 4.4.1 | Weak coupling BCS phase | 42 |
| 4.4.2 | Weak pairing phase | 43 |
| 5 | Conclusions | 45 |
| A | Calculations for the anyonic pairing model | 45 |
| A.1 | Cyclic renormalisation group | 45 |
| A.2 | Wavefunction scalar product and correlation functions | 48 |
| A.3 | Duality and the analogue of the Moore-Read state | 51 |
| B | Calculations for the $p + ip$ model | 53 |
| B.1 | Solution of the gap and chemical potential equations | 53 |
| B.2 | Ground-state wavefunction: exact results versus mean-field results | 54 |
| B.3 | Wavefunction scalar product and one-point correlation functions | 56 |
| B.4 | Two-point correlation functions | 58 |

1 Introduction

Exactly solvable many-body models have played a very important role in various branches of physics, especially in statistical mechanics and condensed matter. They have been fundamental in the understanding of phase transitions and non-perturbative phenomena in low-dimensional and strongly correlated systems. Prominent examples are provided by the 2D Ising model, the 1D anisotropic Heisenberg model, the interacting 1D Bose gas, and the 1D Hubbard model [8, 41]. The solvability and integrability of these and related models emerges from a common algebraic structure, due to the quantum Yang-Baxter equation satisfied by the so called R -matrix. The R -matrix is the basic object of the Quantum Inverse Scattering Method (QISM) [41]. It allows for the construction of a one parameter family of commuting transfer matrices whose expansion, in powers of the spectral parameter, generates an infinite set of conserved quantities including the Hamiltonian of the system. For the anisotropic Heisenberg model, also known as the XXZ model, the R -matrix is the six-vertex trigonometric solution of the Yang-Baxter equation and it depends on a spectral parameter u and the quantum parameter q related to the anisotropy as $\Delta = (q^2 + q^{-2})/2$.

A closely related family of exactly solvable models are the Richardson-Gaudin models, where the most prominent examples are the Richardson model of BCS superconductivity [9, 46, 54, 62, 69] and the Gaudin spin models [23] (for a review see [14]). The common algebraic structure of this family is the classical Yang-Baxter equation satisfied by the classical r -matrix. This latter equation is obtained from the quasi-classical limit of the quantum Yang-Baxter equation through $R(u) \sim 1 + \hbar r(u)$. A feature of these models, unlike the anisotropic Heisenberg model, is the dependence of the Hamiltonian on a large number of parameters. In the Richardson model, they are the energies of the single particle levels and the BCS coupling constant, while in the Gaudin model they are the position of the spins. This abundance of parameters has its origin in the transfer matrix which is the product of R -matrices with shifted spectral parameters. This is called an inhomogeneous transfer matrix. This situation must be compared with the anisotropic Heisenberg model whose transfer matrix is homogeneous, which is the reason why the Hamiltonian of this model only depends on q .

Thus the majority of models constructed so far are based either on a homogeneous transfer matrix (e.g. anisotropic Heisenberg model), or in the quasi-classical limit of an inhomogeneous transfer matrix (Richardson-Gaudin models). It is also of interest to construct physical models from an inhomogeneous transfer matrix before one takes the quasi-classical limit. The first result of this paper is to construct such a model starting from the trigonometric six-vertex R -matrix discussed above. This model describes the pairing interaction of anyonic particles with braiding statistics in momentum space parameterized by q , and for that reason it can be termed an anyonic pairing model. These anyons should be distinguished from the real space anyons which satisfy braiding statistics in 1D [6] or in 2D [44, 64].

The one-body version of the anyonic pairing Hamiltonian we obtain coincides with the quantum mechanical Hamiltonian proposed by Glazek and Wilson in 2002, which furnishes a simple example of a renormalization group with limit cycles [24, 25]. The latter work inspired the construction of a BCS model with s -wave symmetry and time reversal symmetry-breaking where the renormalization group also has limit cycles [45]. The mean-field gap equation of this BCS model has an infinite number of solutions related by discrete scale invariance, which explains its name: Russian doll BCS model. This model was shown in reference [16] to be exactly solvable by the QISM using a rational R matrix.

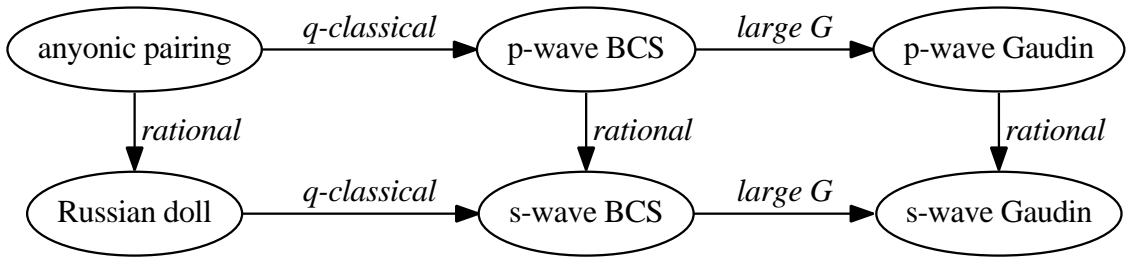


Figure 1: Web of integrable pairing models.

The relation between the mean-field and the exact solution of this model was established in reference [4]. It then comes as no surprise that the Russian doll BCS model can be obtained from the anyonic pairing model in the limit where the trigonometric R -matrix becomes rational. However, if the quasi-classical limit of the anyonic pairing model is taken before the rational limit a BCS model with $p + ip$ -wave symmetry is obtained, as has been reported in [33]. Taking a rational limit of the latter model or a quasi-classical limit of the Russian doll model one arrives to the well known s -wave BCS model of Richardson [54]. Finally, one can take the limit where the BCS coupling constant, of both the s -wave and $p + ip$ -wave models, goes to infinity obtaining two Gaudin models. The web of relations between all these models is shown in Fig. (1).

The first part of this paper, Sect. 2, is devoted to the construction of the anyonic pairing model using the QISM and the derivation of the eigenvalues of the transfer matrix. In Sect. 3 the relationships of the models in Fig. 1 are shown, giving a unified picture of the pairing models that can be obtained from the trigonometric R -matrix. In Appendix A we collect the more technical computation of the wavefunction and scalar products of the anyonic model, as well as its relation with the aforementioned Glazek-Wilson model.

The bulk of the paper, Sect. 4, is devoted to a detailed study of the exactly solvable $p + ip$ -wave model which was initiated in [33]. In recent years this model has received considerable attention due to the existence of vortices with non-trivial braiding statistics [53, 32, 60], with the potential for implementing topological quantum computation [50]. Furthermore, there are some experimental indications that Sr_2RuO_4 is such a chiral p -wave superconductor [42], supporting topological vortices [12, 35]. In the realm of cold atoms there are also possibilities to realize $p + ip$ -wave paired phases [11, 29, 31, 43] through experiments involving Feshbach resonances [21, 22, 34, 51, 66, 67].

We begin our study of the $p + ip$ model using the BCS mean-field theory, to determine the phase diagram in the plane $(1/g, x)$, where $1/g$ is the inverse of the BCS coupling constant and x is the fraction of occupied energy levels. This phase diagram is divided into three regions denoted as weak coupling, weak pairing and strong pairing in the terminology introduced by Read and Green [53]. The strong and weak pairing regions are separated by a line in the $(1/g, x)$ plane where the chemical potential vanishes, giving rise to a second-order phase transition and a topological transition described by a winding number in momentum space introduced by Volovik [60]. The latter two regions are related by a strong-weak duality which connects two ground states having the same total energy, and value of the gap, while the chemical potential differs in the sign. On the other hand, the weak pairing and weak coupling regions are separated by another line in the $(1/g, x)$ plane which can be called the Moore-Read line because the projected BCS state coincides precisely with the Moore-Read pfaffian state related to the Fractional Quantum Hall state at filling fraction $5/2$. All the points of this line have zero total energy and are mapped,

under the duality transformation, into the vacuum state. However the gap does not vanish on this line and the nature of the transition is rather subtle since, as we show below, it is associated to a discontinuity of the ground state energy, or in another words a zeroth order phase transition. Volovik has discussed the existence of a Higgs like phase transition for the $p + ip$ model, meaning a qualitative change in the dispersion relation of the quasi-particles [61]. We find that this type of transition occurs on a line located in the weak coupling region, which is close, but not identical, to the Moore-Read line. A peculiarity of the Read-Green and the Moore-Read lines is that they are insensitive to the particular choice of the energy levels, and in that sense they are topological. This feature is not shared by the Volovik line whose position in the phase diagram depends on the energy level distribution.

The analysis of Sect. 4 continues with the computation of the fidelity susceptibility which confirms, as expected, the singular nature of the Read-Green line, while the Moore-Read line does not show any special feature. Next we analyze the continuum limit of the Bethe ansatz equations of the $p + ip$ model using an electrostatic analogy which allows us to uncover the complex structure of the arcs formed by the roots of the Bethe ansatz equations. We also recover the mean-field gap and chemical potential equations as was done in previous works for the BCS model with s -wave symmetry [23, 55, 56]. The structure of the arcs, the values of the ground state energy, gaps, chemical potential and occupation numbers are compared with the numerical results obtained by solving the Bethe ansatz equations for systems with finite size, finding a reasonable agreement. A detailed analysis of the exact solution allow us to understand the weak-strong duality in terms of a dressing operation that maps exact eigenstates between those two regions. The physical picture that emerges is that the ground state of the weak pairing region is formed by strongly localized pairs and by delocalized pairs with zero energy. We then discuss the zeroth order phase transition and the winding number of the mean-field and exact solutions. For the mean-field solution the winding number vanishes in the strong pairing region while it does not in the weak pairing and weak coupling regions. However in the exact solution the winding number only vanishes in the weak pairing region where it counts the number of Bethe ansatz equation roots that are equal to zero. In this sense the winding number plays the role of a topological order parameter for the weak pairing region. Another qualitative distinction between the weak pairing and weak coupling regions is derived by studying the structure of the vortex wavefunction by means of the Bogolioubov-de Gennes equations. We find that the vortex wavefunction has an oscillatory behaviour in the weak coupling region which does not appear in the weak pairing region.

Finally, in Appendices A and B we discuss several technical issues: relation between the Glazek-Wilson model and the anyonic model, computation of wavefunction scalar products and correlation functions of the anyonic pairing and the $p + ip$ models, a q -deformed version of the Moore-Read state, solution of the gap and chemical potential equations.

2 Construction of an integrable anyonic pairing model

2.1 The Yang–Baxter equation

A systematic method to construct integrable quantum systems is through the Quantum Inverse Scattering Method (QISM) [41]. The key element in this approach is a solution of the Yang–Baxter equation [8, 38], commonly known as an R -matrix. This is a linear

operator acting on a two-fold tensor product space which is dependent on $x \in \mathbb{C}$ known as the spectral parameter. Denoting the R -matrix as $R(x) \in \text{End}(V \otimes V)$, the Yang–Baxter equation reads

$$R_{12}(x/y)R_{13}(x)R_{23}(y) = R_{23}(y)R_{13}(x)R_{12}(x/y) \quad (1)$$

which acts on the three-fold space $V \otimes V \otimes V$. The subscripts above refer to the spaces on which the operators act. E.g.

$$R_{12}(x) = R(x) \otimes I.$$

The specific example we will use is the well-known XXZ solution associated with the quantum algebra $U_q[sl(2)]^1$ [39]

$$R(x) = \left(\begin{array}{cc|cc} (q^2x - q^{-2}x^{-1}) & 0 & 0 & 0 \\ 0 & (x - x^{-1}) & (q^2 - q^{-2}) & 0 \\ \hline 0 & (q^2 - q^{-2}) & (x - x^{-1}) & 0 \\ 0 & 0 & 0 & (q^2x - q^{-2}x^{-1}) \end{array} \right).$$

We define the local L -operator as $L(x) = R(xq^{-1})$ which is a solution of

$$R_{12}(x/y)L_{13}(x)L_{23}(y) = L_{23}(y)L_{13}(x)R_{12}(x/y) \quad (2)$$

as a consequence of (1). It is customary to consider $L(x) \in \text{End}(V \otimes V)$ as acting on the tensor product of an ‘‘auxiliary’’ space and a local ‘‘quantum’’ space. We use the subscript a to denote the auxiliary space and the labels $j = 1, \dots, L$ for the local quantum spaces of a many-body system.

To apply the QISM to construct a pairing Hamiltonian we next introduce the hard-core boson (Cooper pair) operators in terms of fermion operators. Let $\{c_{j\sigma}^\dagger, c_{j\sigma} : j = 1, \dots, L, \sigma = \pm\}$, denote a set of creation and annihilation operators with the usual canonical anticommutation relations and where the labels \pm refer to time-reversed pairs. The hard-core boson operators are defined

$$b_j = c_{j-}c_{j+}, \quad b_j^\dagger = c_{j+}^\dagger c_{j-}^\dagger.$$

We also set $N_j = b_j^\dagger b_j$ as the Cooper pair number operator such that the total number of Cooper pairs in a system is given by the eigenvalue of

$$N = \sum_{j=1}^L N_j.$$

Throughout we will use M to denote the eigenvalues of N .

For each j the local Hilbert space of states is four-dimensional. Excluding the subspace of states which contain unpaired fermions reduces the local Hilbert spaces to dimension two, spanned by the vacuum $|0\rangle$ and the paired state $b_j^\dagger|0\rangle$. Now expressing the linear operators of the quantum space of the L -operator in terms of hard-core boson operators we have

$$L_{aj}(x) = x \begin{pmatrix} q^{2N_j - I} & 0 \\ 0 & q^{I - 2N_j} \end{pmatrix} + (q^2 - q^{-2}) \begin{pmatrix} 0 & b_j \\ b_j^\dagger & 0 \end{pmatrix} - x^{-1} \begin{pmatrix} q^{I - 2N_j} & 0 \\ 0 & q^{2N_j - I} \end{pmatrix}$$

¹It is convenient for our purposes to express the deformation parameter as q^2 rather than the more familiar q .

noting that

$$q^{\gamma N_j} = (q^\gamma - 1)N_j + I.$$

Using the L -operator in this form, we will next apply the QISM to construct an integrable pairing Hamiltonian with anyonic degrees of freedom.

2.2 Transfer matrix, Hamiltonian, and exact solution

The most common use of the QISM is to construct a transfer matrix on a closed chain (to adopt the language of spin models). Here we use this approach with a “twist” in the boundary conditions, which will be chosen in a sector dependent manner as described below. The quantum space for such a model is the L -fold tensor product space $W = V^{\otimes L}$. We introduce the monodromy matrix $T(x) \in \text{End}(V \otimes W)$ defined by

$$T(x) = U_a L_{a1}(xz_1^{-1}) L_{a2}(xz_2^{-1}) \dots L_{aL}(xz_L^{-1})$$

where

$$U = \begin{pmatrix} \exp(-i\alpha') & 0 \\ 0 & \exp(i\alpha') \end{pmatrix}.$$

The monodromy matrix is commonly expressed in a matrix form as

$$T(x) = \begin{pmatrix} T_1^1(x) & T_2^1(x) \\ T_1^2(x) & T_2^2(x) \end{pmatrix}.$$

where the entries are operators acting on W . As a result of (2) and

$$[U \otimes U, R(x)] = 0$$

it follows that

$$R_{ab}(x/y) T_a(x) T_b(y) = T_b(y) T_a(x) R_{ab}(x/y) \quad (3)$$

which is an operator equation on $V \otimes V \otimes W$, with the two auxiliary spaces labelled by a and b .

Defining the transfer matrix to be

$$t(x) = \text{tr}(T(x)) = T_1^1(x) + T_2^2(x).$$

it follows from (3) that the transfer matrices form a commutative family; i.e.

$$[t(x), t(y)] = 0 \quad \forall x, y \in \mathbb{C}. \quad (4)$$

The transfer matrices can be expanded in a Laurent series

$$t(x) = \sum_{j=-L}^L t^{(j)} x^j$$

and because of (4) the co-efficients commute

$$[t^{(j)}, t^{(k)}] = 0, \quad -L \leq j, k \leq L.$$

One may check directly that the transfer matrix commutes with N , so the Hilbert space of states can be decomposed into sectors labelled by the eigenvalues M of N . The leading order terms in the expansion are

$$\begin{aligned} t^{(L)} &= \left(\prod_{j=1}^L z_j^{-1} \right) (\exp(-i\alpha')q^{2N-L} + \exp(i\alpha')q^{L-2N}) \\ t^{(L-1)} &= 0. \end{aligned}$$

We will construct a Hamiltonian in terms of the operator $t^{(L-2)}$, where the choice of the variable α will depend on the sector labelled by M . Setting

$$\begin{aligned} q &= \exp(i\beta) \\ \alpha &= \alpha' + \beta(L - 2M + 2) \end{aligned}$$

we define

$$H = \frac{1}{4 \sin(2\beta) \sin(\alpha)} \left[t^{(L-2)} \prod_{j=1}^L z_j + 2 \cos(\alpha) \sum_{j=1}^L z_j^2 \right].$$

The Hamiltonian may be expressed as

$$H = \sum_{j=1}^L z_j^2 N_j - \frac{\sin(2\beta)}{\sin(\alpha - 2\beta)} \sum_{k>r} z_k z_r (\exp(-i\alpha) d_r^\dagger d_k + \text{h.c.}) \quad (5)$$

with

$$\begin{aligned} d_j &= b_j \prod_{k=j+1}^L q^{4N_k - 2I}, \\ d_j^\dagger &= b_j^\dagger \prod_{k=j+1}^L q^{2I - 4N_k}, \end{aligned} \quad (6)$$

α, β are assumed to be real and h.c. denotes hermitian conjugate. Due to the non-local action of the operators d_j^\dagger, d_j they satisfy

$$\begin{aligned} d_j d_k &= q^4 d_k d_j & j > k \\ d_j^\dagger d_k &= q^{-4} d_k d_j^\dagger & j > k \end{aligned}$$

amongst other relations, and therefore can be viewed as anyonic creation and annihilation operators. By the nature of the above construction, the anyonic Hamiltonian is integrable as it commutes with all terms in the expansion of the transfer matrix. That is

$$[H, t^{(j)}] = 0, \quad j = -L, \dots, L$$

establishing that the $t^{(j)}$ provide a set of conserved operators².

Recall that the derivation of the Hamiltonian was made using a restricted subspace of the Hilbert space obtained by excluding unpaired states. By noting that the second term

²In principle for integrability to hold one would need to check that the number of independent conserved operators is not less than the number of degrees of freedom.

in (5), which describes the scattering of Cooper pairs, vanishes on unpaired states³ it is straightforward to extend the action of the Hamiltonian to the full 4^L -dimensional Hilbert space. We define anyonic creation and annihilation operators $\{a_{j\pm}^\dagger, a_{j\pm} : j = 1, \dots, L\}$ which are defined in terms of the canonical fermion operators through

$$a_{j\sigma} = c_{j\sigma} \prod_{k=j+1}^L q^{2n_{k\sigma}-I},$$

$$a_{j\sigma}^\dagger = c_{j\sigma}^\dagger \prod_{k=j+1}^L q^{I-2n_{k\sigma}}$$

where $n_{j\sigma} = c_{j\sigma}^\dagger c_{j\sigma}$. These operators satisfy the relations

$$\{a_{j\sigma}, a_{j\rho}\} = \{a_{j+}, a_{k-}\} = 0, \quad (7)$$

$$\{a_{j\sigma}, a_{j\rho}^\dagger\} = \delta_{\sigma\rho} I, \quad (8)$$

$$a_{j\sigma} a_{k\sigma} = -q a_{k\sigma} a_{j\sigma} \quad j > k \quad (9)$$

$$a_{j\sigma}^\dagger a_{k\sigma} = -q^{-1} a_{k\sigma} a_{j\sigma}^\dagger \quad j > k \quad (10)$$

and those relations obtained by taking hermitian conjugates. The usual fermionic commutation relations are recovered in the limit $q \rightarrow 1$. Then the Hamiltonian

$$H = \frac{1}{2} \sum_{j=1}^L z_j^2 (n_{j+} + n_{j-}) - \frac{\sin(2\beta)}{\sin(\alpha - 2\beta)} \sum_{k>r} z_k z_r \left(\exp(-i\alpha) a_{r+}^\dagger a_{r-}^\dagger a_{k-} a_{k+} + \text{h.c.} \right)$$

is an extension to the 4^L -dimensional Hilbert space which has the same action as (5) when the unpaired states are excluded.

Having constructed the Hamiltonian through the QISM it is a standard calculation to obtain the exact solution through the algebraic Bethe ansatz. We simply present the key results. Explicit details relevant to the derivation of the formulae below may be found in [26, 40, 41, 62].

The first step is to identify that the vacuum state $|0\rangle$ admits the properties

$$\begin{aligned} T_1^1(x) |0\rangle &= a(x) |0\rangle, \\ T_2^1(x) |0\rangle &= 0, \\ T_1^2(x) |0\rangle &\neq 0, \\ T_2^2(x) |0\rangle &= d(x) |0\rangle \end{aligned}$$

where

$$a(x) = \exp(-i\alpha') \prod_{k=1}^L (q^{-1} x z_k^{-1} - q x^{-1} z_k),$$

$$d(x) = \exp(i\alpha') \prod_{k=1}^L (q x z_k^{-1} - q^{-1} x^{-1} z_k).$$

We then look for eigenstates of $t(x)$ in the form

$$|\Phi(Y)\rangle = \prod_{j=1}^M T_1^2(y_j) |0\rangle$$

³In standard BCS theory this phenomenon is well-known and goes by the name of the *blocking effect*, e.g. see [63].

where $Y = \{y_j\}$. Note that

$$[T_1^2(y_j), T_1^2(y_k)] = 0$$

so the operators may be ordered arbitrarily. Using the algebraic relations amongst the $T_j^i(x)$ operators, this leads to the eigenvalues $\Lambda(x)$ of the transfer matrix being given by [26, 40, 41, 62]

$$\begin{aligned} \Lambda(x) &= \exp(-i\alpha') \prod_{k=1}^L (q^{-1}xz_k^{-1} - qx^{-1}z_k) \prod_{j=1}^M \frac{q^2x^2 - q^{-2}y_j^2}{x^2 - y_j^2} \\ &\quad + \exp(i\alpha') \prod_{k=1}^L (qzx_k^{-1} - q^{-1}x^{-1}z_k) \prod_{j=1}^M \frac{q^{-2}x^2 - q^2y_j^2}{x^2 - y_j^2} \\ &= \exp(-i\alpha) \prod_{k=1}^L (xz_k^{-1} - q^2x^{-1}z_k) \prod_{j=1}^M \frac{x^2 - q^{-4}y_j^2}{x^2 - y_j^2} \\ &\quad + \exp(i\alpha) \prod_{k=1}^L (xz_k^{-1} - q^{-2}x^{-1}z_k) \prod_{j=1}^M \frac{x^2 - q^4y_j^2}{x^2 - y_j^2} \end{aligned}$$

such that the parameters $\{y_j\}$ satisfy the Bethe ansatz equations

$$\exp(-2i\alpha) \prod_{k=1}^L \frac{1 - q^2y_m^{-2}z_k^2}{1 - q^{-2}y_m^{-2}z_k^2} = \prod_{j \neq m}^M \frac{1 - q^4y_m^{-2}y_j^2}{1 - q^{-4}y_m^{-2}y_j^2} \quad m = 1, \dots, M. \quad (11)$$

To obtain the energy expression E for the Hamiltonian (5), it is a matter of expanding the transfer matrix eigenvalues in the Laurent series

$$\Lambda(x) = \sum_{j=-L}^L \Lambda^{(j)} x^j$$

giving

$$\begin{aligned} E &= \frac{1}{4 \sin(2\beta) \sin(\alpha)} \left[\Lambda^{(L-2)} \prod_{j=1}^L z_j + 2 \cos(\alpha) \sum_{j=1}^L z_j^2 \right] \\ &= \frac{\sin(\alpha)}{\sin(\alpha - 2\beta)} \sum_{j=1}^M y_j^2. \end{aligned} \quad (12)$$

We leave to Appendix A.2 the computation of the scalar product and correlators for this model.

From the form of the Hamiltonian (5) and the definition of the operators d_j , eq. (6) one can see that the model parameters can be restricted to the domain $0 \leq \alpha, \beta \leq \pi$. If $\alpha = 0$ the Hamiltonian (5) reduces to

$$H = \left(\sum_{r=1}^L z_r d_r^\dagger \right) \left(\sum_{k=1}^L z_k d_k \right).$$

Formally eq. (12) yields that the energies are zero. However in this limit the roots y_j can be divergent, such that non-zero energies do occur.

It is possible to generalise the above construction in a number of ways. Instead of using the closed chain transfer matrix construction, one can adopt the open chain version developed by Sklyanin [58]. In this manner a Hamiltonian is obtained which not only involves scattering interactions between the anyonic pair operators given by (6), but also their complex conjugates. A second route is to use different solutions of the Yang–Baxter equation. An obvious choice would be to employ Baxter’s eight-vertex solution [7, 8]. But this solution suffers from the fact that it is not $U(1)$ invariant which prohibits the construction of a Hamiltonian which conserves particle number. Beyond this there are however many known solutions of the Yang-Baxter equation which do possess $U(1)$ symmetries, particularly those associated with representations of the quantum algebras $U_q[g]$ where g is a classical simple Lie algebra (e.g. see [37]). In principle these can be applied for the construction of models, which in particular cases will provide anyonic generalisations of integrable pairing models based on bosonic or fermionic degrees of freedom.

3 Limiting cases

3.1 Russian doll and s -wave BCS models

An example of a many-body system which admits a cyclic Renormalization Group (RG) equation analogous to the Glazek-Wilson Hamiltonian (see (103) of Appendix A.1) was studied in [45]. The many-body Hamiltonian was taken to be the s -wave BCS model with complex-valued coupling parameter, later to become known as the Russian Doll (RD) BCS model. The cyclic RG was discovered through a mean-field analysis. Subsequently in [16] it was proved that the RD BCS model is integrable, and in [4] the connection between the Bethe ansatz solution and the RG equation was exposed. Next we will show that the RD BCS model can be obtained as a limiting case of the anyonic pairing model (5). Moreover the exact solution for the usual s -wave BCS model, which was first found in [54], is obtained by performing a second limiting procedure.

We introduce a new variable η and define the parameters ε_k , $k = 1, \dots, L$ and v_j , $j = 1, \dots, M$ through

$$\begin{aligned} z_k &= \exp(2\beta\varepsilon_k/\eta) \\ y_j &= \exp(2\beta v_j/\eta) \end{aligned}$$

and redefine the Hamiltonian (5) by a simple rescaling and additional conserved term

$$H \mapsto \frac{\eta}{\sin(2\beta)}(H - N)$$

so the energy expression (12) becomes

$$E = \frac{\eta \sin(\alpha)}{\sin(\alpha - 2\beta) \sin(2\beta)} \sum_{j=1}^M y_j^2 - \frac{\eta}{\sin(2\beta)} M.$$

Now we take what is known as the *rational limit* $\beta \rightarrow 0$ to obtain the following expressions for the Hamiltonian, Bethe ansatz equations, and energy respectively

$$H = 2 \sum_{j=1}^L \varepsilon_j N_j - G \sum_{k>r}^L (\exp(-i\alpha) b_r^\dagger b_k + \text{h.c.}) \quad (13)$$

$$\exp(-2i\alpha) \prod_{k=1}^L \frac{v_j - \varepsilon_k - i\eta/2}{v_j - \varepsilon_k + i\eta/2} = \prod_{m \neq j}^M \frac{v_j - v_m - i\eta}{v_j - v_m + i\eta}, \quad j = 1, \dots, N \quad (14)$$

$$E = 2 \sum_{j=1}^M v_j + GM \cos(\alpha). \quad (15)$$

where $G = \eta/\sin(\alpha)$. This is the exact solution for the Russian Doll BCS model in terms of the parameterisation used in [16]. Applying the same limiting procedure to the expressions (112,117) derived in Appendix A.2 yields the wavefunction scalar product and one-point functions given in [16].

Performing a second limiting procedure to the Russian Doll Hamiltonian yields the s -wave Hamiltonian. To make this result explicit we implement the following change of variable $\alpha \rightarrow \eta\alpha$ and add the conserved quantity $-GN$ to the Hamiltonian (13). Taking the *quasi-classical limit* $\eta \rightarrow 0$ we obtain from (13,14,15)

$$H = 2 \sum_{j=1}^L \varepsilon_j N_j - G \sum_{k,r=1}^L b_r^\dagger b_k \quad (16)$$

$$\frac{2}{G} + \sum_{k=1}^L \frac{1}{v_j - \varepsilon_k} = \sum_{j \neq m}^M \frac{2}{v_m - v_j}, \quad j = 1, \dots, M \quad (17)$$

$$E = 2 \sum_{j=1}^M v_j \quad (18)$$

where $G = 1/\alpha$. Up to a change in notational conventions this is precisely the exact solution first given in [54].

3.2 The $p + ip$ -wave BCS model

The Hamiltonian of the BCS pairing model with $p + ip$ -wave symmetry was introduced in reference [33]

$$H = \sum_{\mathbf{k}} \frac{\mathbf{k}^2}{2m} c_{\mathbf{k}}^\dagger c_{\mathbf{k}} - \frac{G}{4m} \sum_{\mathbf{k} \neq \pm \mathbf{k}'} (k_x - ik_y)(k'_x + ik'_y) c_{\mathbf{k}}^\dagger c_{-\mathbf{k}}^\dagger c_{-\mathbf{k}'} c_{\mathbf{k}'} \quad (19)$$

where $c_{\mathbf{k}}, c_{\mathbf{k}}^\dagger$ are destruction and creation operators of two-dimensional polarised fermions with momentum $\mathbf{k} = (k_x, k_y)$, m is their mass and G is a dimensionless coupling constant which is positive for an attractive interaction. We remark that we impose no constraint on the choice for the ultraviolet cut-off, which we denote as ω . Likewise the distribution of the momenta \mathbf{k} is arbitrary other than the assumption that all momentum states arise in time-reversed pairs \mathbf{k} and $-\mathbf{k}$. In particular this means that a one-dimensional system is obtained by simply setting all $k_y = 0$.

We shall discuss now how this Hamiltonian can be obtained from another limiting case of the Hamiltonian (5), which establishes the integrability of the $p + ip$ -wave BCS model. The strategy here is to take the quasi-classical limit first, rather than the rational limit. While this general approach has previously appeared in the literature to construct integrable Hamiltonians in the context of Gaudin algebras [1, 2, 14, 15], the connection with the $p + ip$ model has thus far not been made apparent for reasons we will discuss below.

Introducing the parameterisation

$$\begin{aligned}\alpha &= -i\gamma t \\ \beta &= -i\gamma p\end{aligned}$$

and taking the limit $\gamma \rightarrow 0$ leads to the Hamiltonian

$$H = \sum_{j=1}^L z_j^2 N_j - \frac{2p}{t-2p} \sum_{k>r}^L z_k z_r (b_r^\dagger b_k + \text{h.c.})$$

with the Bethe ansatz equations and energies given respectively by

$$\begin{aligned}-2t - 4p \sum_{k=1}^L \frac{z_k^2}{y_m^2 - z_k^2} &= -8p \sum_{j \neq m}^M \frac{y_j^2}{y_j^2 - y_m^2}, \\ E &= \frac{t}{t-2p} \sum_{j=1}^M y_j^2\end{aligned}\tag{20}$$

Next we set

$$G = \frac{2p}{t-2p} = \frac{2}{\alpha/\beta - 2}\tag{21}$$

in terms of which we have

$$H = \sum_{j=1}^L z_j^2 N_j - G \sum_{k>r}^L z_k z_r (b_r^\dagger b_k + \text{h.c.}),\tag{22}$$

$$\frac{G^{-1} - L + 2M - 1}{y_m^2} + \sum_{k=1}^L \frac{1}{y_m^2 - z_k^2} = \sum_{j \neq m}^M \frac{2}{y_m^2 - y_j^2},\tag{23}$$

$$E = (1 + G) \sum_{j=1}^M y_j^2.\tag{24}$$

To show that (22) is equivalent to (19), we first define the Cooper pair operators

$$\tilde{b}_{\mathbf{k}}^\dagger = c_{\mathbf{k}}^\dagger c_{-\mathbf{k}}^\dagger, \quad \tilde{b}_{\mathbf{k}} = c_{-\mathbf{k}} c_{\mathbf{k}}, \quad \tilde{N}_{\mathbf{k}} = \tilde{b}_{\mathbf{k}}^\dagger \tilde{b}_{\mathbf{k}},$$

which have odd symmetry (consistent with p -wave pairing):

$$\tilde{b}_{-\mathbf{k}} = -\tilde{b}_{\mathbf{k}}, \quad \tilde{N}_{\mathbf{k}} = \tilde{N}_{-\mathbf{k}}.$$

We let \mathbf{K}_+ denote the set of momenta where $k_x > 0$ and no restriction placed on k_y , so that we avoid issues with double counting. Excluding the unpaired states and setting $m = 1$, the Hamiltonian (19) takes the form

$$H = \sum_{\mathbf{k} \in \mathbf{K}_+} z_{\mathbf{k}}^2 \tilde{N}_{\mathbf{k}} - G \sum_{\mathbf{k} \neq \mathbf{k}' \in \mathbf{K}_+} z_{\mathbf{k}} z_{\mathbf{k}'} \exp(-i\phi_{\mathbf{k}}) \exp(i\phi_{\mathbf{k}'}) \tilde{b}_{\mathbf{k}}^\dagger \tilde{b}_{\mathbf{k}'}\tag{25}$$

where $z_{\mathbf{k}} = |\mathbf{k}|$ and $\exp(i\phi_{\mathbf{k}}) = (k_x + ik_y)/\mathbf{k}^2$. Performing the unitary transformation

$$\tilde{b}_{\mathbf{k}}^\dagger = \exp(i\phi_{\mathbf{k}}) b_{\mathbf{k}}^\dagger, \quad \tilde{b}_{\mathbf{k}} = \exp(-i\phi_{\mathbf{k}}) b_{\mathbf{k}}\tag{26}$$

and using the integers rather than \mathbf{k} to enumerate the momentum states in the half plane brings (25) into (19).

Note that the main results derived for the exact solution of the $p + ip$ model, viz. (23,24), are functions of the squares of the Bethe roots. Throughout the subsequent analyses (with the exception of Appendices B.3 and B.4) we will simplify the notation by making the substitution

$$y_j^2 \mapsto y_j. \quad (27)$$

In terms of the original parameterisation, we may now write that the exact eigenstates of the Hamiltonian (19) with M fermion pairs are given by

$$|\psi\rangle = \prod_{j=1}^M C(y_j)|0\rangle, \quad C(y) = \sum_{\mathbf{k} \in \mathbf{K}_+} \frac{k_x - ik_y}{\mathbf{k}^2 - y} c_{\mathbf{k}}^\dagger c_{-\mathbf{k}}^\dagger \quad (28)$$

where the rapidities y_j , $j = 1, \dots, M$ satisfy the Bethe ansatz equations

$$\frac{q}{y_j} + \frac{1}{2} \sum_{\mathbf{k} \in \mathbf{K}_+} \frac{1}{y_j - \mathbf{k}^2} - \sum_{l \neq j}^M \frac{1}{y_j - y_l} = 0, \quad m = 1, \dots, M \quad (29)$$

with $2q = 1/G - L + 2M - 1$. The total energy of the state (28) is given by

$$E = (1 + G) \sum_{j=1}^M y_j. \quad (30)$$

This limiting case is closely related to other models which have been constructed using the hyperbolic Gaudin algebras [1, 2, 14, 15]. In fact the conserved operators for the Hamiltonian (22) which are obtained by taking the quasi-classical limit of the operators $\{\tilde{t}(qz_j) : j = 1, \dots, L\}$ are equivalent to those which are discussed in [1, 2, 14, 15] with an important difference due to the coupling parameter of the overarching anyonic model being defined in a sector-dependent manner. To make this explicit, expressing the leading term expansion as

$$\tilde{t}(qz_k) \sim I - 2p\gamma\tau_k$$

we find

$$\tau_k = (2G^{-1} - L + 2M)N_k - \sum_{l \neq k}^L \left(\frac{2z_k z_l}{z_k^2 - z_l^2} (b_k^\dagger b_l + b_k b_l^\dagger) + \frac{z_k^2 + z_l^2}{z_k^2 - z_l^2} (2N_k N_l - N_k - N_l) \right). \quad (31)$$

Besides a constant term, the difference with the conserved operators in [1, 2, 14, 15] is the M - and L -dependence on the co-efficient of N_k . Through the conserved operators we can write for each sector with fixed M

$$H = \frac{G}{2} \sum_{k=1}^L z_k^2 (\tau_k - M)$$

The eigenvalues λ_k of the τ_k are

$$\lambda_k = \sum_{j=1}^M \frac{z_k^2 + y_j^2}{z_k^2 - y_j^2}$$

which follows from taking the leading terms in the expansion of (109) in Appendix A.2. One may check, with the help of (23), that

$$\begin{aligned} E &= (1 + G) \sum_{j=1}^M y_j^2 \\ &= \frac{G}{2} \sum_{k=1}^L z_k^2 (\lambda_k - M) \end{aligned}$$

as required.

It is important to clarify here the reason why the conserved operators are said to be associated with hyperbolic Gaudin algebras. Introducing the scaling parameter ν we set

$$\varepsilon_k = \frac{1}{\nu} \ln(z_k), \quad v_j = \frac{1}{\nu} \ln(y_j). \quad (32)$$

Through this change of variables the Bethe ansatz equations (23) can be expressed as

$$\frac{2}{G} - L + 2M + \sum_{k=1}^L \coth(\nu(v_m - \varepsilon_k)) = 2 \sum_{j \neq m}^M \coth(\nu(v_m - v_j)) \quad (33)$$

and in a similar way the expressions for τ_k and λ_k can be written in terms of hyperbolic functions. In this form, we can now take the rational limit to recover the s -wave BCS model from the $p + ip$ model. We redefine the Hamiltonian (22) as

$$H \mapsto \frac{1}{\nu} (H - (1 + G)N).$$

Then setting $G \mapsto \nu G$ and taking the limit $\nu \rightarrow 0$, (22,23,24) reproduce (16,17,18).

3.3 The Gaudin models

The Gaudin model can be considered as the $G \rightarrow \infty$ limit of the corresponding s - wave and p -wave models introduced above. In the s -wave model the $U(1)$ symmetry is promoted to a $SU(2)$ symmetry and the Gaudin model can be regarded as a rotational invariant spin chain with local spin 1/2 operators \mathbf{S}_i whose dynamics is described by a set of commuting operators

$$R_i = \sum_{j \neq i}^L \frac{\mathbf{S}_i \cdot \mathbf{S}_j}{\varepsilon_i - \varepsilon_j}, \quad [R_i, R_j] = 0$$

These operators are simultaneously diagonalized by the Richardson ansatz in terms of a set of rapidities ε_j satisfying the $G \rightarrow \infty$ limit of the Bethe ansatz equations (11), namely

$$\sum_{k=1}^L \frac{1}{v_j - \varepsilon_k} = \sum_{j \neq m}^M \frac{2}{v_m - v_j}, \quad j = 1, \dots, N$$

The p -wave Gaudin model corresponds to the trigonometric version considered earlier with the commuting operators given by the $G \rightarrow \infty$ limit of the operators τ_k defined in eq. (31). The corresponding Bethe ansatz equations are given by the $G \rightarrow \infty$ limit of (29), or equivalently (33).

4 Analysis of the $p + ip$ model

4.1 Ground-state phase diagram from BCS mean-field theory

To undertake the mean-field analysis of the $p + ip$ model it is more convenient to work with the Hamiltonian

$$\mathcal{H} = \sum_{\mathbf{k}} \frac{\mathbf{k}^2}{2m} c_{\mathbf{k}}^{\dagger} c_{\mathbf{k}} - \frac{G}{4m} \sum_{\mathbf{k}, \mathbf{k}'} (k_x - ik_y)(k'_x + ik'_y) c_{\mathbf{k}}^{\dagger} c_{-\mathbf{k}}^{\dagger} c_{-\mathbf{k}'} c_{\mathbf{k}'} \quad (34)$$

which differs from (19) only in that the double sum is now not restricted to $\mathbf{k} \neq \pm \mathbf{k}'$. The differences between using (19) and (34) will be discussed at the end of Subsection 4.1.1.

The derivation of the gap and chemical potential equations which give the mean-field solution of (34) follows now standard techniques which are a straightforward extension of the original methods of the BCS paper [5]. Here we will only outline the main steps. First we assume that the number of fermions is even and that in the ground state of the system all fermions are paired. Our convention will again be to use N to denote the Cooper pair number operator and M for the eigenvalues of N . The BCS order parameter associated to (34) is

$$\hat{\Delta} = \frac{G}{m} \sum_{\mathbf{k}} (k_x + ik_y) \langle c_{-\mathbf{k}} c_{\mathbf{k}} \rangle$$

in terms of which the Hamiltonian (34) can be approximated as

$$\mathcal{H} \approx \sum_{\mathbf{k}} \xi_{\mathbf{k}} c_{\mathbf{k}}^{\dagger} c_{\mathbf{k}} - \frac{1}{4} \sum_{\mathbf{k}} \left(\hat{\Delta} (k_x - ik_y) c_{\mathbf{k}}^{\dagger} c_{-\mathbf{k}}^{\dagger} + h.c. \right) + \frac{|\hat{\Delta}|^2}{4G} + \mu M$$

where $\xi_{\mathbf{k}} = \mathbf{k}^2/2m - \mu/2$ and $\mu/2$ is the chemical potential. This Hamiltonian can be diagonalized by a Bogoliubov transformation. By minimising the energy, and fixing the expectation value of the number of Cooper pairs to be M , it is found that the gap $\Delta = |\hat{\Delta}|$ and chemical potential are the solutions of the equations

$$\sum_{\mathbf{k} \in \mathbf{K}_+} \frac{\mathbf{k}^2}{\sqrt{(\mathbf{k}^2 - \mu)^2 + \mathbf{k}^2 \Delta^2}} = \frac{1}{G} \quad (35)$$

$$\mu \sum_{\mathbf{k} \in \mathbf{K}_+} \frac{1}{\sqrt{(\mathbf{k}^2 - \mu)^2 + \mathbf{k}^2 \Delta^2}} = 2M - L + \frac{1}{G} \quad (36)$$

where we have set $m = 1$ and $2L$ is the total number of momentum states below the cut-off ω . The mean-field expression for the ground-state energy is

$$E_0 = \frac{1}{2} \sum_{\mathbf{k} \in \mathbf{K}_+} \mathbf{k}^2 \left(1 - \frac{2\mathbf{k}^2 + \Delta^2 - 2\mu}{2\sqrt{(\mathbf{k}^2 - \mu)^2 + \mathbf{k}^2 \Delta^2}} \right). \quad (37)$$

The normalised ground state is given by

$$|\Psi\rangle = \prod_{\mathbf{k} \in \mathbf{K}_+} (u_{\mathbf{k}} I + v_{\mathbf{k}} c_{\mathbf{k}}^{\dagger} c_{-\mathbf{k}}^{\dagger}) |0\rangle \quad (38)$$

where

$$\begin{aligned} |u_{\mathbf{k}}|^2 &= \frac{1}{2} \left(1 + \frac{\mathbf{k}^2 - \mu}{\sqrt{(\mathbf{k}^2 - \mu)^2 + \mathbf{k}^2 \Delta^2}} \right) \\ |v_{\mathbf{k}}|^2 &= \frac{1}{2} \left(1 - \frac{\mathbf{k}^2 - \mu}{\sqrt{(\mathbf{k}^2 - \mu)^2 + \mathbf{k}^2 \Delta^2}} \right) \end{aligned}$$

and the phases must be chosen such that

$$\frac{(k_x + ik_y) \hat{\Delta}^* v_{\mathbf{k}}}{u_{\mathbf{k}}} = 2E(\mathbf{k}) - \mathbf{k}^2 + \mu$$

is real. Above, $E(\mathbf{k})$ is the quasiparticle energy spectrum

$$E(\mathbf{k}) = \frac{1}{2} \sqrt{(\mathbf{k}^2 - \mu)^2 + \mathbf{k}^2 \Delta^2}. \quad (39)$$

To obtain an approximation for the ground state with a fixed number of Cooper pairs M , one can take a projection of (38). Writing (38) as

$$|\Psi\rangle = \left(\prod_{\mathbf{k} \in \mathbf{K}_+} u_{\mathbf{k}}^{-1} \right) \exp \left(\sum_{\mathbf{k} \in \mathbf{K}_+} \frac{v_{\mathbf{k}}}{u_{\mathbf{k}}} c_{\mathbf{k}}^\dagger c_{-\mathbf{k}}^\dagger \right) |0\rangle,$$

projection onto a fixed number of M pairs gives

$$|\psi\rangle = \left[\sum_{\mathbf{k} \in \mathbf{K}_+} \mathbf{g}(\mathbf{k}) c_{\mathbf{k}}^\dagger c_{-\mathbf{k}}^\dagger \right]^M |0\rangle \quad (40)$$

where

$$\mathbf{g}(\mathbf{k}) = \frac{v_{\mathbf{k}}}{u_{\mathbf{k}}} = \frac{2E(\mathbf{k}) - \mathbf{k}^2 + \mu}{(k_x + ik_y) \hat{\Delta}^*}. \quad (41)$$

4.1.1 The Moore-Read and Read-Green lines

By analysing the above mean-field results we can piece together the various phases of the model. To some extent this has been undertaken in [53], and we will first review their findings. Then we will extend the analysis to expose a duality that exists in the ground-state phase diagram.

Following [53], note that the spectrum is gapless at $\mu = 0$ as $|\mathbf{k}| \rightarrow 0$. Furthermore, the behaviour of $\mathbf{g}(\mathbf{k})$ as $|\mathbf{k}| \rightarrow 0$ depends on the sign of μ ,

$$\mathbf{g}(\mathbf{k}) \sim \begin{cases} k_x - ik_y, & \mu < 0, \\ 1/(k_x + ik_y), & \mu > 0. \end{cases}$$

It was argued in [53] that $\mu = 0$ corresponds to a topological phase transition, a subject we will return to later in Subsection 4.3. From (36) it is seen that $\mu = 0$ necessarily implies

$$M = \frac{1}{2} \left(L - \frac{1}{G} \right)$$

Introducing the filling fraction $x = M/L$ and defining $g = GL$ we equivalently have

$$x = \frac{1}{2} \left(1 - \frac{1}{g} \right). \quad (42)$$

We will refer to (42) as the Read-Green (RG) line of the phase diagram.

In real space the state (40) takes the form of a pfaffian

$$\psi(\mathbf{r}_1, \dots, \mathbf{r}_{2M}) = \mathcal{A}[\hat{\mathbf{g}}(\mathbf{r}_1 - \mathbf{r}_2) \dots \hat{\mathbf{g}}(\mathbf{r}_{2M-1} - \mathbf{r}_{2M})]$$

where \mathcal{A} denotes the antisymmetrization of the positions and $\hat{\mathbf{g}}(\mathbf{r})$ is the Fourier transform of $\mathbf{g}(\mathbf{k})$. We will refer to the case $\mu = 0$ as the Read-Green (RG) state. For $\mu > 0$ the large distance behaviour is $\hat{\mathbf{g}}(\mathbf{r}) \sim 1/(x + iy)$, which asymptotically reproduces the Moore-Read (MR) state found in studies of the Fractional Quantum Hall Effect [49] (see Appendix B.1 for the derivation of this result and its comparison with the exact wavefunctions in real space). In momentum space co-ordinates the (unnormalised) MR state of M Cooper pairs is

$$|MR\rangle = \left[\sum_{\mathbf{k} \in \mathbf{K}_+} \frac{1}{k_x + ik_y} c_{\mathbf{k}}^\dagger c_{-\mathbf{k}}^\dagger \right]^M |0\rangle. \quad (43)$$

Upon closer inspection of the mean-field equations we find that the MR state (43) coincides (up to normalisation) with the projected ground state (40) whenever

$$\Delta^2 = 4\mu \quad (44)$$

The result is easily verified by simply substituting (44) into (39,41). Furthermore, substituting (44) into (35,36) and adding these equations yields

$$M = L - \frac{1}{G},$$

or in terms of the filling fraction

$$x = 1 - \frac{1}{g}. \quad (45)$$

We will refer to (45) as the MR line of the phase diagram. Finally, we substitute (44) into (37) to obtain

$$E_0 = 0. \quad (46)$$

This means that the condensation energy of the state equals the energy of the Fermi sea!

From the above considerations we gain an initial insight into topological properties of the model. Both the RG line given by (42), for which the excitation spectrum becomes gapless as $|\mathbf{k}| \rightarrow 0$, and the MR line given by (45), for which the ground-state energy is zero, hold *independent* of the choice of distribution for the momenta \mathbf{k} . These are properties of the model that are protected (in a topological sense to be discussed in Subsection 4.3) from perturbations of the system which are reflected by changes in the momentum distribution.

Both the RG and MR lines can be viewed as boundary lines in the ground-state phase diagram relative to a duality property of the mean-field solution, which is our next item

to discuss. First we introduce parameters a and b related to the chemical potential and the gap by

$$a, b = \mu - \frac{\Delta^2}{2} \pm \Delta \sqrt{\frac{\Delta^2}{4} - \mu} \quad (47)$$

which simply allows us to write the quadratic term under the square root in (35,36) in terms of its roots:

$$\sqrt{(\mathbf{k}^2 - \mu)^2 + \mathbf{k}^2 \Delta} = \sqrt{(\mathbf{k}^2 - a)(\mathbf{k}^2 - b)}.$$

The parameters a and b can either both be real, or form a complex pair in which case we denote them as $\epsilon \pm i\delta$. In either case they satisfy the relation

$$\mu^2 = ab.$$

We see from (37) that in terms of a and b the ground-state energy reads

$$E_0 = \frac{1}{2} \sum_{\mathbf{k} \in \mathbf{K}_+} \mathbf{k}^2 \left(1 - \frac{2\mathbf{k}^2 - a - b}{2\sqrt{(\mathbf{k}^2 - a)(\mathbf{k}^2 - b)}} \right) \quad (48)$$

which is independent of the sign of μ . On the other hand, the sign of the μ coincides, by eq. (36), with that of

$$q_0 = L \left(x - \frac{1}{2} + \frac{1}{2g} \right). \quad (49)$$

This implies the existence of a duality between phases which we will denote as weak pairing and strong pairing, adopting the terminology of [53]. Specifically, the two ground states with filling fractions x_W (with $\mu > 0$) and x_S (with $\mu < 0$) satisfying

$$x_W + x_S = 1 - \frac{1}{g} \quad (50)$$

share the same values of a, b, g, μ^2 . Besides differing in the sign of μ , they also differ in the values of Δ . One can check that the required map which preserves (47) is

$$\begin{aligned} \Delta^2 &\mapsto \Delta^2 - 4\mu \\ \mu &\mapsto -\mu \end{aligned}$$

Finally, from (48) we see these ground states have the same mean-field energy, and from (39) the same excitation spectrum above them.

Taking into account all these considerations, the ground state of the model consists of three phases detailed in Table 1. In the weak coupling BCS phase where $x > 1 - 1/g$, a and b form a complex pair parameterized by ϵ and δ . When $x = 1 - 1/g$, the MR line, both a and b are equal and real. This line is dual to the vacuum. From (39) the mean-field solution predicts this line is gapped, so it is not clear at this stage in what sense the MR line might be considered a phase transition. We shall come back to this issue later on when we discuss the solution of the model in terms of the Bethe ansatz equations. The two regions denoted weak pairing and strong pairing, for which the parameters a and b are real and negative, are separated by the critical RG line where the chemical potential $\mu = 0$ and the excitation gap vanishes. The RG line is self-dual.

| Phase | a, b | μ, Δ | x |
|-------------------|------------------------|------------------------|-----------------------------------|
| Weak coupling BCS | $\epsilon \pm i\delta$ | $\mu > \Delta^2/4$ | $x > 1 - g^{-1}$ |
| Moore-Read line | $a = b = -\mu$ | $\mu = \Delta^2/4$ | $x_{MR} = 1 - g^{-1}$ |
| Weak pairing | $a < b < 0$ | $0 < \mu < \Delta^2/4$ | $(1 - g^{-1})/2 < x < 1 - g^{-1}$ |
| Read-Green line | $a < b = 0$ | $\mu = 0$ | $x_{RG} = (1 - g^{-1})/2$ |
| Strong pairing | $a < b < 0$ | $\mu < 0$ | $x < (1 - g^{-1})/2$ |

Table 1: Phases of the $p + ip$ model in terms of the mean-field variables μ, Δ, a, b .

To solve the mean-field gap (35) and chemical potential (36) equations for the case of large L it is useful to undertake a continuum limit whereby the sums are replaced by integrals. Making the change of variable $\bar{\epsilon} = \mathbf{k}^2/\omega$ we introduce a density function $\bar{\rho}(\bar{\epsilon})$ with the choice of normalisation

$$\int_0^1 d\bar{\epsilon} \bar{\rho}(\bar{\epsilon}) = 1.$$

The densities are chosen as

$$\bar{\rho}(\bar{\epsilon}) = \frac{1}{2\sqrt{\bar{\epsilon}}} \quad (51)$$

which corresponds to free fermions in one dimension (1D), and

$$\bar{\rho}(\bar{\epsilon}) = 1 \quad (52)$$

for free fermions in two dimensions (2D). The integral approximations of (35,36) are

$$\frac{1}{g} = \int_0^1 d\bar{\epsilon} \frac{\bar{\epsilon} \bar{\rho}(\bar{\epsilon})}{\sqrt{(\bar{\epsilon} - \bar{a})(\bar{\epsilon} - \bar{b})}}, \quad (53)$$

$$2 \left| x - \frac{1}{2} + \frac{1}{2g} \right| = \sqrt{\bar{a}\bar{b}} \int_0^1 d\bar{\epsilon} \frac{\bar{\rho}(\bar{\epsilon})}{\sqrt{(\bar{\epsilon} - \bar{a})(\bar{\epsilon} - \bar{b})}}, \quad (54)$$

where $\bar{a} = a/\omega, \bar{b} = b/\omega$. From (37) we obtain the ground-state energy per pair as

$$e_0 = \frac{\omega}{2x} \int_0^1 d\bar{\epsilon} \bar{\epsilon} \bar{\rho}(\bar{\epsilon}) \left(1 - \frac{2\bar{\epsilon} - \bar{a} - \bar{b}}{2\sqrt{(\bar{\epsilon} - \bar{a})(\bar{\epsilon} - \bar{b})}} \right). \quad (55)$$

The integral equation approximations become exact in the thermodynamic limit $L \rightarrow \infty$, which requires that $G \rightarrow 0, M \rightarrow \infty$ in order for $g = GL, x = M/L$ to remain finite. Solutions of (53,54) are given in Appendix B.1. Numerical results are presented in Figs. 3 and 4 below.

To conclude here, we turn to the comparison between the Hamiltonians (19) and (34). Excluding the subspace of unpaired states we have

$$H(G) = (1 + G)\mathcal{H}(G/(1 + G))$$

which shows that H is equivalent to \mathcal{H} up to a scaling factor $1 + G$ and the redefinition of the coupling $G \mapsto G/(1 + G)$. For systems with an even number of fermions, the mean-field ground states of H and \mathcal{H} are equal in the thermodynamic limit since we take $G \rightarrow 0$.

4.1.2 The Volovik line

The energy gap between the ground and first excited states is the minimum of the quasiparticle excitation energies as given by (39). In order to make comparison with later results for finite-sized systems where the total fermion number is fixed, we will consider an elementary excitation to be associated with two quasiparticle excitations. From (39) we find that the gap E_{gap} is

$$E_{\text{gap}}(\mathbf{k}) = \begin{cases} |\mu|, & \mu \leq \Delta^2/2, \\ \frac{1}{2}\sqrt{\Delta^2(4\mu - \Delta^2)}, & \mu \geq \Delta^2/2. \end{cases}$$

For $\mu > \Delta^2/2$ the quasiparticle energy has a minimum at a non zero momentum \mathbf{k} different from zero, while for $\mu \leq \Delta^2/2$ the minimum is achieved at $\mathbf{k} = 0$. This situation is reminiscent of the Higgs transition that takes places for a scalar field with a quartic potential [61]. For this reason we call the case $\mu = \Delta^2/2$ the Volovik line in the $p+ip$ phase diagram. In this instance eliminating Δ from the gap and chemical potential equations (35,36) gives

$$\begin{aligned} \sum_{\mathbf{k} \in \mathbf{K}_+} \frac{\mathbf{k}^2}{\sqrt{\mathbf{k}^4 + \mu^2}} &= \frac{1}{G}, \\ \mu \sum_{\mathbf{k} \in \mathbf{K}_+} \frac{1}{\sqrt{\mathbf{k}^4 + \mu^2}} &= 2M - L + \frac{1}{G}. \end{aligned}$$

Further eliminating the $1/G$ term we obtain the equation of the Volovik line

$$x = \frac{1}{2} - \frac{1}{2L} \sum_{\mathbf{k} \in \mathbf{K}_+} \frac{\mathbf{k}^2 - \mu}{\sqrt{\mathbf{k}^4 + \mu^2}} \quad (56)$$

which lies in the weak coupling BCS phase. In contrast to the RG (42) and MR (45) line equations, the Volovik line is dependent on the distribution of the momenta \mathbf{k} and consequently is not topologically protected. In the continuum limit the equation (56) reads

$$x = \frac{1}{2} - \frac{1}{2} \int_0^1 d\bar{\varepsilon} \bar{\rho}(\bar{\varepsilon}) \frac{\bar{\varepsilon} - \bar{\mu}}{\sqrt{\bar{\varepsilon}^2 + \bar{\mu}^2}} \quad (57)$$

which relates the filling fraction x with the value of the normalized chemical potential $\bar{\mu}$. In 2D the gap equation (53) becomes

$$\frac{1}{g} = -\bar{\mu} + \sqrt{1 + \bar{\mu}^2}$$

which can be easily inverted to yield $\bar{\mu}$ as a function of g . Plugging that result into the integral of (57) gives the Volovik line for the 2D model

$$x = \frac{1}{2} \left(1 - g^{-1} + \frac{1}{2}(g - g^{-1}) \log \frac{g + g^{-1} + 2}{g - g^{-1}} \right). \quad (58)$$

In 1D the gap equation (53) yields

$$\frac{1}{g} = \frac{1}{3\bar{\mu}} F_{2,1} \left(\frac{1}{2}, \frac{3}{4}, \frac{7}{4}, -\frac{1}{\bar{\mu}^2} \right)$$

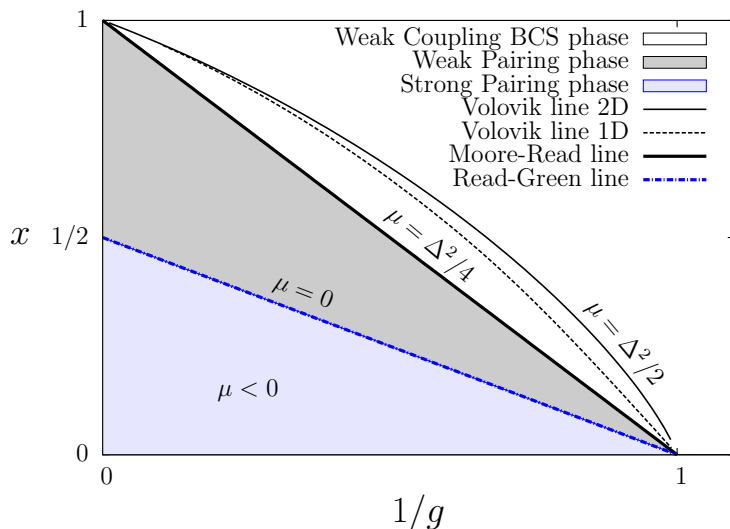


Figure 2: Ground-state phase diagram of the $p + ip$ model in terms of the inverse coupling $1/g$ and filling fraction $x = M/L$. Phase boundaries are given by the Read-Green line ($\mu = 0$) and the Moore-Read line ($\mu = \Delta^2/4$). The phase boundary conditions are independent of the choice of the momentum distribution, and independent of the ultraviolet cut-off. Also shown are the Volovik lines corresponding to 1D and 2D momentum distributions.

which together with the integration of (57) gives

$$x = \frac{1}{2} \left(1 - g^{-1} + F_{2,1} \left(\frac{1}{4}, \frac{1}{2}, \frac{5}{4}, -\frac{1}{\bar{\mu}^2} \right) \right)$$

which is the equation of the Volovik line in 1D. In Fig. 2 we depict the Volovik lines, of the 1D and 2D models, on the the phase diagram of the $p + ip$ model. One can see that they lie close to the MR line although do not coincide with it. As explained earlier the Volovik line depends on the choice of the energy level density $\rho(\varepsilon)$, while the MR and RG lines are independent of it.

4.1.3 Fidelity susceptibility

The notion of fidelity has been adopted in a variety of ways to characterise quantum phase transitions [65, 68]. Here we focus on one such formulation, which is the fidelity susceptibility [28].

The fidelity susceptibility χ_F is defined as

$$\chi_F = \left\langle \frac{d\Psi}{dG} \left| \frac{d\Psi}{dG} \right\rangle - \left\langle \frac{d\Psi}{dG} \left| \Psi \right\rangle \left\langle \Psi \left| \frac{d\Psi}{dG} \right\rangle \right.$$

For the mean-field wavefunction this reduces to

$$\chi_F = \sum_{\mathbf{k} \in \mathbf{K}_+} \left\langle \frac{d\psi_{\mathbf{k}}}{dG} \left| \frac{d\psi_{\mathbf{k}}}{dG} \right\rangle = \sum_{\mathbf{k} \in \mathbf{K}_+} \left(\frac{du_{\mathbf{k}}}{dG} \right)^2 + \left(\frac{dv_{\mathbf{k}}}{dG} \right)^2.$$

The derivatives of $u_{\mathbf{k}}$ and $v_{\mathbf{k}}$ with respect to G can be computed in terms of

$$\frac{d\mu}{dG} = c, \quad \frac{d\Delta}{dG} = d.$$

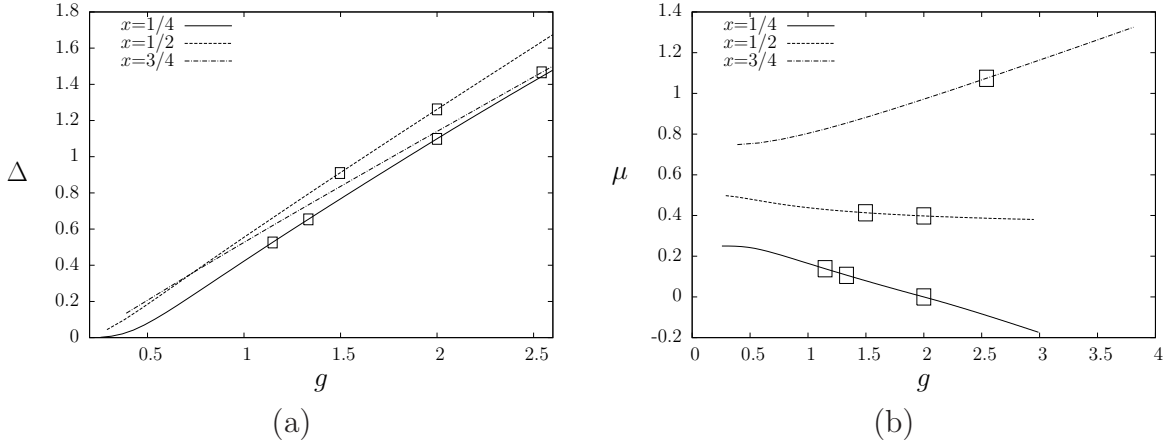


Figure 3: Mean-field order parameter, Δ , and chemical potential, μ , solution of the gap and chemical potential equations in 2D for filling fractions $x = 1/4, 1/2$ and $3/4$, vs. g . The rectangles over the curves indicate, from left to right, the Volovik, Moore-Read and Read-Green points ($x = 1/4$); the Volovik and Moore-Read points ($x = 1/2$), and the Volovik point ($x = 3/4$).

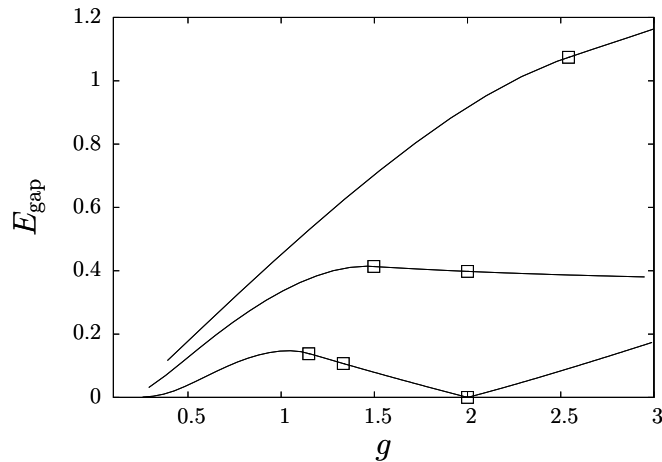


Figure 4: The mean-field energy gap E_{gap} versus coupling constant g for a 2D momentum density distribution as given by (52). From top to bottom the curves shown correspond to the filling fractions $x = 3/4, 1/2, 1/4$. The squares over the curves indicate, from left to right, the Volovik, Moore-Read, and Read-Green points respectively.

which never vanish for $G > 0$, as can be seen from Fig. 3. Now

$$\left(\frac{du_{\mathbf{k}}}{dG}\right)^2 + \left(\frac{dv_{\mathbf{k}}}{dG}\right)^2 = \frac{\epsilon_{\mathbf{k}} (c\Delta + d(\epsilon_{\mathbf{k}} - \mu))^2}{4 ((\epsilon_{\mathbf{k}} - \mu)^2 + \epsilon_{\mathbf{k}}\Delta^2)^2}$$

In the mean-field theory gapless excitations occur when $\epsilon_0 = \mu = 0$. Now

$$\lim_{\epsilon_0 \rightarrow 0} \lim_{\mu \rightarrow 0} \left[\left(\frac{du_0}{dG}\right)^2 + \left(\frac{dv_0}{dG}\right)^2 \right] = \infty.$$

This indicates the fidelity susceptibility is divergent on the Read-Green line. The expression of χ_F in the continuum limit is given by

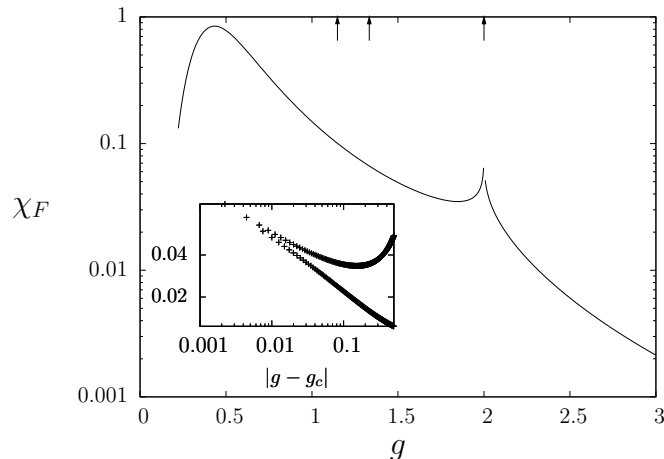


Figure 5: Plot of the mean-field fidelity susceptibility (59) as a function of the coupling g for $x = 1/4$. The 2D momentum distribution (52) is used and the fidelity susceptibility is in units of L^3 . The singularity at $g_c = 2$ is apparent. Arrows indicate from left to right the Volovik, Moore-Read, and Read-Green points respectively. The inset emphasises the logarithmic character of this singularity, with the distance to the critical point g_c shown on a logarithmic scale. The two data sets correspond to both cases $g > g_c$ and $g < g_c$.

$$\chi_F = \frac{L^3}{4} \int_0^1 d\bar{\varepsilon} \bar{\rho}(\bar{\varepsilon}) \varepsilon \left[\frac{\bar{c}\bar{\Delta} + \bar{d}(\bar{\varepsilon} - \bar{\mu})}{(\bar{\varepsilon} - \bar{\mu})^2 + \bar{\varepsilon}\bar{\Delta}^2} \right]^2 \quad (59)$$

where

$$\frac{d\bar{\mu}}{dg} = \bar{c}, \quad \frac{d\bar{\Delta}}{dg} = \bar{d}.$$

In Fig. 5 we plot χ_F as a function of g for $x = 1/4$. The results show a logarithmic divergence at the Read-Green point $g_c = 2$, reflecting that the model is critical here.

4.2 Analysis of the Bethe ansatz equations in the continuum limit

4.2.1 The electrostatic analogy

For the s -wave BCS model, the relationship between the mean-field gap and chemical potential equations and the exact Bethe ansatz solution was first explored by Gaudin [23]. This was achieved by use of an electrostatic analogy, whereby the Bethe ansatz equations represent the equilibrium conditions for a two-dimensional system of fixed and mobile charges. Further studies along this line for the s -wave case can be found in [55, 56]. Our aim below is to extend this approach for the $p + ip$ model. In the general framework of exactly solvable models based on hyperbolic Gaudin algebras this type of study has previously been conducted in [1]. There the mapping from the hyperbolic form of the Bethe ansatz equation such as (33) to a set of algebraic equations was implemented by a change of variable. However this change of variable is not the same as (32), so the algebraic form considered in [1] is different from (23).

Taking into account the change of notational conventions as described by (27), let us

write the Bethe ansatz equation (23) as

$$-\frac{1}{2} \sum_{k=1}^L \frac{1}{y_m - z_k^2} - \frac{q_0}{y_m} + \sum_{j \neq m}^M \frac{1}{y_m - y_j} = 0, \quad m = 1, \dots, M \quad (60)$$

where q_0 is given by (49). This equation admits an electrostatic analogy associating $-1/2$ charges at the fixed positions z_k^2 , a $-q_0$ charge at the origin, and mobile $+1$ charges with positions y_j . With these assignments (60) amounts to the vanishing of the total electric field acting on the charge y_m . The continuum limit of (60) is given by (we shall follow the conventions of references [23, 55]):

$$\int_{\Omega} d\varepsilon \frac{\rho(\varepsilon)}{\varepsilon - y} - \frac{q_0}{y} - P \int_{\Gamma} |dy'| \frac{r(y')}{y' - y} = 0, \quad \forall y \in \Gamma \quad (61)$$

where $\Omega = (0, \omega)$ denotes the interval on the real line where lie the energy levels which can be associated to a negative charge density $-\rho(\varepsilon)$ such that

$$\int_0^{\omega} d\varepsilon \rho(\varepsilon) = \frac{L}{2}.$$

The function $r(y)$ denotes the charge density associated to the roots y_m which lie on an arc Γ of the complex plane. It satisfies

$$\int_{\Gamma} |dy| r(y) = M$$

while the energy (24) in the continuum limit is given by

$$\int_{\Gamma} |dy| y r(y) = E. \quad (62)$$

For the ground-state roots the topology of the arc Γ depends crucially on the domain of the phase diagram one is exploring. In each phase Γ consists of the union of several types of arcs whose properties are given in Table 2. Table 3 displays the arcs associated to the different phases of the model. We shall first comment on the results contained in these tables and will give the derivation later.

An arc of type Γ_A is a segment of the real line $(0, \varepsilon_A)$ which is contained in the real interval Ω . At $G = 0$, all the roots y_m associated to the ground state lie on Γ_A , where $\varepsilon_A = \mu$ only depends on the filling fraction x . When the coupling is switched on, $g > 0$, the roots closer to the Fermi level form a complex arc Γ_B parameterized by its end points $a, b = \varepsilon \pm i\delta$, and which cuts the real axis at ε_A whose value has also changed slightly. In the weak coupling BCS phase, Γ is the union of the arcs Γ_A and Γ_B . This type of arc is the familiar one encountered in the solution of the s -wave model [23, 55]. As g increases, the arc Γ_B enlarges and bends towards the negative real axis. At the Moore-Read line the complex arc closes and is denoted by Γ_C . This arc cuts the real axis at $\varepsilon_A > 0$ and $a = b < 0$. Some real roots may still remain, so that Γ at the Moore-Read line is the union $\Gamma_A \cup \Gamma_C$. In the weak pairing phase the closed arc Γ_C remains but there appear some new roots on the negative real axis forming the open arc $\Gamma_D = (a, b)$. Hence $\Gamma = \Gamma_A \cup \Gamma_C \cup \Gamma_D$. As g increases further, the closed arc Γ_C shrinks and Γ_D becomes larger until g reaches the Read-Green line, where Γ_C disappears. Finally in the strong pairing phase there are only negative real roots. In Fig. 6 we display the types of arcs depending on the region of the phase diagram together with the exact numerical roots.

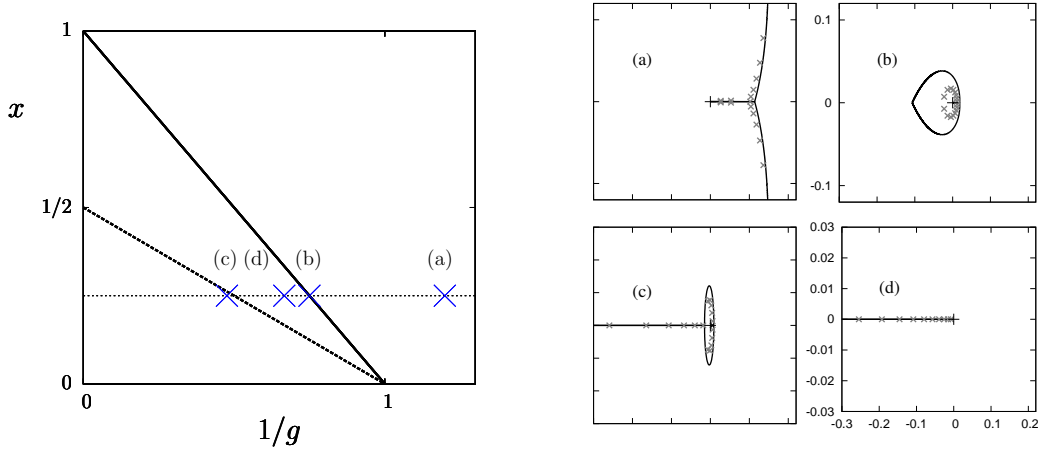


Figure 6: Representation of the electrostatic arcs in several regions of the phase diagram. The roots of the Bethe ansatz equations for $L = 64$ and $M = 16$ are also shown. For the four smaller figures, the same horizontal scale is used which is shown explicitly for case (d). Cases (a) and (b) have the same vertical scale, as do cases (c) and (d). We note that while the roots lie close to the electrostatic arc in cases (a), (c) and (d), the agreement is not as good in case (b) which lies near the Moore-Read line.

| Type | Reality | Topology | Parameters | Meaning |
|------------|---------|----------|---------------------------------------|-------------|
| Γ_A | real | open | $(0, \varepsilon_A) \subseteq \Omega$ | Fermi pairs |
| Γ_B | complex | open | $\epsilon \pm i\delta$ | BCS pairs |
| Γ_C | complex | closed | $\varepsilon_A, a = b$ | BCS pairs |
| Γ_D | real | open | $(a, b) \not\subseteq \Omega$ | BEC pairs |

Table 2: Classification of the arcs containing the roots of the Bethe ansatz equation (61).

| Phase | Γ |
|-------------------|--|
| Weak coupling BCS | $\Gamma_A \cup \Gamma_B$ |
| Moore-Read line | $\Gamma_A \cup \Gamma_C$ |
| Weak pairing | $\Gamma_A \cup \Gamma_C \cup \Gamma_D$ |
| Read-Green line | Γ_D |
| Strong pairing | Γ_D |

Table 3: Structure of the electrostatic arcs in the different phases of the $p + ip$ model.

Next we consider the solution of (61) in the different regions of the phase diagram.

4.2.2 Weak coupling BCS phase

In this region $\Gamma = \Gamma_A \cup \Gamma_B$, where $\Gamma_A = (0, \varepsilon_A)$, $\varepsilon_A < \omega$ and Γ_B is a complex arc with end points $\epsilon \pm i\delta$. In the continuum limit, the roots belonging to Γ_A lie between the z_k^2 . Recalling that the charge associated to the y_m is $+1$, while that associated to the z_k^2 is $-1/2$, one finds that the effect of the arc Γ_A can be taken into account by writing (61) as

$$-\int_0^{\varepsilon_A} d\varepsilon \frac{\rho(\varepsilon)}{\varepsilon - y} + \int_{\varepsilon_A}^{\omega} d\varepsilon \frac{\rho(\varepsilon)}{\varepsilon - y} - \frac{q_0}{y} - P \int_{\Gamma_B} |dy'| \frac{r(y')}{y' - y} = 0, \quad \forall y \in \Gamma_B. \quad (63)$$

To solve this equation we introduce a function $h(y)$ which is analytic outside Γ_B , Ω and 0 , and has a branch cut on the arc Γ_B , such that

$$r(y) |dy| = \frac{1}{2\pi i} (h_+(y) - h_-(y)) dy, \quad y \in \Gamma_B \quad (64)$$

where $h_+(y)$ and $h_-(y)$ are the limiting values of $h(y)$ to the right and left of Γ_B . The appropriate ansatz for $h(y)$ is

$$h(y) = R(y) \left[\int_0^\omega d\varepsilon \frac{\varphi(\varepsilon)}{\varepsilon - y} - \frac{Q}{y} \right] \quad (65)$$

where

$$R(y) = \sqrt{(y-a)(y-b)} = \sqrt{(y-\varepsilon)^2 + \delta^2} \quad (66)$$

such that $R(\varepsilon)$ is positive on the interval (ω_A, ω) and negative on $(0, \omega_A)$. In particular $R(0) < 0$. Using (64) one can write the last term of (63) as

$$P \int_{\Gamma_B} |dy'| \frac{r(y')}{y' - y} = \int_{L_B} \frac{dy'}{2\pi i} \frac{h(y')}{y' - y} \quad (67)$$

where L_B is a counterclockwise contour surrounding Γ_B . Plugging (65) into (67) and deforming the contour L_B around $\Omega, 0$ and ∞ one finds

$$\int_{L_B} \frac{dy'}{2\pi i} \frac{h(y')}{y' - y} = - \int_0^{\omega_A} d\varepsilon \frac{\varphi(\varepsilon) |R(\varepsilon)|}{\varepsilon - y} + \int_{\omega_A}^\omega d\varepsilon \frac{\varphi(\varepsilon) R(\varepsilon)}{\varepsilon - y} - \frac{Q R(0)}{y} - \int_0^\omega d\varepsilon \varphi(\varepsilon) - Q.$$

The solution of the electrostatic equation (63) is obtained with the choices

$$\varphi(\varepsilon) = \frac{\rho(\varepsilon)}{|R(\varepsilon)|}, \quad Q = \frac{q_0}{R(0)}, \quad \int_0^\omega d\varepsilon \frac{\rho(\varepsilon)}{|R(\varepsilon)|} = -Q = \frac{q_0}{|R(0)|}. \quad (68)$$

Observe that the last equation in (68) coincides, up to a rescaling of the variables, with the chemical potential equation (54) (use $|R(0)| = \sqrt{ab} = |\mu|$). In the s -wave model the analogue of (68) provides the gap equation. However for the $p + ip$ model the roles of the gap and chemical potential equations are reversed. To find the gap equation from the electrostatic model one has to compute the number of roots on the arc Γ :

$$M = \int_{\Gamma_A} |dy| r(y) + \int_{\Gamma_B} |dy| r(y) = 2 \int_0^{\varepsilon_A} d\varepsilon \rho(\varepsilon) + \int_{L_B} \frac{dy}{2\pi i} h(y) \quad (69)$$

Plugging (65) into (69) and deforming the contour L_B as done above, one finds

$$\frac{1}{2G} = \int_0^\omega d\varepsilon \frac{\varepsilon \rho(\varepsilon)}{\sqrt{(\varepsilon - \varepsilon)^2 + \delta^2}}$$

where we have also used (68). This is the gap equation (53). The energy of the solution can be computed from (62)

$$E = \int_{\Gamma_A} |dy| y r(y) + \int_{\Gamma_B} |dy| y r(y) = 2 \int_0^{\varepsilon_A} d\varepsilon \varepsilon \rho(\varepsilon) + \int_{L_B} \frac{dy}{2\pi i} y h(y). \quad (70)$$

As in the case of equation (68), we substitute (65) into (70) and after the contour deformation of L_B one finds

$$E = \int_0^\omega d\varepsilon \rho(\varepsilon) \varepsilon \left(1 - \frac{\varepsilon - \epsilon}{\sqrt{(\varepsilon - \epsilon)^2 + \delta^2}} \right) \quad (71)$$

in agreement with (55). This formula is similar to the one found for the s -wave model except for the fact that is missing a constant term $-\delta^2/4$ corresponding to the condensation energy [23, 55]. Finally, the equation for the arc Γ_B is given by the equipotential equation

$$\operatorname{Re} \left[\int_{\epsilon - i\delta}^y dy' h(y') \right] = 0, \quad y \in \Gamma_B$$

while the density of roots is

$$r(y) = \frac{1}{\pi} |h(y)|, \quad y \in \Gamma_B.$$

4.2.3 Moore–Read line

This case is reached when the arc Γ_B studied in the previous subsection closes, i.e. $\delta = 0$, so that $a = b = \epsilon$. The function $R(y)$ defined in eq. (66) becomes $R(y) = y - a$, so it no longer has a branch cut. To find the closed arc Γ_C one introduces an analytic function $s(y)$ satisfying

$$r(y) |dy| = s(y) dy, \quad y \in \Gamma_C.$$

The Bethe ansatz equation is similar to (63), i.e.

$$- \int_0^{\varepsilon_A} d\varepsilon \frac{\rho(\varepsilon)}{\varepsilon - y} + \int_{\varepsilon_A}^\omega d\varepsilon \frac{\rho(\varepsilon)}{\varepsilon - y} - \frac{q_0}{y} - P \int_{\Gamma_C} |dy'| \frac{r(y')}{y' - y} = 0, \quad \forall y \in \Gamma_C \quad (72)$$

where ε_A is the point where Γ_C cuts the positive real axis. The analogue of (67) is

$$P \int_{\Gamma_C} |dy'| \frac{r(y')}{y' - y} = \int_{\Gamma_C} dy' \frac{s(y')}{y' - y}, \quad (73)$$

where Γ_C is the counterclockwise contour containing the complex roots. To solve (72) we choose the following ansatz

$$s(y) = \frac{1}{i\pi} \left[\int_{\Omega} d\varepsilon \frac{\rho(\varepsilon)}{\varepsilon - y} + \frac{q_0}{y} \right] \quad (74)$$

which is motivated by the two level s -wave model where the roots form a closed loop when the coupling constant is less than half the distance between the two levels [23, 55]. Introducing (74) into (73) one can check that (72) holds (we use that $\int_{\Gamma_C} dy'/(y'-y) = i\pi$ for $y \in \Gamma_C$). The total number of roots M is given by

$$M = 2 \int_0^{\varepsilon_A} d\varepsilon \rho(\varepsilon) + \int_{\Gamma_C} dy s(y) = 2q_0 \implies x = 1 - \frac{1}{g}$$

which shows that the criterion for the Moore–Read line is reproduced. The chemical potential equation is equivalent to the vanishing of the potential $s(y)$ at the point a where Γ_C cuts the real axis, i.e.

$$q_0 = -a \int_0^\omega d\varepsilon \frac{\rho(\varepsilon)}{\varepsilon - a} \iff s(a) = 0.$$

The latter condition follows from continuity of the weak coupling case since the density of roots on the arc Γ_B also vanishes at the end points.

The equation of the arc Γ_C is given by

$$\text{Im} \left[\int_{y_0}^y dy' s(y') \right] = 0, \quad y \in \Gamma_C \quad (75)$$

where y_0 is a point of Γ_C which can be taken as a . Doing the integral one finds

$$\text{Re} \left[\int_\Omega d\varepsilon \rho(\varepsilon) \log \left(\frac{\varepsilon - y}{\varepsilon - y_0} \right) - q_0 \log \frac{y}{y_0} \right] = 0. \quad (76)$$

In 1D this equation becomes, in normalized variables (i.e. $y \rightarrow \omega y$)

$$\text{Re} \left[\sqrt{y} \log \left(\frac{\sqrt{y} + 1}{\sqrt{y} - 1} \right) - \sqrt{y_0} \log \left(\frac{\sqrt{y_0} + 1}{\sqrt{y_0} - 1} \right) + \log \left(\frac{y - 1}{y_0 - 1} \right) - \left(1 - \frac{1}{g}\right) \log \frac{y}{y_0} \right] = 0,$$

while in 2D it is

$$\text{Re} \left[-y \log \left(1 - \frac{1}{y} \right) + y_0 \log \left(1 - \frac{1}{y_0} \right) + \log \left(\frac{y - 1}{y_0 - 1} \right) - \left(1 - \frac{1}{g}\right) \log \frac{y}{y_0} \right] = 0.$$

These eqs. have two real solutions, corresponding to the intersections points of Γ_c with the real axis: $y_0 = a/\omega$ and $y = \varepsilon_A/\omega$. The total energy can be computed in a way similar to eq. (70) and the result is

$$E = 2 \int_0^{\varepsilon_A} d\varepsilon \varepsilon \rho(\varepsilon) + \int_{L_C} dy y s(y) = 0,$$

which agrees with the mean-field result (46). This result can also be obtained as a limit of eq.(71) by setting $\delta = 0$ and $\epsilon = a < 0$.

4.2.4 Weak pairing phase

This is the most complicated phase concerning the structure of the arc Γ which consists now of three pieces, $\Gamma = \Gamma_A \cup \Gamma_C \cup \Gamma_D$, where $\Gamma_A = (0, \varepsilon_A)$, $\Gamma_D = (a, b)$ and Γ_C is a closed arc that touches the points $\varepsilon_B = b$ and ε_A on the real line. Combining the results of the two previous cases we introduce a function $h(y)$ associated to the open arc Γ_D

$$h(y) = R(y) \left[\int_0^\omega d\varepsilon \frac{\varphi(\varepsilon)}{\varepsilon - y} - \frac{Q}{y} \right] \quad (77)$$

and a function $s(y)$ associated to the closed arc Γ_C , i.e.

$$s(y) = \frac{1}{i\pi} R(y) \left[\int_0^\omega d\varepsilon \frac{\varphi(\varepsilon)}{\varepsilon - y} - \frac{Q'}{y} \right], \quad (78)$$

where

$$R(y) = \sqrt{(y-a)(y-b)}, \quad a < b < 0$$

which is always positive for $\varepsilon \in \Omega$. The electrostatic equation (61) reads,

$$- \int_0^{\varepsilon_A} d\varepsilon \frac{\rho(\varepsilon)}{\varepsilon - y} + \int_{\varepsilon_A}^\omega d\varepsilon \frac{\rho(\varepsilon)}{\varepsilon - y} - \frac{q_0}{y} = \int_{L_D} \frac{dy'}{2\pi i} \frac{h(y')}{y' - y} + \int_{L_C} dy' \frac{s(y')}{y' - y}, \quad y \in \Gamma_C \text{ or } \Gamma_D$$

and it is solved by the ansatz (77, 78) provided

$$\varphi(\varepsilon) = \frac{\rho(\varepsilon)}{R(\varepsilon)}, \quad Q = -\frac{q_0}{R(0)}, \quad Q = Q' \quad (79)$$

and

$$\int_0^\omega d\varepsilon \frac{\rho(\varepsilon)}{R(\varepsilon)} = -Q = \frac{q_0}{R(0)}. \quad (80)$$

The last equation coincides with the chemical potential equation (54) since $\mu = R(0) = ab > 0$. On the other hand the gap eq.(53) is obtained from the counting of the number of roots M

$$M = 2 \int_0^{\varepsilon_A} d\varepsilon \rho(\varepsilon) + \int_{\Gamma_C} dy s(y) + \int_{L_D} \frac{dy}{2\pi i} h(y) \implies \int_0^\omega d\varepsilon \frac{\varepsilon \rho(\varepsilon)}{\sqrt{(\varepsilon-a)(\varepsilon-b)}} = \frac{1}{2G}. \quad (81)$$

The total energy is given by

$$\begin{aligned} E &= 2 \int_0^{\varepsilon_A} d\varepsilon \varepsilon \rho(\varepsilon) + \int_{\Gamma_C} dy y s(y) + \int_{L_D} \frac{dy}{2\pi i} y h(y) \\ &= \int_0^\omega d\varepsilon \rho(\varepsilon) \varepsilon \left(1 - \frac{\varepsilon - (a+b)/2}{\sqrt{(\varepsilon-a)(\varepsilon-b)}} \right) \end{aligned} \quad (82)$$

which coincides with (55). Finally the equation for the closed arc Γ_C is the same as (75) with $s(y)$ replaced by (78). The results obtained so far must reproduce those found earlier for the Moore-Read line. Indeed, if $a \rightarrow b$, one can check that the function $s(y)$ given in (78) coincides with (74).

4.2.5 Read–Green line

This case can be obtained from the previous one taking the limit $b \rightarrow 0$. One can easily prove that the number of roots on Γ_A and Γ_C is zero so that all the roots lie in the open arc Γ_D . The gap and chemical potential equations and energy are given by (80,81,82) setting $b = 0$. The criticality of this line can be seen from the fact that the function $R(\varepsilon)/2$, which is the mean-field energy of the excitations, vanishes as $\sqrt{\varepsilon} \propto |k|$ when $|k| \rightarrow 0$. Note that this also means that the density of roots is divergent at the origin, as can be deduced from (77).

4.2.6 Strong pairing phase

In this case all the roots lie on the open arc $\Gamma_D = (a, b)$ belonging to the negative real axis. As in the weak pairing phase we introduce the function $h(y)$ given by (77), so that the electrostatic equation becomes

$$\int_0^\omega d\varepsilon \frac{\rho(\varepsilon)}{\varepsilon - y} - \frac{q_0}{y} = \int_{L_D} \frac{dy'}{2\pi i} \frac{h(y')}{y' - y}, \quad y \in \Gamma_D.$$

The solution of this equation is provided by

$$\varphi(\varepsilon) = \frac{\rho(\varepsilon)}{R(\varepsilon)}, \quad Q = \frac{q_0}{R(0)}$$

and

$$\int_\Omega \varphi(\varepsilon) = -Q = \frac{|q|}{R(0)}.$$

Notice the change of sign of the equation for Q as compared to (79). Computing the number of roots on the arc gives the gap equation:

$$\frac{1}{2G} = \int_0^\omega d\varepsilon \frac{\varepsilon \rho(\varepsilon)}{\sqrt{(\varepsilon - a)(\varepsilon - b)}}.$$

The total energy is given by

$$E = \int_{L_D} \frac{dy}{2\pi i} y h(y) = \int_0^\omega d\varepsilon \rho(\varepsilon) \varepsilon \left(1 - \frac{\varepsilon - (a + b)/2}{\sqrt{(\varepsilon - a)(\varepsilon - b)}} \right).$$

4.3 Topological properties of the ground state

4.3.1 Dressing and duality

Above we established, through use of the electrostatic analogy, that the continuum limit of the Bethe ansatz equations for the ground state is in agreement with the mean-field solution. However with reference to Fig. 6, we see a noticeable discrepancy between the theoretical arc and the position of the roots near the Moore-Read line. Here we re-examine

the Bethe ansatz equations in the case of finite-sized systems to clarify some subtle issues about the nature of the ground state. Using an algebraic approach we will introduce the concept of dressing of states, which gives a different perspective on the duality that was seen in the mean-field analysis.

For a generic splitting of the set of roots Y into nonintersecting sets Y' and Z such that $Y = Y' \cup Z$, we can express the Bethe ansatz equations (23) as

$$\begin{aligned} G^{-1} - L + 2M - 1 + \sum_{k=1}^L \frac{y_m}{y_m - z_k^2} \\ = \sum_{y_j \in Y', y_j \neq y_m} \frac{2y_m}{y_m - y_j} + \sum_{y_j \in Z} \frac{2y_m}{y_m - y_j}, \quad y_m \in Y' \end{aligned} \quad (83)$$

$$\begin{aligned} G^{-1} - L + 2M - 1 + \sum_{k=1}^L \frac{y_m}{y_m - z_k^2} \\ = \sum_{y_j \in Z, y_j \neq y_m} \frac{2y_m}{y_m - y_j} + \sum_{y_j \in Y'} \frac{2y_m}{y_m - y_j}, \quad y_m \in Z. \end{aligned} \quad (84)$$

Setting $|Y'| = M'$ and $|Z| = P$ we take the sum over elements in Z in (84) to give

$$\begin{aligned} P(G^{-1} - L + 2M - 1) + \sum_{y_m \in Z} \sum_{k=1}^L \frac{y_m}{y_m - z_k^2} \\ = \sum_{y_j \in Z, y_m \in Z, y_j \neq y_m} \frac{2y_m}{y_m - y_j} + \sum_{y_j \in Y', y_m \in Z} \frac{2y_m}{y_m - y_j} \\ = P(P - 1) + \sum_{y_j \in Y', y_m \in Z} \frac{2y_m}{y_m - y_j} \end{aligned} \quad (85)$$

Suppose that at some limiting value of G we have

$$\begin{aligned} y_m &\neq 0 && \text{for all } y_m \in Y', \\ y_m &= 0 && \text{for all } y_m \in Z. \end{aligned}$$

Taking note that $M' + P = M$ equation (85) informs us that

$$P = G^{-1} - L + 2M \quad \Rightarrow \quad P = L - 2M' - G^{-1}, \quad (86)$$

while from (83) we obtain

$$\begin{aligned} G^{-1} - L + 2M - 1 + \sum_{k=1}^L \frac{y_m}{y_m - z_k^2} &= \sum_{y_j \in Y', y_j \neq y_m} \frac{2y_m}{y_m - y_j} + 2P, \quad y_m \in Y' \\ \Rightarrow G^{-1} - L + 2M' - 1 + \sum_{k=1}^L \frac{y_m}{y_m - z_k^2} &= \sum_{y_j \in A, y_j \neq y_m} \frac{2y_m}{y_m - y_j}, \quad y_m \in Y'. \end{aligned} \quad (87)$$

Equation (87) is simply the set of Bethe ansatz equations for a system of M' Cooper pairs. The above calculations suggest that given such a solution set Y' , we can augment it with P additional roots which all have zero value to obtain the solution set Y , provided that P is given by (86). It is important to check that this solution set is indeed valid for there

are known examples where the roots of the Bethe ansatz equations must be distinct, most noticeably the repulsive Bose gas [36].

A fairly straightforward calculation, using proof by induction, leads to the following commutator identity for H in the form (22)

$$[H, C^P(0)] = PQ^\dagger C^{P-1}(0)(GL - 1 - GP - 2GN) \quad (88)$$

where

$$Q^\dagger = \sum_{k=1}^L z_k b_k^\dagger.$$

If we partition the Hilbert space of states into subspaces defined by the eigenvalues M' of the Cooper pair number operator N , there exists a subspace on which the commutator (88) vanishes whenever $P = L - 2M' - G^{-1}$ which is precisely equation (86). That is to say given any eigenstate $|\phi(Y')\rangle$ with M' Cooper pairs, we can construct a new eigenstate $|\phi(Y)\rangle = C^P(0)|\phi(Y')\rangle$ of $M = M' + P$ Cooper pairs and the same energy as $|\phi(Y')\rangle$ provided (86) holds. Whenever this is the case we say that the state $|\phi(Y)\rangle$ is a *dressing* of the state $|\phi(Y')\rangle$.

To explore in more depth the consequences of this result, we first note that P must necessarily be a non-negative integer. In terms of the filling fraction $x' = M'/L$, non-negativity of P implies that

$$x' < \frac{1}{2} \left(1 - \frac{1}{g}\right)$$

so that the state $|\phi(Y')\rangle$ belongs to the strong pairing phase. Letting $x = M/L = (M' + P)/L$ denote the filling of the dressed state we find

$$x + x' = 1 - \frac{1}{g}$$

which is simply the duality relation (50) obtained from the mean-field theory. We can immediately conclude that $|\phi(Y)\rangle$ belongs to the weak pairing phase. However one significant point about this derivation of the duality is that it only applies in particular cases when the coupling g is *rational*. This aspect has some ramifications to which we will return later.

For the moment, we will consider a simple example of dressing. Starting with the sector of the Hilbert space where the number of Cooper pairs is zero there is only one state, that being the vacuum $|0\rangle$. We can dress this state with M additional Cooper pairs where, by equation (86), we must choose

$$M = P = L - G^{-1}. \quad (89)$$

There is no reason yet to expect that the dressed state will be the ground state in the sector with M Cooper pairs. However we do recognise that (89) is precisely the equation of the MR line (45) found from mean-field theory, for which the mean-field ground-state energy is zero. The dressed state will have the same energy as the vacuum, which is also zero. Performing the dressing gives us

$$C^M(0)|0\rangle = \left[\sum_{k=1}^L \frac{b_k^\dagger}{z_k} \right]^M |0\rangle = \left[\sum_{\mathbf{k} \in \mathbf{K}_+} \frac{c_{\mathbf{k}}^\dagger c_{-\mathbf{k}}^\dagger}{k_x + ik_y} \right]^M |0\rangle$$

which is precisely the MR state (43). Recall that the projected mean-field wavefunction gives the MR state as the ground state on the MR line with zero energy. We can show that this is indeed the ground-state. In fact, in all instances dressing a ground state in the strong pairing phase leads to a ground state in the weak pairing phase, which we now show follows from the Perron-Frobenius theorem.

By adding an appropriate constant term to (22) we obtain an operator with strictly negative entries for each sector of M' pairs. The Perron-Frobenius theorem tells us that the ground-state vector of this operator can be normalised such that all components of the vector are strictly positive. Applying the dressing operator $C^P(0)$ with P given by (86) to the ground-state of M' pairs leads to an eigenstate of (22) in the weak pairing phase, which also has strictly positive components. By the Perron-Frobenius theorem, this must be the ground state in the weak pairing phase for $M' + P$ pairs.

It is of importance to compare this result with the previous discussions of the solution in the thermodynamic limit described in Subsection 4.2. There, it was concluded that on the MR line the ground-state roots formed a closed arc in the complex plane. In the finite system, we have now found that all ground-state roots are zero on the MR line. In both instances the ground-state energy was found to be zero. One way to resolve this apparent contradiction would be to suggest that the assumption used in Subsection 4.2, viz. that in the thermodynamic limit the ground-state roots form a dense arc in complex plane, was not valid. To investigate this matter further we next turn our attentions to the numerical solution of the Bethe ansatz equations.

4.3.2 Numerical solution of the Bethe ansatz equations for finite systems

First we will discuss the behaviour of the roots in the three different regions. Later we will discuss properties across all regions. The numerical solutions of the Bethe ansatz equations are obtained starting from the initial condition $y_m \rightarrow (1+G)\mathbf{k}^2$ ($m = 1, \dots, M$) as $G \rightarrow 0$, with the \mathbf{k} chosen to fill the Fermi sea. As g increases, the roots y_m , closest to the Fermi level become complex pairs. When g approaches the MR-line the roots bend towards the origin, and at the value $x = x_{MR}$ all the roots collapse onto the origin. At larger values of g one enters the weak pairing phase where all the roots are non-zero, except at some rational values of g where a fraction of the roots collapse again. Finally, in the strong pairing regime all the roots become real and they belong to the interval (a, b) on the negative real axis. The RG-line is obtained when $b = 0$, in which case the quasiparticle energy (39) becomes gapless.

In the weak coupling regime the parameters a, b appearing in (47) give the end points of the complex arcs shown in Figs. 7(a) - 7(d) for the 1D and 2D models (recall Table 1). On the MR line a and b become real and equal, giving $E = 0$ from (48), and the complex arc closes satisfying eq. (76).

Fig. 7(e) shows how the roots approach this closed arc for increasing values of M at $g = 1.99$ and $x = 1/2$. For $g = 2$ and $x = M/L = 1/2$ (MR line) all roots collapse to the origin in any finite system. The continuous arc is the solution of eq. (76) corresponding to $g = 2, x = 1/2$, where $L \rightarrow \infty$ is taken before $g \rightarrow 2$. However the exact solution of the Bethe ansatz equations (29) is $y_m = 0, \forall m$, exactly giving the Moore-Read state [49] $C(0)^M|0\rangle$ which also has total energy $E = 0$. In Fig. 7(f) we plot the real part of the Bethe ansatz equations roots for a 2D momentum distribution in a system with $M = 8, L = 32$. The Moore-Read points, in which all the roots collapse to zero, are clearly noticeable. This fact presents a paradoxical situation where the thermodynamic limit does not commute with the limit where the coupling g approaches the MR line from

the weak coupling BCS phase.

In the strong pairing phase we expect from the calculations in the continuum limit that the ground-state roots should be real and negative. Moreover, the Perron-Frobenius theorem indicates that there can only be one such set of roots with this property. This fact makes the numerical analysis of the ground-state roots fairly efficient in the strong pairing phase, since the solution converges quickly to the unique real and negative solution set. In all instances we considered we always found a numerical solution set of real and negative roots in this phase.

To illustrate the results for this phase we define the discrete root density to be

$$r(y_j) = \frac{1}{(M-1)(y_{j+1} - y_j)}. \quad (90)$$

which we have plotted in Fig. 8 for a system with $L = 450$ and $M = 150$. The results compare the cases $g = 3$, the Read-Green line, and $g = 20$. As discussed in Subsection 4.2.6 the continuum limit of the Bethe ansatz equations predicts a divergence in the root density at the origin when the coupling is on the Read-Green line. The numerical results support this picture with the value of the root density at the origin for $g = 3$ several times larger than for $g = 20$.

In Fig. 9 we plot the exact and mean-field energy of the ground state of a 2D system, showing results for the two filling fractions $x = 1/2, 1/4$. Observe that at the MR coupling the exact and mean-field energies coincide, i.e. $E = 0$. For $x = 1/4$ there is a departure between the exact and mean-field results in the strong pairing phase, which disappears for large systems.

In Fig. 10(a) we plot the expectation values of the Cooper pair density $\langle N_n \rangle$ (using 117 in Appendix A.2). In Fig. 10(b) we plot the exact and mean-field values of the the fluctuation parameter C defined as

$$C = \frac{1}{L} \sum_{j=1}^L (\langle N_j \rangle - \langle N_j \rangle^2). \quad (91)$$

In both of these instances there is reasonably good agreement between the mean-field and the exact results.

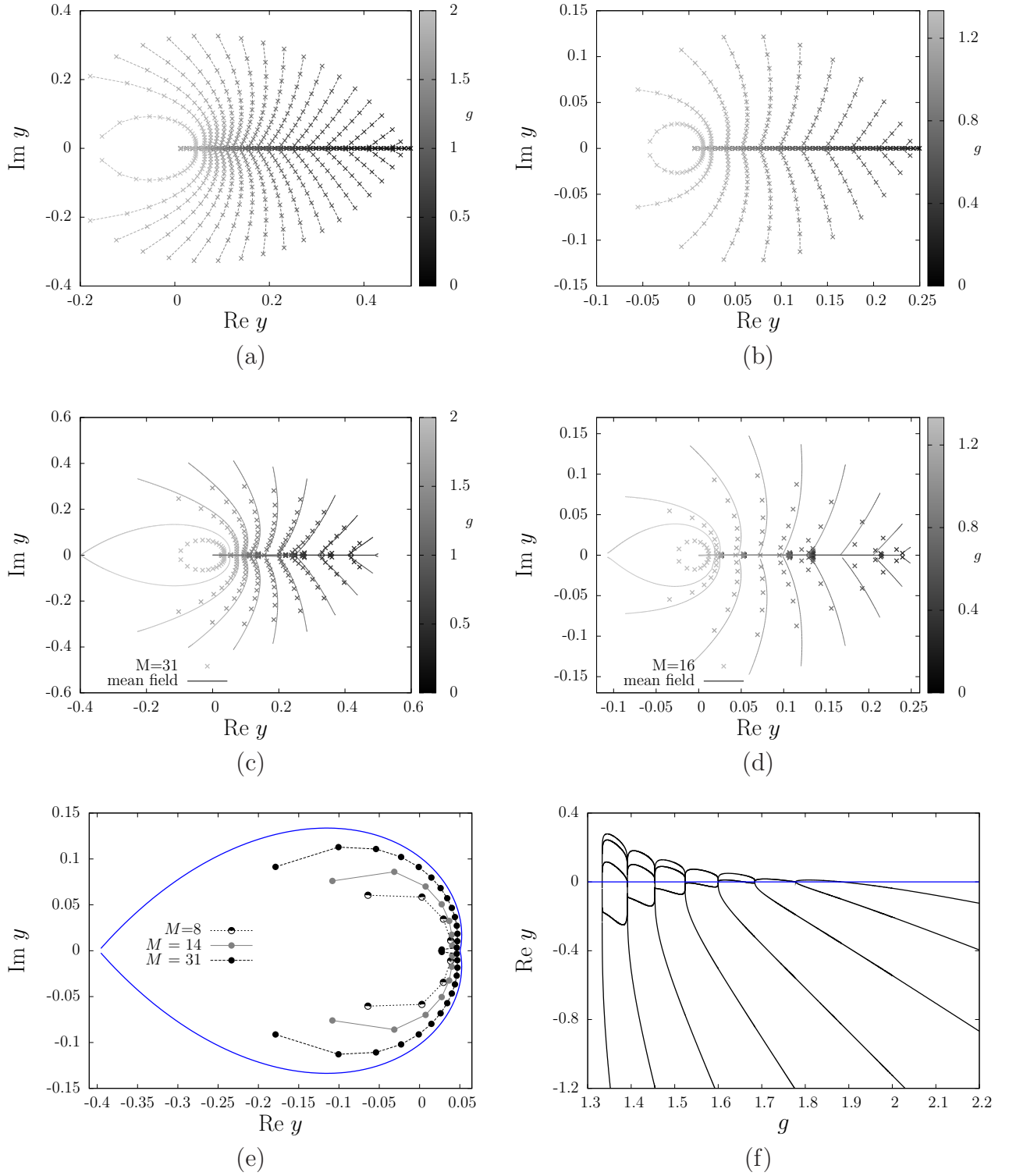


Figure 7: Real and imaginary parts of the roots of the Bethe ansatz equations in several regimes for several values of the coupling constant g . In the cases (c,d,e) the corresponding electrostatic arcs are also shown: (a) 1D model, $M = 31, L = 62$, (b) 1D model, $M = 16, L = 64$, (c) 2D model, $M = 31, L = 62$, (d) 2D model, $M = 16, L = 64$ (e) 2D model, $g = 1.99, M = 8, 14, 31, L = 2M$. Notice that the MR point is $g = 2, x = 1/2$. (f) Real part of the Bethe ansatz equation roots for 2D momentum distribution with $M = 8, L = 32$. The range of g covers both the weak pairing and strong pairing phases. The dressing points, in which some of the roots collapse to zero, can be seen to occur at regular intervals between $g_{MR} = 4/3$ and $g_{RG} = 2$.

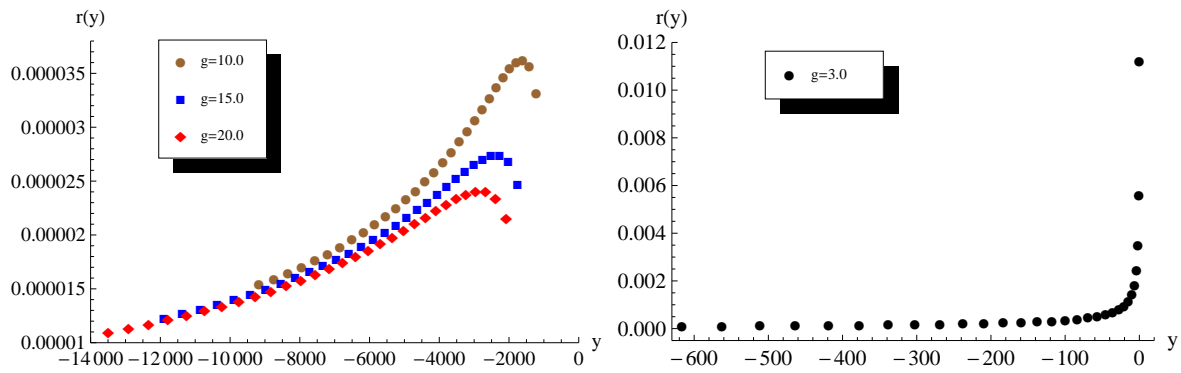


Figure 8: Discrete root densities as given by (90) for $L = 450$ and $M = 150$. The momenta have been chosen as $|\mathbf{k}| = m$, $m = 1, \dots, 450$. The left graph shows results for the coupling choices $g = 10, 15, 20$, which correspond to the strong pairing phase. The support of the discrete root density lies on the negative real axis, and in each case the maximum value does not occur at the endpoint. For comparison, the right graph shows analogous results for $g = 3$ corresponding to the Read–Green line. Here the maximum value of the discrete root density occurs at the endpoint of the support at $y = 0$. Note also the different scale for the vertical axis.

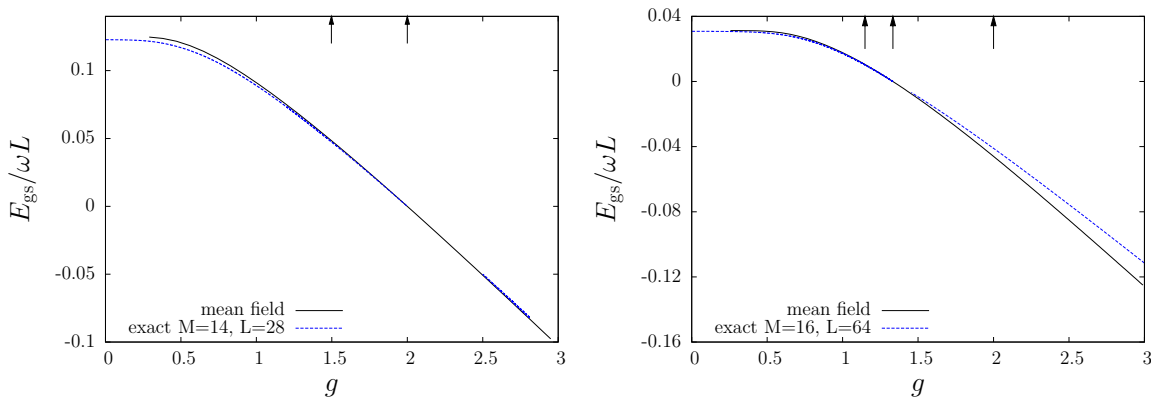


Figure 9: Comparison between the exact and mean-field ground state energy in 2D for $x = 1/2$, $M = 14$, $L = 28$ (left) and $x = 1/4$, $M = 16$, $L = 64$ (right). The arrows indicate, from left to right, the values of the coupling g corresponding to the Volovik, Moore-Read and Read-Green lines. For $x = 1/2$ the latter point is absent.

4.3.3 A zeroth-order quantum phase transition

We have already observed that the MR line has the peculiar property that the behaviour of the roots of the Bethe ansatz equations in the limits $g \rightarrow g_{MR}$, $L \rightarrow \infty$ depends on the order in which the limits are taken. Another curious property of the MR line is the discontinuity of the ground-state energy $E(g, x)$ in the thermodynamic limit as the filling fraction x approaches the value x_{MR} from the weak pairing region. To derive this result, for finite L we take the one-pair state and dress it to give the dual GS in the weak pairing region. The filling x_I of the dressed state is given by (50), setting $x_{II} = 1/L$, i.e. $x_I = x_{MR} - 1/L$, which approaches $x_{MR} = 1 - 1/g$ as $L \rightarrow \infty$. Since the MR pairs carry no energy, the ground-state energy of the dressed state coincides with the one-pair energy. To compute this energy we consider the Bethe ansatz equation for one Cooper

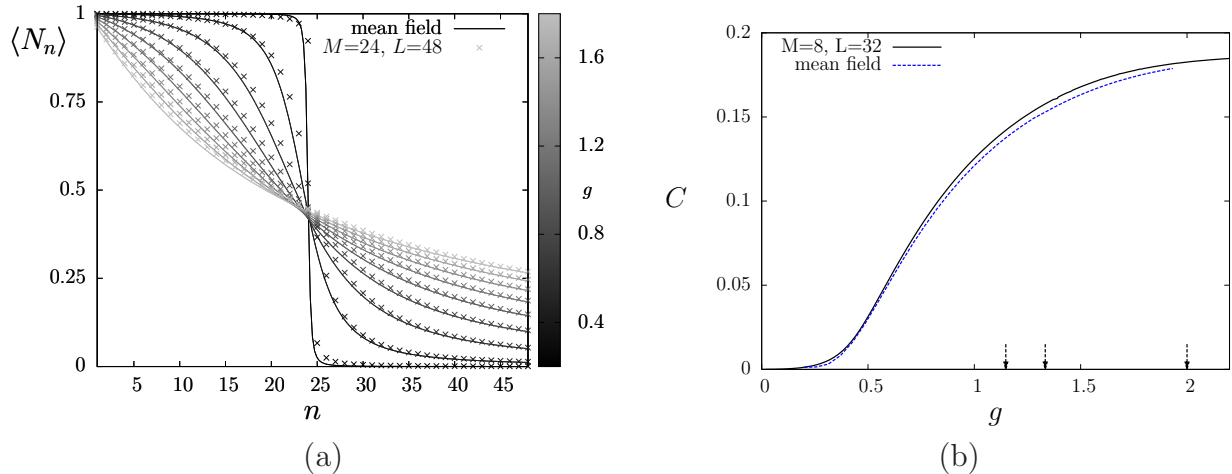


Figure 10: a) Cooper pair expectation values of the n -th level, $\langle N_n \rangle$, for a 2D momentum distribution system with $M = 24$, $L = 48$, for several values of g . The values of g corresponding to the weak coupling BCS phase. The mean-field counterpart of this magnitude is also shown for each value of g and $x=1/2$ (continuous lines). (b) The parameter C as given by (91), measuring fluctuations of the expected value of the occupation number is plotted as a function of g . Results are shown using the roots of the Bethe ansatz equations for a $M=8$, $L=32$ system, and for mean-field case in the continuum limit with $x = 1/4$. The arrows indicate the Volovik, Moore-Read and Read-Green points.

pair and take the continuum limit (i.e. eq. (29) with $M = 1$). For simplicity we take the momentum distribution to be that for free particles in 2D, i.e. $\rho(\varepsilon) = L/\omega$. This leads to

$$L - \frac{1}{G} - 1 = \sum_{\mathbf{k} \in \mathbf{K}_+} \frac{y}{y - \mathbf{k}^2} \implies 1 - \frac{1}{g} = y \int_0^\omega \frac{d\varepsilon}{\omega} \frac{1}{y - \varepsilon}.$$

This equation has a unique negative energy solution $y < 0$ satisfying

$$1 - \frac{1}{g} = \frac{y}{\omega} \log \left(\frac{y}{y - \omega} \right)$$

which we denote as $y = \mathcal{E}(g)$. From here one derives the aforementioned discontinuity on the MR line $x_{MR} = 1 - g^{-1}$,

$$\lim_{L \rightarrow \infty} E(g, x_I) = \mathcal{E}(g) \neq E(g, x_{MR}) = 0$$

which may reasonably be termed a zeroth-order quantum phase transition. We note that in thermodynamic systems analogous zeroth-order transitions have been discussed in [10, 13, 48].

All of the above considerations point towards the MR line signifying a phase boundary which has significantly different properties to the RG line. In the latter case, both the excitation spectrum is gapless and the mean-field fidelity susceptibility is divergent. These are not properties associated with the MR line.

4.3.4 Winding number of wavefunctions

Here we formulate a description of the three phases in terms of the ground-state wavefunction topology. To this end we will use a winding number approach.

Let us consider a continuous map $S^2 \rightarrow S^2$, given by a function $\mathbf{g} : (X, Y) \rightarrow (\mathbf{g}_X, \mathbf{g}_Y)$ where (X, Y) and $(\mathbf{g}_X, \mathbf{g}_Y)$ are the stereographic coordinates of the spheres. The winding number is defined as

$$w = \frac{1}{\pi} \int \frac{d\mathbf{g}_X d\mathbf{g}_Y}{(1 + \mathbf{g}_X^2 + \mathbf{g}_Y^2)^2} = \frac{1}{\pi} \int_{\mathbb{R}^2} dX dY \frac{\partial J(\mathbf{g}_X, \mathbf{g}_Y)}{\partial(X, Y)} \frac{1}{(1 + \mathbf{g}_X^2 + \mathbf{g}_Y^2)^2} \quad (92)$$

The function $\frac{\partial J(\mathbf{g}_X, \mathbf{g}_Y)}{\partial(X, Y)}$ is the Jacobian of \mathbf{g} . An alternative way to write (92) is

$$w = \frac{1}{\pi} \int_{\mathbb{R}^2} dX dY \left(\frac{\partial \mathbf{g}}{\partial z} \frac{\partial \bar{\mathbf{g}}}{\partial \bar{z}} - \frac{\partial \mathbf{g}}{\partial \bar{z}} \frac{\partial \bar{\mathbf{g}}}{\partial z} \right) \frac{1}{(1 + \mathbf{g}\bar{\mathbf{g}})^2} \quad (93)$$

where $\mathbf{g} = \mathbf{g}_X + i\mathbf{g}_Y$ and $z = X + iY$.

To start, we consider the exact eigenstate of (19) for one Cooper pair, as given by (28). In the limit $L \rightarrow \infty$ with one Cooper pair there are only two ground-state phases, the weak coupling BCS phase and the strong pairing phase, with the transition point given by $g = 1$ at which the ground-state energy is zero. In first quantized formulation we have that the momentum-space wavefunction is

$$\mathbf{g}(\mathbf{k}) = \frac{k_x - ik_y}{\mathbf{k}^2 - E}$$

where E denotes the energy. In terms of the complex variable $z = k_x + ik_y$, the Jacobian is given by

$$J = \frac{\partial \mathbf{g}}{\partial z} \frac{\partial \bar{\mathbf{g}}}{\partial \bar{z}} - \frac{\partial \mathbf{g}}{\partial \bar{z}} \frac{\partial \bar{\mathbf{g}}}{\partial z} = \frac{(z\bar{z})^2 - E\bar{E}}{(z\bar{z} - E)^2(z\bar{z} - \bar{E})^2}.$$

The winding number is then obtained as

$$\begin{aligned} w &= \frac{1}{\pi} \int_{\mathbb{R}^2} dk_x dk_y \frac{(z\bar{z})^2 - E\bar{E}}{[z\bar{z} + (z\bar{z} - E)(z\bar{z} - \bar{E})]^2} \\ &= \int_0^\infty du \frac{u^2 - E\bar{E}}{[u + (u - E)(u - \bar{E})]^2} \\ &= - \left[\frac{u}{u - (E + \bar{E})u + u^2 + E\bar{E}} \right]_0^\infty \end{aligned}$$

which yields

$$w = \begin{cases} 1, & E = 0, \\ 0, & E \neq 0. \end{cases} \quad (94)$$

In this manner we find a topological change in the wavefunction when the energy is zero, or equivalently $g = 1$, consistent with the phase diagram Fig. 2. However in both the weak coupling BCS phase and the strong pairing phase the wavefunction topology is trivial.

It is useful to contrast the above with the analogous result for the mean-field wavefunction. Up to a factor of $\hat{\Delta}^*$ which can be omitted, we have from (41,47)

$$\mathbf{g}(z, \bar{z}) = \frac{e(z, \bar{z}) - z\bar{z} + \mu}{z}, \quad e(z, \bar{z}) = \sqrt{(z\bar{z} - a)(z\bar{z} - b)}$$

where $\mu^2 = ab$. The Jacobian is given by

$$J = \frac{1}{(2z\bar{z} e(z, \bar{z}))^2} \left[((a + b)z\bar{z} - 2ab - 2\mu e(z, \bar{z}))^2 - (z\bar{z})^2 (2z\bar{z} - a - b - 2e(z, \bar{z}))^2 \right].$$

We have found numerically that

$$w = \begin{cases} 1, & \mu > 0, \\ a/(a-1), & \mu = 0, \\ 0, & \mu < 0 \end{cases} \quad (95)$$

where $\mu = 0$ corresponds to a choice $a < 0, b = 0$. In this case the winding number is not an integer at $\mu = 0$. The reason for this is that setting $\mu = 0$ gives

$$\mathbf{g}(z, \bar{z}) = \sqrt{\frac{\bar{z}}{z}} (\sqrt{z\bar{z} - a} - \sqrt{z\bar{z}})$$

which is not continuous at $z = 0$. The above shows very different topological predictions between the exact wavefunction and the mean-field wavefunction, specifically with the mean-field wavefunction having non-trivial topology in the weak coupling BCS phase.

To gain a further understanding of the many-body system, next we consider the exact wavefunction for two Cooper pairs:

$$\psi(z_1, \bar{z}_1, z_2, \bar{z}_2) = \begin{cases} \mathbf{g}(z_1, \bar{z}_1, E_1)\mathbf{g}(z_2, \bar{z}_2, E_2) + \mathbf{g}(z_1, \bar{z}_1, E_2)\mathbf{g}(z_2, \bar{z}_2, E_1), & z_1 \neq z_2, \\ 0, & z_1 = z_2 \end{cases} \quad (96)$$

where $\mathbf{g}(z, \bar{z}, E)$ is the one-pair wavefunction and E_1, E_2 are roots of the Bethe ansatz equations (30), which can either be real or a complex conjugate pair. In order to apply the winding number approach described above we reduce (96) to a complex-valued function by setting

$$\mathbf{g}(z, E_1, E_2, c) = \mathbf{g}(z, E_2, E_1, c) = \psi(z, z + c, E_1, E_2)$$

for some $c \neq 0$. Numerically we find

$$w = \begin{cases} 2, & E_1 = 0, \quad E_2 = 0, \\ 1, & E_1 = 0, \quad E_2 \neq 0, \\ 0, & E_1 \neq 0, \quad E_2 \neq 0. \end{cases}$$

This result shows that the winding number coincides with the number of MR pairs. Equation (93) is given an interesting interpretation if we parameterize $\mathbf{g}(z, \bar{z})$ as in the BCS model

$$\mathbf{g}(z, \bar{z}) = \frac{v(z, \bar{z})}{u(z, \bar{z})}, \quad u(z, \bar{z})\bar{u}(z, \bar{z}) + v(z, \bar{z})\bar{v}(z, \bar{z}) = 1$$

where u and v are well defined functions in the complex plane. It can be shown that

$$w = \frac{1}{2\pi i} \int_{\mathbb{R}^2} dX dY [\partial_X(\bar{u} \partial_Y u + \bar{v} \partial_Y v) - \partial_Y(\bar{u} \partial_X u + \bar{v} \partial_X v)]. \quad (97)$$

and from the Gauss theorem

$$w = \lim_{r \rightarrow \infty} \int_0^{2\pi} \frac{d\theta}{2\pi i} (\bar{u} \partial_\theta u + \bar{v} \partial_\theta v) \quad (98)$$

where $X + iY = re^{i\theta}$. This expression indicates that w measures the angular dependence of the wave function $\mathbf{g}(z, \bar{z})$. The result (95) for the BCS wavefunction can be derived

analytically from (98), by noticing that the proper definition of u and v depend on the sign of the chemical potential, i.e.

$$\begin{aligned} u &= \frac{z\Delta}{\sqrt{2e(z, \bar{z})(e(z, \bar{z}) - z\bar{z} + \mu)}}, & v &= \sqrt{\frac{e(z, \bar{z}) - z\bar{z} + \mu}{2e(z, \bar{z})}}, & \mu > 0, \\ u &= \sqrt{\frac{e(z, \bar{z}) + z\bar{z} - \mu}{2e(z, \bar{z})}}, & v &= \frac{\bar{z}\Delta}{\sqrt{2e(z, \bar{z})(e(z, \bar{z}) + z\bar{z} - \mu)}}, & \mu < 0 \end{aligned}$$

which leads to

$$w = \lim_{r \rightarrow \infty} |u(r, 0)|^2 = 1, \quad \mu > 0, \quad w = - \lim_{r \rightarrow \infty} |v(r, 0)|^2 = 0, \quad \mu < 0.$$

Similarly, equation (94) can be derived from (98) using the following expression of the u and v functions corresponding to the one pair wavefunction

$$\begin{aligned} u &= \frac{z}{\sqrt{1 + z\bar{z}}}, & v &= \frac{1}{\sqrt{1 + z\bar{z}}}, & E &= 0, \\ u &= \frac{z\bar{z} - E}{\sqrt{|z\bar{z} - E|^2 + z\bar{z}}}, & v &= \frac{\bar{z}}{\sqrt{|z\bar{z} - E|^2 + z\bar{z}}}, & E &\neq 0. \end{aligned}$$

In the general case of an exact wavefunction with M pairs, having P vanishing rapidities, the asymptotic expression of u and v immediately yields the expected value of w , i.e.

$$u \sim z^M \bar{z}^{M-P}, \quad v \sim \bar{z}^{M-P} \implies w = P.$$

This result shows that non-trivial topology of the wavefunction can only be found in the weak pairing phase.

As a final comment we note that the winding number w appears in a completely different context, namely the $O(3)$ non-linear sigma model in 2D. The order parameter of the latter model is a three component unit vector \vec{n} , which can be constructed out of the two component spinor $\psi = (u, v)$, as $\vec{n} = \psi^\dagger \vec{\sigma} \psi$. Using this parametrization the winding number w can be written as

$$w = \frac{1}{8\pi} \int_{\mathbb{R}^2} d^2\mathbf{x} \quad \vec{n} \cdot (\partial_\mu \vec{n} \times \partial_\nu \vec{n}) \epsilon^{\mu\nu}$$

where $\epsilon^{\mu\nu}$ is the 2D Levi-Civita tensor. This term appears in the action of the $O(3)$ non-linear sigma model multiplied by a parameter θ , which is defined modulo 2π . In a famous work, Haldane mapped the 1D antiferromagnetic Heisenberg model of spin S into the $O(3)$ non-linear sigma model with $\theta = 2\pi S$ [30]. The gapped nature of the integer spin chains then follows from the gapped nature of the non-linear sigma model with $\theta = 0 \pmod{2\pi}$.

4.4 Vortex wavefunctions

So far we have discussed the $p + ip$ model for a constant value of the order parameter Δ , which describes the system in the bulk. It is however of interest to study the effect of vortices. As shown by Read and Green [53] there are vortices with zero energy when the chemical potential μ is positive. We shall show below that the structure of the vortex wavefunction for $\mu > 0$ depends on the region of the phase diagram, with different behaviours in the weak coupling BCS and weak pairing regimes. However the transition between these two regimes is smooth in the mean-field analysis.

We shall consider the Bogoliubov-de Gennes (BdG) equations in the simplest situation of a single vortex with rotational invariance characterized by an order parameter

$$\Delta(\mathbf{r}) = ie^{il\varphi} |\Delta(r)|$$

where l is the vorticity and r, φ are the polar coordinates centered on the vortex. (We shall closely follow the results of references [29, 53, 59] with the appropriate notational changes: the mass is equal to 1, the gap Δ and the chemical potential in this paper are twice those considered in the cited references.) The BdG equations are a set of coupled equations for the functions $u_n(\mathbf{r}), v_n(\mathbf{r})$, corresponding to energies E_n , which determine the Bogoliubov quasiparticle operators γ_n by

$$\gamma_n = \int d^2r [u_n^*(\mathbf{r})a(\mathbf{r}) + v_n^*(\mathbf{r})a^\dagger(\mathbf{r})]$$

where $a(\mathbf{r}), a^\dagger(\mathbf{r})$ are annihilation and creation operators of polarised electrons. The zero energy solutions, i.e. $E_n = 0$, can be chosen to satisfy the reality condition $u_n(\mathbf{r}) = v_n(\mathbf{r})$, in which case the quasiparticle operator γ_n corresponds to a Majorana fermion. For odd vorticity, $l = 2n - 1$, the BdG equation for $u(\mathbf{r})$ can be most conveniently written in terms of a function $\chi(r)$ defined through

$$u(\mathbf{r}) = \chi(r) \exp\left(-\frac{1}{2} \int_0^r dr' |\Delta(r')|\right)$$

and it reads

$$-\chi'' - \frac{\chi'}{r} + \left(\frac{|\Delta^2(r)|}{4} + \frac{n^2}{r^2}\right) \chi = \mu \chi.$$

Let us suppose that the order parameter $|\Delta(r)|$ vanishes inside a core of radius a and that it reaches its bulk value, Δ_0 , outside i.e.

$$|\Delta(r)| = \begin{cases} 0, & 0 < r < a, \\ \Delta_0, & a < r < \infty. \end{cases}$$

The previous equation becomes

$$\begin{aligned} r^2 \chi'' + r \chi' + [\mu r^2 - n^2] \chi &= 0, & 0 < r < a, \\ r^2 \chi'' + r \chi' + \left[\left(\mu - \frac{\Delta_0^2}{4}\right) r^2 - n^2\right] \chi &= 0, & a < r < \infty. \end{aligned} \quad (99)$$

Notice that the coefficient multiplying the r^2 term in the second equation changes sign when crossing the MR line $\mu = \Delta_0^2/4$. This fact leads to two different type of equations corresponding to the weak coupling and weak pairing regimes. (We do not consider the strong coupling regime where the vortices have a trivial topological structure [29, 53, 59].)

4.4.1 Weak coupling BCS phase

For the weak coupling BCS phase $\mu > \Delta_0^2/4$ we make the change of variables

$$\mu = k_0^2, \quad \mu - \frac{\Delta_0^2}{4} = k^2,$$

Eq. (99) becomes

$$\begin{aligned} x^2 \chi_{xx} + x \chi_x + [x^2 - n^2] \chi &= 0, & x = k_0 r, & & 0 < r < a \\ y^2 \chi_{yy} + y \chi_y + [y^2 - n^2] \chi &= 0, & y = kr, & & a < r < \infty \end{aligned}$$

whose solutions are Bessel functions. Let us denote by I and II the regions $0 < r < a$ and $a < r < \infty$ respectively. Imposing that χ is regular at $r = 0$ and infinity one has

$$\begin{aligned}\chi_I &= AJ_n(k_0r), \\ \chi_{II} &= BJ_n(kr) + CY_n(kr).\end{aligned}$$

The constants A, B, C are found by matching the function $u(r)$ and its derivative $u'(r)$ at the boundary $r = a$. The relation between u and χ in the regions I and II is

$$\begin{aligned}u_I(r) &= \chi_I(r), \\ u_{II}(r) &= \chi_{II}(r)e^{-\Delta_0 r/2}.\end{aligned}\tag{100}$$

Hence

$$\begin{aligned}u_I(a) &= u_{II}(a) \implies \chi_I(a) = \chi_{II}(a)e^{-a\Delta_0/2}, \\ u'_I(a) &= u'_{II}(a) \implies \chi'_I(a) = (\chi'_{II}(a) - \frac{\Delta_0}{2}\chi_{II}(a))e^{-a\Delta_0/2}.\end{aligned}$$

Combining these two equations one can write

$$\begin{aligned}\chi_I(a) &= \chi_{II}(a)e^{-a\Delta_0/2}, \\ \chi'_I(a) + \frac{\Delta_0}{2}\chi_I(a) &= \chi'_{II}(a)e^{-a\Delta_0/2}\end{aligned}$$

with the explicit expressions

$$\begin{aligned}AJ_n(k_0a) &= (BJ_n(ka) + CY_n(ka))e^{-a\Delta_0/2}, \\ A\left(k_0J'_n(k_0a) + \frac{\Delta_0}{2}J_n(k_0a)\right) &= k(BJ'_n(ka) + CY'_n(ka))e^{-a\Delta_0/2}.\end{aligned}$$

This then leads to

$$\begin{aligned}\frac{B}{A} &= \frac{1}{2}a\pi e^{a\Delta_0/2} \left[kY'_n(ka)J_n(k_0a) - Y_n(ka) \left(k_0J'_n(k_0a) + \frac{\Delta_0}{2}J_n(k_0a) \right) \right], \\ \frac{C}{A} &= \frac{1}{2}a\pi e^{a\Delta_0/2} \left[-kJ'_n(ka)J_n(k_0a) + J_n(ka) \left(k_0J'_n(k_0a) + \frac{\Delta_0}{2}J_n(k_0a) \right) \right].\end{aligned}$$

For an infinitesimal core, $a \rightarrow 0$, the zero mode is localized on an isolated vortex with wavefunction

$$u(r) = J_n(kr) e^{-\Delta_0 r/2}, \quad r > 0 \quad (\mu > \Delta_0^2/4).$$

This result reproduces the one found by Gurarie and Radzihovsky [29]. The function $u(r)$ has an oscillatory and decaying asymptotic behaviour dominated by Δ_0 , i.e.

$$u(r) \sim \frac{\cos(kr + \phi_0)}{\sqrt{r}} e^{-r\Delta_0/2}, \quad r \rightarrow \infty.$$

4.4.2 Weak pairing phase

To study the weak pairing case $0 < \mu < \Delta_0^2/4$ we make the change of variables

$$\mu = k_0^2, \quad -\mu + \frac{\Delta_0^2}{4} = k^2,$$

which corresponds to the replacement $k \rightarrow ik$ in the previous case. The equation for χ becomes

$$\begin{aligned} x^2 \chi_{xx} + x \chi_x + [x^2 - n^2] \chi &= 0, & x = k_0 r, & & 0 < r < a, \\ y^2 \chi_{yy} + y \chi_y - [y^2 + n^2] \chi &= 0, & y = kr, & & a < r < \infty. \end{aligned}$$

whose solutions are Bessel functions in region *I* and modified Bessel functions in region *II*:

$$\begin{aligned} \chi_I &= A J_n(k_0 r), \\ \chi_{II} &= B I_n(kr) + C K_n(kr). \end{aligned}$$

The computation of A, B, C is similar to the previous one. The final solution is

$$\begin{aligned} \frac{B}{A} &= -a e^{a \Delta_0/2} \left[k K'_n(ka) J_n(k_0 a) - K_n(ka) \left(k_0 J'_n(k_0 a) + \frac{\Delta_0}{2} J_n(k_0 a) \right) \right], \\ \frac{C}{A} &= -a e^{a \Delta_0/2} \left[-k I'_n(ka) J_n(k_0 a) + I_n(ka) \left(k_0 J'_n(k_0 a) + \frac{\Delta_0}{2} J_n(k_0 a) \right) \right]. \end{aligned} \quad (101)$$

In the limit $a \rightarrow 0$ one obtains

$$u(r) = I_n(kr) e^{-\Delta_0 r/2}, \quad r > 0 \quad (\mu < \Delta_0^2/4)$$

in agreement with [29]. It is important to notice that the exponential factor $e^{-\Delta_0 r/2}$ in equation (100) is essential to get a convergent asymptotic behaviour of $u(r)$. Assuming that the coefficient B , given in eq. (101), is non zero one finds for $B \neq 0$

$$u(r) \sim \frac{1}{\sqrt{r}} \exp \left[-r \left(\frac{\Delta_0}{2} - \sqrt{\frac{\Delta_0^2}{4} - \mu} \right) \right], \quad r \rightarrow \infty,$$

while if $B = 0$, the asymptotic behaviour of $u(r)$ changes to

$$u(r) \sim \frac{1}{\sqrt{r}} \exp \left[-r \left(\frac{\Delta_0}{2} + \sqrt{\frac{\Delta_0^2}{4} - \mu} \right) \right], \quad r \rightarrow \infty.$$

which is a more localized vortex. The condition for this to happen is

$$B = 0 \implies k \frac{K'_n(ka)}{K_n(ka)} - k_0 \frac{J'_n(k_0 a)}{J_n(k_0 a)} = \frac{\Delta_0}{2}. \quad (102)$$

This equation has an infinite number of solutions for a as a function of μ and Δ_0 . In the case where $ka, k_0 a \gg 1$, the solutions of eq. (102) are

$$k_0 a \sim \frac{\pi}{4} + \frac{n\pi}{2} + \arctan \left(\frac{k + \Delta_0/2}{k_0} \right) \pmod{\pi}.$$

Hence there is a minimal core size in order to have these more localized vortices. In Fig. 11 we plot the function $u(r)$ for several values of the coupling constant g . In the weak coupling regime the function $u(r)$ has an oscillatory behaviour, while in the weak pairing regime the oscillations are absent. We observe that the different qualitative behaviour depends on the region of the phase diagram.

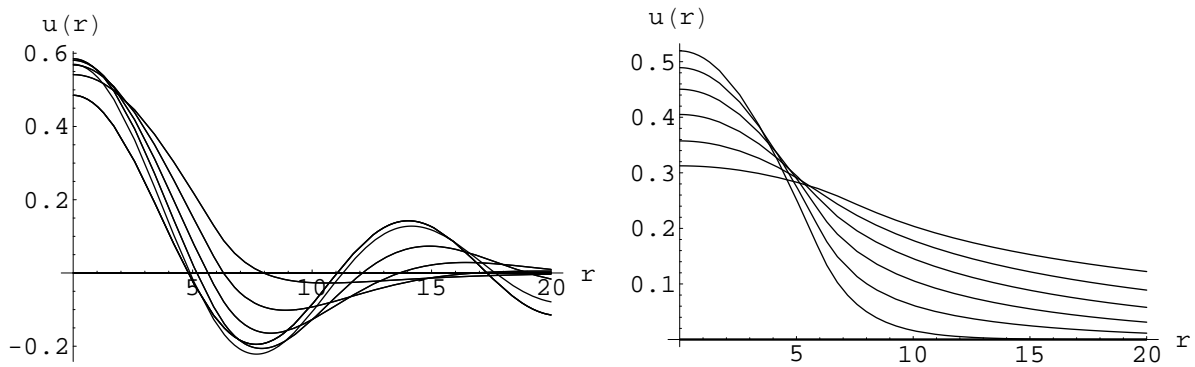


Figure 11: The wavefunction $u(r)$ for the vortex solution with $l = -1$ for $x = 1/4$ and several values of the coupling constant g . The size of the core is $a = 6$ in units of $\sqrt{\omega}$. Left: weak coupling BCS region for $g = 0.3 - 0.13$ in steps of 0.2. Right: weak pairing region for $g = 1.4 - 1.9$ in steps of 0.1.

5 Conclusions

In summary, we have constructed an exactly solvable pairing model which contains in various limits some of the most studied pairing models of current studies such as: the Richardson model with s -wave symmetry, the $p + ip$ BCS model, the Russian doll BCS model and the Gaudin models with s -wave and p -wave symmetries. We have computed the wavefunctions scalar products and one-point and two-point correlators. Furthermore, we have carried out an in depth study of the $p + ip$ model combining the exact solution with mean-field methods. We have found the phase diagram of this model characterizing the various phases in terms of the fidelity susceptibility, topological invariants, and other quantities such as the ground state energy, gap, chemical potential and occupation numbers. We have also studied the structure of the vortex wave function which is shown to depend on the region of the phase diagram. The richness of the $p + ip$ model calls for further studies concerning its behaviour. This task can be greatly facilitated by the existence of an exact solution for studies such as entanglement [17], correlation functions [3, 18] and quenching [19, 20].

Acknowledgments We thank I. Cirac, J. Dukelsky, N. Read, S. Rombouts and G.E. Volovik for helpful comments. M.I. and G.S. are supported by the CICYT project FIS2006-04885. G.S. also acknowledges ESF Science Programme INSTANS 2005-2010. J.L. and S.-Y.Z. are funded by the Australian Research Council through Discovery Grant DP0663772. C.D. and J.L. acknowledge the Royal Society Travel Grants Scheme.

A Calculations for the anyonic pairing model

A.1 Cyclic renormalisation group

In this Appendix we discuss how the Hamiltonian (5) is related to a known Hamiltonian, viz. the Galazek–Wilson model [24, 25]. This model was introduced as a simple example of a quantum mechanical system which admits a cyclic renormalisation group (RG) map. As will be shown below, the Galazek–Wilson is simply the one-body version of the anyonic pairing Hamiltonian (5). Cyclic behaviour of the RG also occurs in the many-body system, and we will demonstrate how the RG equation is easily obtained from the Bethe ansatz

equations.

The model introduced in [24, 25], which we will denote as H_{GW} , is defined by the matrix

$$H_{GW}(n, m) = \sqrt{\mathcal{E}_n \mathcal{E}_m} (\delta_{n,m} - g - ih \operatorname{sign}(n - m)) \quad (103)$$

where $\mathcal{M} < n, m < \mathcal{N}$. In [24, 25] the \mathcal{E}_n are assumed to scale exponentially $\mathcal{E}_n = \mu^n$, $\mu > 1$ under which there is a discrete scale invariance $n \rightarrow n + 1$ such that

$$H(n + 1, m + 1) = \mu H(n, m).$$

However this scale invariance is broken by the infra-red and ultra-violet cutoffs \mathcal{M} and \mathcal{N} .

In [24, 25] the RG is performed by a Gaussian elimination procedure for the highest component of the wavefunction in the Schrödinger equation, reducing \mathcal{N} to $\mathcal{N} - 1$. Under this process the result of the RG is that the coupling h remains invariant while the coupling g renormalises as

$$g_{\mathcal{N}-1} = \frac{g_{\mathcal{N}} + h^2}{1 - g_{\mathcal{N}}}. \quad (104)$$

Reparameterising the couplings in terms of angles $\phi_{\mathcal{N}}$, χ through

$$\begin{aligned} \tan(\phi_{\mathcal{N}}) &= \frac{g_{\mathcal{N}}}{h}, \\ \tan(\chi) &= h \end{aligned}$$

the RG equation becomes

$$\tan(\phi_{\mathcal{N}-1}) = \frac{\tan(\phi_{\mathcal{N}}) + \tan(\chi)}{1 - \tan(\phi_{\mathcal{N}}) \tan(\chi)} = \tan(\phi_{\mathcal{N}} + \chi)$$

or equivalently, iterating the RG equation p times,

$$\phi_{\mathcal{N}-p} = \phi_{\mathcal{N}} + p\chi.$$

A cycle occurs in the RG after p steps if $\chi = \pi/p$ since

$$g_{\mathcal{N}-p} = h \tan(\phi_{\mathcal{N}-p}) = h \tan(\phi_{\mathcal{N}} + p\chi) = h \tan(\phi_{\mathcal{N}} + \pi) = g_{\mathcal{N}}$$

with the RG period given by

$$p = \frac{\pi}{\arctan(h)}.$$

Next we show that (103) is equivalent to the one-pair version of (5). The first thing to observe is that for the one-pair version of (5) the string operators (6) appearing in the definition of the anyonic creation and annihilation operators can be removed by a unitary transformation. The Hamiltonian is then given in terms of the hard-core boson operators as

$$H_{\text{one-pair}} = \sum_{j=1}^L z_j^2 N_j - \frac{\sin(2\beta)}{\sin(\alpha - 2\beta)} \sum_{k>r}^L z_k z_r (\exp(-i\alpha) b_r^\dagger b_k + \text{h.c.})$$

with the Hilbert space spanned by the one-body states

$$|j\rangle = b_j^\dagger |0\rangle, \quad j = 1, \dots, L.$$

Here the energy is

$$E_{\text{one-pair}} = \frac{\sin(\alpha)}{\sin(\alpha - 2\beta)} y^2$$

such that

$$\exp(-2i\alpha) \prod_{k=1}^L \frac{1 - q^2 y^{-2} z_k^2}{1 - q^{-2} y^{-2} z_k^2} = 1.$$

Setting

$$\mathcal{E}_k = z_k^2, \quad g = \tan(2\beta) \cot(\alpha), \quad h = \tan(2\beta) \quad (105)$$

yields

$$H_{GW} = (1 - g)H_{\text{one-pair}}, \quad \mathcal{N} - \mathcal{M} = L.$$

To derive the RG equations from the Bethe ansatz, we only assume that the variables z_k are distinct and ordered $0 < z_1 < z_2 < \dots < z_L$. We may then write

$$\exp(-2i\alpha) \cdot \frac{1 - q^2 y^{-2} z_L^2}{1 - q^{-2} y^{-2} z_L^2} \cdot \prod_{k=1}^{L-1} \frac{1 - q^2 y^{-2} z_k^2}{1 - q^{-2} y^{-2} z_k^2} = 1.$$

Assuming $|z_L| \gg |y|$, which is a reasonable assumption for low energy states in a weakly coupled system, we can eliminate the highest energy degree of freedom of the Hamiltonian by making the approximation

$$\begin{aligned} \frac{1 - q^2 y^{-2} z_L^2}{1 - q^{-2} y^{-2} z_L^2} &\approx q^4, \\ \Rightarrow \exp(-2i\alpha + 4i\beta) \prod_{k=1}^{L-1} \frac{1 - q^2 y^{-2} z_k^2}{1 - q^{-2} y^{-2} z_k^2} &\approx 1. \end{aligned}$$

Thus for one RG step we have the renormalised coupling

$$\alpha_{\mathcal{N}-1} = \alpha_{\mathcal{N}} - 2\beta, \quad (106)$$

while β remains invariant. Substituting back into (105) shows that, in terms of the H_{GW} coupling parameters, h is invariant while

$$\begin{aligned} g_{\mathcal{N}-1} &= \tan(2\beta) \cot(\alpha_{\mathcal{N}-1}) \\ &= \tan(2\beta) \cot(\alpha_{\mathcal{N}} - 2\beta) \\ &= \tan(2\beta) \frac{\cot(\alpha_{\mathcal{N}}) + \tan(2\beta)}{1 - \tan(2\beta) \cot(\alpha_{\mathcal{N}})} \\ &= \frac{g_{\mathcal{N}} + h^2}{1 - g_{\mathcal{N}}} \end{aligned}$$

in agreement with (104).

For the many-body Hamiltonian (5), a completely analogous approach can be taken to establish the existence of the cyclic RG equation. Starting with the Bethe ansatz equations (11) we can make the same approximation as in the one-pair case by eliminating the highest energy level, i.e. if $|z_L| \gg |y_m|$ for all $m = 1, \dots, M$ then

$$\frac{1 - q^2 y_m^{-1} z_L^2}{1 - q^{-2} y_m^{-1} z_L^2} \approx q^4 \quad \forall m = 1, \dots, M$$

and (11) gives

$$\exp(-2i\alpha + 4i\beta) \prod_{k=1}^{L-1} \frac{1 - q^2 y_m^{-2} z_k^2}{1 - q^{-2} y_m^{-2} z_k^2} = \prod_{j \neq m}^M \frac{1 - q^4 y_m^{-2} y_j^2}{1 - q^{-4} y_m^{-2} y_j^2} \quad m = 1, \dots, M.$$

This leads to exactly the same RG equation (106) for α , with β again invariant.

A.2 Wavefunction scalar product and correlation functions

One of the byproducts of formulating the model via the QISM is that it readily provides access to the evaluation of correlation functions. Again, we will only outline these calculations. We will follow the general procedures of [40], where explicit details of derivations can be found.

It is convenient to first rescale the L -operator as

$$\tilde{L}(x) = \left(\begin{array}{cc|cc} 1 & 0 & 0 & 0 \\ 0 & \frac{q^{-1}x - qx^{-1}}{qx - q^{-1}x^{-1}} & \frac{q^2 - q^{-2}}{qx - q^{-1}x^{-1}} & 0 \\ - & - & - & - \\ 0 & \frac{q^2 - q^{-2}}{qx - q^{-1}x^{-1}} & \frac{q^{-1}x - qx^{-1}}{qx - q^{-1}x^{-1}} & 0 \\ 0 & 0 & 0 & 1 \end{array} \right) \quad (107)$$

such that it has the properties

$$\begin{aligned} \tilde{L}(x) \Big|_{q=1} &= I \otimes I \\ \tilde{L}(x) \Big|_{x=q} &= P \end{aligned}$$

with P the permutation operator. We also rescale the matrix U to be

$$\tilde{U} = \begin{pmatrix} \exp(-2i\alpha') & 0 \\ 0 & 1 \end{pmatrix}.$$

These rescalings have the net effect of working with rescaled elements of the monodromy matrix

$$\tilde{T}_j^i(x) = \exp(-i\alpha') \left(\prod_{k=1}^L \frac{1}{qx z_k^{-1} - q^{-1}x^{-1} z_k} \right) T_j^i(x)$$

The transfer matrix eigenvalues of $\tilde{t}(x) = \tilde{T}_1^1(x) + \tilde{T}_2^2(x)$ are now

$$\tilde{\Lambda}(x) = \tilde{a}(x) \prod_{j=1}^M \frac{q^2 x y_j^{-1} - q^{-2} y_j x^{-1}}{x y_j^{-1} - y_j x^{-1}} + \tilde{d}(x) \prod_{j=1}^M \frac{q^{-2} x y_j^{-1} - q^2 y_j x^{-1}}{x y_j^{-1} - y_j x^{-1}}$$

with

$$\begin{aligned}\tilde{a}(x) &= \exp(-2i\alpha') \prod_{k=1}^L \frac{q^{-1}xz_k^{-1} - qx^{-1}z_k}{qxz_k^{-1} - q^{-1}x^{-1}z_k} \\ \tilde{d}(x) &= 1\end{aligned}$$

One reason for working with the the rescaled monodromy matrix is that it provides a compact solution of the “inverse problem” of expressing the local operators b_j , b_j^\dagger , N_j in terms of the elements of the monodromy matrix. The result, which is obtained by a minor generalisation of the methods used in [16, 40, 47], is

$$\begin{aligned}b_j &= \left(\prod_{k=1}^{j-1} \tilde{t}(qz_k) \right) \tilde{T}_2^1(qz_j) \left(\prod_{k=1}^j \tilde{t}^{-1}(qz_k) \right), \\ b_j^\dagger &= \left(\prod_{k=1}^{j-1} \tilde{t}(qz_k) \right) \tilde{T}_1^2(qz_j) \left(\prod_{k=1}^j \tilde{t}^{-1}(qz_k) \right), \\ I - N_j &= \left(\prod_{k=1}^{j-1} \tilde{t}(qz_k) \right) \tilde{T}_2^2(qz_j) \left(\prod_{k=1}^j \tilde{t}^{-1}(qz_k) \right).\end{aligned}$$

Note that the operators $\{\tilde{t}(qz_j) : j = 1, \dots, L\}$ are conserved. Explicitly these are

$$\tilde{t}(qz_k) = \tilde{L}_{k(k-1)}(qz_k z_{k-1}^{-1}) \dots \tilde{L}_{k1}(qz_k z_1^{-1}) \tilde{U}_k \tilde{L}_{kL}(qz_k z_L^{-1}) \dots \tilde{L}_{k(k+1)}(qz_k z_{k+1}^{-1}) \quad (108)$$

where

$$\begin{aligned}\tilde{L}_{kl}(qz_k z_l^{-1}) &= \frac{qz_k z_l^{-1} + q^{-1}z_k^{-1}z_l}{(q - q^{-1})(q^2 z_k z_l^{-1} - q^{-2}z_k^{-1}z_l)} (q^{2N_k + 2N_l - 2} + q^{2 - 2N_k - 2N_l}) \\ &\quad + \frac{q^2 - q^{-2}}{q^2 z_k z_l^{-1} - q^{-2}z_k^{-1}z_l} (b_k^\dagger b_l + b_k b_l^\dagger) \\ &\quad - \frac{(q + q^{-1})(z_k z_l^{-1} + z_k^{-1}z_l)}{(q - q^{-1})(q^2 z_k z_l^{-1} - q^{-2}z_k^{-1}z_l)} I.\end{aligned}$$

The eigenvalues of $\tilde{t}(qz_k)$ are

$$\tilde{\Lambda}(qz_k) = \prod_{j=1}^M \frac{q^{-1}z_k y_j^{-1} - q y_j z_k^{-1}}{q z_k y_j^{-1} - q^{-1} y_j z_k^{-1}}. \quad (109)$$

Next we consider the scalar products between the states $\langle \tilde{\Phi}(W) |$, $|\tilde{\Phi}(Y)\rangle$, where

$$\langle \tilde{\Phi}(W) | = \langle 0 | \prod_{j=1}^L \tilde{T}_2^1(w_j), \quad (110)$$

$$|\tilde{\Phi}(Y)\rangle = \prod_{j=1}^L \tilde{T}_1^2(y_j) |0\rangle. \quad (111)$$

If $W = \{w_i\}$ is a set of solutions of the Bethe ansatz equations (11), and $Y = \{y_j\}$ are arbitrary parameters, then the Slavnov formula for the the scalar product is [57]

$$\langle \tilde{\Phi}(W) | \tilde{\Phi}(Y)\rangle = \mathcal{C}(W, Y) \det(F(W, Y)) \quad (112)$$

where elements of the matrix $F(W, Y)$ are given by

$$F(W, Y)_{ij} = \frac{(q^2 - q^{-2})\tilde{d}(w_i)}{(y_j w_i^{-1} - y_j^{-1} w_i)} \left(\tilde{a}(y_j) \prod_{m \neq i}^M (y_j w_m^{-1} q^2 - y_j^{-1} w_m q^{-2}) + \tilde{d}(y_j) \prod_{m \neq i}^M (y_j w_m^{-1} q^{-2} - y_j^{-1} w_m q^2) \right), \quad (113)$$

and

$$\mathcal{C}(W, Y) = \frac{1}{\prod_{k>l}^M (y_k y_l^{-1} - y_k^{-1} y_l) (w_l w_k^{-1} - w_l^{-1} w_k)}. \quad (114)$$

Note that

$$\mathcal{C}(Y, Y) = \frac{1}{\prod_{p=1}^M \prod_{q \neq p}^M (y_p y_q^{-1} - y_p^{-1} y_q)}.$$

We remark that the Slavnov formula (112) is a *scalar* product as opposed to an *inner* product. However for the anyonic pairing model we expect, due to a lack of symmetries, that generically there are no degeneracies in the energy spectrum for fixed particle number. In such an instance the eigenstates must be real, up to an overall phase factor, in which case the scalar product between any two eigenstates is equivalent to the inner product up to a phase.

An application of the Slavnov formula (112) is that it allows us to compute the normalised wavefunction overlap between two states with *different* values of the coupling parameter α . Specifically this permits us to compute the *fidelity*, as defined in [65, 68], which has been proposed as a technique to identify quantum phase transitions (for a review see [28]). To make this point transparent, we start with the explicit form of the monodromy matrix elements in terms of the elements of the L -operators which is

$$\tilde{T}_j^i(x) = \sum_{k_1, \dots, k_L=1}^L \tilde{g}_j^{k_L} \left[\tilde{L}_{k_L}^{k_L-1}(x z_L^{-1}) \right]_L \dots \left[\tilde{L}_{k_2}^{k_1}(x z_2^{-1}) \right]_2 \left[\tilde{L}_{k_1}^i(x z_1^{-1}) \right]_1.$$

Since \tilde{g} is a diagonal matrix we can then write

$$\tilde{T}_j^i(x) = \tilde{g}_j^j \sum_{k_1, \dots, k_{L-1}=1}^L \left[\tilde{L}_j^{k_{L-1}}(x z_L^{-1}) \right]_L \dots \left[\tilde{L}_{k_2}^{k_1}(x z_2^{-1}) \right]_2 \left[\tilde{L}_{k_1}^i(x z_1^{-1}) \right]_1 \quad (115)$$

and each of the operators

$$\left[\tilde{L}_{k_j}^{k_j-1}(x z_j^{-1}) \right]_j \quad (116)$$

is not explicitly dependent on α . Consequently the explicit α -dependence of $\tilde{T}_j^i(x)$ is only in terms of an overall phase. Thus we can take the set W to be a solution of the Bethe ansatz equations for a given coupling, say α_1 , and the set Y , which in general may be arbitrary, to be a solution to the Bethe ansatz equations with a second choice of the coupling, say α_2 . This is not to say that the eigenstates of the Hamiltonian (5) are independent of α , but rather the dependence is implicit through the solution sets W and Y of the Bethe ansatz equations. In this way the normalised wavefunction overlaps between ground states with different values of the coupling α can be computed, which is

in essence the computation of the fidelity.⁴ Note however we cannot compute the overlaps between ground states with different values of q nor the z_k , since these parameters appear explicitly in the operator elements (116).

Using the Slavnov formula and the solution of the inverse problem the form factors (matrix elements) for the local operators b_j, b_j^\dagger can also be written, although we will not give details here (however see Appendix B.4 for an example). Our main objects of interest for now are the one-point correlation functions, or expectation values, of the Cooper pair number operators N_j . We begin with the following form factor between two Bethe states [40]

$$\begin{aligned} & \langle \tilde{\Phi}(W) | \tilde{T}_2^2(x) | \tilde{\Phi}(Y) \rangle \\ &= \mathcal{C}(W, Y) \tilde{d}(x) \theta(x) \prod_{j=1}^M \frac{(xy_j^{-1}q^{-2} - x^{-1}y_jq^2)}{(xy_j^{-1} - x^{-1}y_j)} \det(F(W, Y) + Q(W, y; x)), \end{aligned}$$

where

$$\theta(x) = \prod_{k=1}^M \frac{xw_k^{-1} - x^{-1}w_k}{xy_k^{-1} - x^{-1}y_k},$$

and $Q(W, Y; x)$ is a rank-one matrix with elements

$$\begin{aligned} Q(W, Y; x)_{ij} &= \frac{(q^2 - q^{-2}) \tilde{d}(w_i) \tilde{d}(y_j)}{(xw_i^{-1} - x^{-1}w_i)(xw_i^{-1}q^{-1} - x^{-1}w_iq)} \\ &\times \prod_{k=1}^M (y_j y_k^{-1} q^{-2} - y_j^{-1} y_k q^2) \left(1 - \frac{\tilde{a}(x)}{\tilde{d}(x)} \prod_{k \neq i}^M \frac{xw_k^{-1} q^2 - x^{-1} w_k q^{-2}}{xw_k^{-1} q^{-2} - x^{-1} w_k q^2} \right). \end{aligned}$$

This expression enables us to compute the expectation value

$$\begin{aligned} \langle N_m \rangle &= \frac{\langle \tilde{\Phi}(Y) | N_m | \tilde{\Phi}(Y) \rangle}{\langle \tilde{\Phi}(Y) | \tilde{\Phi}(Y) \rangle} \\ &= 1 - t^{-1}(qz_m) \frac{\langle \tilde{\Phi}(Y) | \tilde{T}_2^2(qz_m) | \tilde{\Phi}(Y) \rangle}{\langle \tilde{\Phi}(Y) | \tilde{\Phi}(Y) \rangle} \\ &= 1 - \frac{\det(F(Y, Y) + Q(Y, Y; qz_m))}{\det F(Y, Y)}. \end{aligned} \tag{117}$$

Note that for the present case because $\tilde{a}(qz_m) = 0$, $\tilde{d}(x) = 1$ we have the following simplification for the matrix $Q(Y, Y; qz_m)$:

$$Q(Y, Y; qz_m)_{ij} = \frac{(q^2 - q^{-2})}{(qz_m y_i^{-1} - q^{-1} z_m^{-1} y_i)(z_m y_i^{-1} - z_m^{-1} y_i)} \prod_{k=1}^M (y_j y_k^{-1} q^{-2} - y_j^{-1} y_k q^2).$$

A.3 Duality and the analogue of the Moore-Read state

The $p + ip$ model was derived from the anyonic pairing model in a limit where the parameters α, β go to zero while keeping their ratio fixed, which gives the coupling constant $G = 2/(\alpha\beta^{-1} - 2)$ (recall (21)). One may ask whether the results obtained in this section

⁴In the context of the s -wave model this property has been exploited in [19, 20] to study quenching dynamics.

have an analogue in the anyonic pairing model. To answer this question we first look for a solution of the Bethe ansatz equations (11) with the property that all the roots vanish, i.e. $y_j \rightarrow 0$ ($j = 1, \dots, M$). From eq. (11) this implies

$$\exp(4i\beta(L - M - \frac{\alpha}{2\beta} + 1)) = \lim_{y_j \rightarrow 0} \prod_{j \neq m}^M \frac{q^{-2}y_m^2 - q^2y_j^2}{q^2y_m^2 - q^{-2}y_j^2} \quad m = 1, \dots, M.$$

The RHS of this equation is identically equal to 1 in the limit $\beta \rightarrow 0$, which is why there is such a solution in the $p + ip$ model. One can readily check that this result remains true for any β provided

$$y_m^2 \propto e^{2\pi im/M}, \quad m = 1, \dots, M,$$

which implies

$$M = L - \frac{\alpha}{2\beta} + 1 = L - G^{-1}.$$

This equation coincides with the condition (89) for the existence of a MR state in the $p + ip$ model. In the latter equation the parameter G should not be confused with the coupling constant of the anyonic pairing model given by $G_{AP} = \sin(2\beta)/\sin(\alpha - 2\beta)$, except in the limit $\alpha, \beta \rightarrow 0$. The corresponding eigenstate of the anyonic pairing model has zero energy and it is an anyonic deformation of the MR state. Explicitly the state is

$$|AMR\rangle = \left(\sum_{j=1}^L \frac{d_j^\dagger}{z_j} \right)^M |0\rangle.$$

As in the $p + ip$ model we can look for a set of roots Y , where a subset Z of P roots vanish, while the other set Y' with M' roots do not. The Bethe ansatz equations for the roots in Z yield

$$\exp(4i\beta(L - P - 2M' - \frac{\alpha}{2\beta} + 1)) = \lim_{y_j \rightarrow 0} \prod_{y_j \in Z, y_j \neq y_m}^M \frac{q^{-2}y_m^2 - q^2y_j^2}{q^2y_m^2 - q^{-2}y_j^2} \quad y_m \in Z$$

while for the roots in Y' the Bethe ansatz equations become

$$\exp(-2i\alpha) \prod_{k=1}^L \frac{1 - q^2y_m^{-2}z_k^2}{1 - q^{-2}y_m^{-2}z_k^2} = \prod_{y_j \in Y', y_j \neq y_m}^M \frac{1 - q^4y_m^{-2}y_j^2}{1 - q^{-4}y_m^{-2}y_j^2} \quad y_m \in Y'.$$

Hence the roots in Y' satisfy the same Bethe ansatz equations as the original model, provided

$$P = L - 2M' - \frac{\alpha}{2\beta} + 1 = L - 2M' - G^{-1}$$

which is the same condition as found in (86). Hence we expect that the duality symmetry of the $p + ip$ model to also be a property of the anyonic pairing model.

B Calculations for the $p + ip$ model

B.1 Solution of the gap and chemical potential equations

In this appendix we collate some results for the dimensionless parameters \bar{a} and \bar{b} which are solutions of equations (53,54). In all instances the results for the strong pairing phase can be deduced from those of the weak pairing phase through use of the duality relation (50). Below, the convention for the elliptic integrals are as in [27]:

$$E(\phi, k) = \int_0^\phi dx \sqrt{1 - k^2 \sin^2 x},$$

$$F(\phi, k) = \int_0^\phi dx \frac{1}{\sqrt{1 - k^2 \sin^2 x}}.$$

With the density functions as given by (51,52), performing the integrals in (53,54) one finds the following results.

1D case

Weak coupling BCS phase: ($\bar{a}, \bar{b} = \bar{\epsilon} \mp i\bar{\delta}$)

$$\frac{2}{g} = \sqrt{R}(F(\phi, k) - 2E(\phi, k)) + 2\frac{\sqrt{1 - 2\bar{\epsilon} + R^2}}{1 + R},$$

$$4\left(x - \frac{1}{2} + \frac{1}{2g}\right) = \sqrt{R}F(\phi, k)$$

where

$$R = \sqrt{\bar{\epsilon}^2 + \bar{\delta}^2}, \quad \phi = 2 \arctan(1/\sqrt{R}), \quad k^2 = \frac{1}{2} \left(1 + \frac{\bar{\epsilon}}{R}\right).$$

Moore–Read line: ($\bar{a} = \bar{b} < 0, \bar{a} = -|\bar{a}|$)

$$\frac{1}{g_{MR}} = 1 - \sqrt{|\bar{a}|} \arctan(1/\sqrt{|\bar{a}|}).$$

Weak pairing phase: ($\bar{a} = -|\bar{a}|, \bar{b} = -|\bar{b}|, |\bar{a}| > |\bar{b}|$)

$$\frac{1}{g} = \sqrt{\frac{1 + |\bar{a}|}{1 + |\bar{b}|}} - \sqrt{|\bar{a}|} E(\psi, m),$$

$$2\left(x - \frac{1}{2} + \frac{1}{2g}\right) = \sqrt{|\bar{b}|} F(\psi, m)$$

where

$$\psi = \arcsin(1/\sqrt{1 + |\bar{b}|}), \quad m^2 = 1 - \frac{|\bar{b}|}{|\bar{a}|}.$$

Read–Green line: ($\bar{a} = -|\bar{a}| < 0, \bar{b} = 0$)

$$\frac{1}{g_{RG}} = \sqrt{1 + |\bar{a}|} - \sqrt{|\bar{a}|}.$$

2D case

Weak coupling BCS: ($\bar{a}, \bar{b} = \bar{\epsilon} \mp i\bar{\delta}$)

$$\begin{aligned} \frac{1}{g} &= \sqrt{1 + R^2 - 2\bar{\epsilon}} - R + \bar{\epsilon} \log \left(\frac{1 - \bar{\epsilon} + \sqrt{1 + R^2 - 2\bar{\epsilon}}}{-\bar{\epsilon} + R} \right), \\ 2 \left(x - \frac{1}{2} + \frac{1}{2g} \right) &= R \log \left(\frac{1 - \bar{\epsilon} + \sqrt{1 + R^2 - 2\bar{\epsilon}}}{-\bar{\epsilon} + R} \right), \end{aligned}$$

where

$$R = \sqrt{\bar{\epsilon}^2 + \bar{\delta}^2}.$$

Moore–Read line: ($\bar{a} = \bar{b} < 0, \bar{a} = -|\bar{a}|$)

$$\frac{1}{g_{MR}} = 1 - |\bar{a}| \log(1 + 1/|\bar{a}|).$$

Weak pairing phase: ($\bar{a} = -|\bar{a}|, \bar{b} = -|\bar{b}|, |\bar{a}| > |\bar{b}|$)

$$\begin{aligned} \frac{1}{g} &= \sqrt{(1 + |\bar{a}|)(1 + |\bar{b}|)} - \sqrt{|\bar{a}\bar{b}|} + (|\bar{a}| + |\bar{b}|) \log \left(\frac{\sqrt{|\bar{a}|} + \sqrt{|\bar{b}|}}{\sqrt{1 + |\bar{a}|} + \sqrt{1 + |\bar{b}|}} \right), \\ \left(x - \frac{1}{2} + \frac{1}{2g} \right) &= \sqrt{|\bar{a}\bar{b}|} \log \left(\frac{\sqrt{1 + |\bar{a}|} + \sqrt{1 + |\bar{b}|}}{\sqrt{|\bar{a}|} + \sqrt{|\bar{b}|}} \right). \end{aligned}$$

Read–Green line: ($\bar{a} = -|\bar{a}| < 0, \bar{b} = 0$)

$$\frac{1}{g_{RG}} = \sqrt{1 + |\bar{a}|} - |\bar{a}| \log \left(\frac{1}{\sqrt{|\bar{a}|}} + \sqrt{1 + \frac{1}{|\bar{a}|}} \right).$$

B.2 Ground-state wavefunction: exact results versus mean-field results

We first recall from eq. (28) that for the $p + ip$ model

$$C(y) = \sum_{\mathbf{k} \in \mathbf{K}_+} \frac{k_x - ik_y}{\mathbf{k}^2 - y} c_{\mathbf{k}}^\dagger c_{-\mathbf{k}}^\dagger,$$

while in 1D this simplifies to

$$C(y) = \sum_{k > 0} \frac{k}{k^2 - y} c_k^\dagger c_{-k}^\dagger.$$

In the latter formulae we extended the domain of the momentum variables to include negative values of k_x which is done to properly account for the antisymmetry of the wavefunction. Now we will compare the exact wavefunction with the mean-field one. Recalling (40) we have

$$|\psi\rangle = \left(\sum_{\mathbf{k}} \mathbf{g}(\mathbf{k}) c_{\mathbf{k}}^{\dagger} c_{-\mathbf{k}}^{\dagger} \right)^M |0\rangle$$

This expression can be viewed as an average of the exact wavefunction (28) which involves a product of pair operators characterized by the roots y_m . Read and Green have shown [53] that in the limit where $\mathbf{k} \rightarrow 0$ the BCS wavefunction behaves as

$$\mathbf{g}(\mathbf{k}) \sim \begin{cases} k_x - ik_y, & \mu < 0, \quad (\text{strong - coupling}), \\ 1/(k_x + ik_y), & \mu > 0, \quad (\text{weak - coupling}). \end{cases}$$

This behaviour can be compared with the wavefunction associated to the roots appearing in (28),

$$\mathbf{g}(\mathbf{k}, y) = \frac{k_x - ik_y}{\mathbf{k}^2 - y} \sim \begin{cases} k_x - ik_y, & \text{if } |\mathbf{k}| \ll \sqrt{|y|}, \\ 1/(k_x + ik_y), & \text{if } |\mathbf{k}| \gg \sqrt{|y|} \end{cases}$$

which in real space leads to

$$\hat{\mathbf{g}}(\mathbf{r}, y) = \int_{-\infty}^{\infty} \int_{-\infty}^{\infty} d^2\mathbf{k} e^{i\mathbf{k}\cdot\mathbf{r}} \mathbf{g}(\mathbf{k}, y) \sim \frac{\bar{z}}{|z|} K_1(|z|\sqrt{-y})$$

where $z \in \mathbb{C}$ and $K_1(z)$ is a Bessel function. Using the asymptotic results $K_1(z) \sim 1/z$ ($|z| \ll 1$) and $K_1(z) \sim e^{-z} \sqrt{\pi/2z}$ ($|z| \gg 1$) one finds

$$\hat{\mathbf{g}}(\mathbf{r}, y) \sim \begin{cases} \bar{z}|z|^{-3/2} e^{-|z|\sqrt{-y}}, & |z| \gg 1/\sqrt{|y|}, \\ 1/z, & |z| \ll 1/\sqrt{|y|}. \end{cases}$$

Hence at short distances all the pairs behave as in the Moore-Read wavefunction and at large distances they show the typical behaviour associated to localized BCS pairs with a correlation length

$$\xi_y = \frac{1}{\text{Re}(\sqrt{-y})}. \quad (118)$$

If most of the roots y lie near the origin then the overall behaviour of the exact wavefunction will be well described by the Moore-Read wavefunction.

In 1D the real-space wavefunction associated to a root y is given by

$$\mathbf{g}(x, y) = \int_{-\infty}^{\infty} dk e^{ikx} \frac{k}{k^2 - y} = i\pi \text{sign}(x) e^{-|x|\sqrt{-y}}$$

which decays exponentially with a correlation length given by (118).

B.3 Wavefunction scalar product and one-point correlation functions

The wavefunction scalar product and one-point correlation functions of the $p + ip$ model can be obtained directly as a limiting case of the results in Appendix A.2. The elements of the L -operator (107) act locally, to leading order in γ , as

$$\begin{aligned}\tilde{L}_1^1(x) &\sim I - 2p\gamma \frac{x + x^{-1}}{x - x^{-1}}(I - N), \\ \tilde{L}_2^1(x) &\sim \frac{4p\gamma}{x - x^{-1}}b, \\ \tilde{L}_1^2(x) &\sim \frac{4p\gamma}{x - x^{-1}}b^\dagger, \\ \tilde{L}_2^2(x) &\sim I - 2p\gamma \frac{x + x^{-1}}{x - x^{-1}}N.\end{aligned}$$

Now using (115) we have to leading order

$$\begin{aligned}\tilde{T}_1^2(x) &\sim 4p\gamma \sum_{j=1}^L \frac{1}{xz_k^{-1} - x^{-1}z_k} b_j^\dagger \\ &= 4xp\gamma \left(\sum_{j=1}^L \frac{z_j b_j^\dagger}{x^2 - z_j^2} \right).\end{aligned}$$

We define the operator (cf. (28))

$$C(x) = \sum_{j=1}^L \frac{z_j b_j^\dagger}{x^2 - z_j^2} \quad (119)$$

such that the states of the system are of the form

$$|\phi(Y)\rangle = \prod_{j=1}^M C(y_j) |0\rangle \quad (120)$$

where $Y = \{y_j\}$ are a solution set of the Bethe ansatz equations (23). The formula for the scalar products of the states (120) follows from taking the appropriate limit of (112). For the limit of the matrix (113) the result is

$$F(W, Y)_{ij} \sim \frac{4p\gamma^2 \prod_{l \neq i}^M (y_j w_l^{-1} - y_j^{-1} w_l)}{(y_j w_i^{-1} - y_j^{-1} w_i)} \left(-2t - 2p \sum_{r=1}^L \frac{y_j^2 + z_r^2}{y_j^2 - z_r^2} + 4p \sum_{m \neq i}^M \frac{y_j^2 + w_m^2}{y_j^2 - w_m^2} \right).$$

Recalling the Bethe ansatz equations in the form (20), we can substitute into the above to eliminate t :

$$\begin{aligned}F(W, Y)_{ij} &\sim 4p\gamma^2 y_j w_i \prod_{l \neq i}^M (y_j w_l^{-1} - y_j^{-1} w_l) \\ &\times \left(4p \sum_{k=1}^L \frac{z_k^2}{(w_i^2 - z_k^2)(y_j^2 - z_k^2)} + 8p \sum_{m \neq i}^M \frac{w_m^2}{(w_m^2 - w_i^2)(y_j^2 - w_m^2)} \right).\end{aligned}$$

To simplify the calculation we introduce the diagonal matrices

$$\begin{aligned}\Gamma(W, Y)_{ij} &= \delta_{ij} \left(\frac{w_j}{y_j} \right) \frac{y_j w_j^{-1} - y_j^{-1} w_j}{\prod_{k=1}^M (y_j w_k^{-1} - y_j^{-1} w_k)}, \\ \Pi(W, Y)_{ij} &= \delta_{ij} \frac{1}{16p^2 \gamma^2 w_j^2}\end{aligned}$$

such that

$$\begin{aligned}\det(\Pi(W, Y)) &= \left(\frac{1}{16p^2 \gamma^2} \right)^M \left(\prod_{j=1}^M w_j^{-2} \right), \\ \det(\Gamma(W, Y)) &= \prod_{j=1}^M \left(\frac{w_j}{y_j} \right) \Upsilon(W, Y)\end{aligned}$$

where

$$\Upsilon(W, Y) = \frac{\prod_{j=1}^M (y_j w_j^{-1} - y_j^{-1} w_j)}{\prod_{j=1}^M \prod_{k=1}^M (y_j w_k^{-1} - y_j^{-1} w_k)}.$$

Note that

$$\Upsilon(Y, Y) = \mathcal{C}(Y, Y)$$

with $\mathcal{C}(W, Y)$ given by (114). Now defining

$$G(W, Y) = \lim_{\gamma \rightarrow 0} \Pi(W, Y) F(W, Y) \Gamma(W, Y)$$

leads to

$$G(W, Y)_{ij} = \frac{(y_j^2 - w_j^2)}{(y_j^2 - w_i^2)} \left(\sum_{k=1}^L \frac{z_k^2}{(w_i^2 - z_k^2)(y_j^2 - z_k^2)} + 2 \sum_{m \neq i}^M \frac{w_m^2}{(w_m^2 - w_i^2)(y_j^2 - w_m^2)} \right).$$

We will also need

$$\begin{aligned}\frac{\mathcal{C}^2(W, Y)}{\Upsilon^2(W, Y)} &= \frac{\prod_{j \neq k}^M (y_j w_k^{-1} - y_j^{-1} w_k)}{\prod_{m > l}^M (y_m y_l^{-1} - y_m^{-1} y_l) (w_l w_m^{-1} - w_l^{-1} w_m)} \\ &\quad \times \frac{\prod_{a \neq b}^M (y_a w_b^{-1} - y_a^{-1} w_b)}{\prod_{p > q}^M (y_p y_q^{-1} - y_p^{-1} y_q) (w_q w_p^{-1} - w_q^{-1} w_p)} \\ &= \prod_{k=1}^M \prod_{j \neq k}^M \frac{(y_j^2 - w_k^2)^2}{(y_j^2 - y_k^2)(w_k^2 - w_j^2)}.\end{aligned}$$

Keeping in mind that $C(x)$ differs from the leading term in the expansion of $\tilde{T}_1^2(x)$ by a scale factor, we now have

$$\langle \phi(W) | \phi(Y) \rangle = \frac{\prod_{k=1}^M \prod_{j \neq k}^M (y_j^2 - w_k^2)}{\prod_{j < k}^M (y_j^2 - y_k^2)(w_k^2 - w_j^2)} \det(G(W, Y)).$$

Finally we can make explicit the square of the normalised wavefunction scalar product $\mathcal{F}(W, Y)$ (equivalent to the square of the fidelity) between two states as a function of the Bethe roots, but independent of the coupling G . The result is

$$\begin{aligned}\mathcal{F}(W, Y)^2 &= \frac{\langle \phi(W) | \phi(Y) \rangle^2}{\langle \phi(W) | \phi(W) \rangle \langle \phi(Y) | \phi(Y) \rangle} \\ &= \frac{\mathcal{C}^2(W, Y)}{\Upsilon^2(W, Y)} \frac{\det(G(W, Y))^2}{\det(G(W, W)) \det(G(Y, Y))} \\ &= \prod_{k=1}^M \prod_{j \neq k}^M \frac{(y_j^2 - w_k^2)^2}{(y_j^2 - y_k^2)(w_j^2 - w_k^2)} \frac{\det(G(W, Y))^2}{\det(G(W, W)) \det(G(Y, Y))}\end{aligned}$$

and we note

$$\begin{aligned}G(Y, Y)_{ii} &= \sum_{k=1}^L \frac{z_k^2}{(y_i^2 - z_k^2)^2} - 2 \sum_{m \neq i}^M \frac{y_m^2}{(y_i^2 - y_m^2)^2}, \\ G(Y, Y)_{ij} &= \frac{2y_j^2}{(y_j^2 - y_i^2)^2}, \quad i \neq j.\end{aligned}\tag{121}$$

In a similar manner we obtain the formula for the one-point correlation functions from the limit of (117). The result is

$$\langle N_m \rangle = 1 - \frac{\det(G(Y, Y) - z_m \mathcal{W}_m(Y))}{\det(G(Y, Y))}\tag{122}$$

with $G(Y, Y)$ given by (121) and

$$(\mathcal{W}_m(Y))_{ij} = \frac{z_m}{(y_i^2 - z_m^2)^2}.\tag{123}$$

B.4 Two-point correlation functions

Finally we turn our attention to the more technically demanding problem of calculating two-point correlation functions. We will derive formulae for both the off-diagonal case $\langle b_m^\dagger b_n \rangle$ and the diagonal case $\langle N_m N_n \rangle$. For the calculation of these results we extend the methods used in [18, 52, 69] which were developed for the s -wave model.

First we consider the off-diagonal case. For any fixed n we may express the state $|\phi(Y)\rangle$ as

$$|\phi(Y)\rangle = \prod_{\beta=1}^M C(y_\beta) |0\rangle = \prod_{\beta=1}^M \left(\tilde{C}_n(y_\beta) + A_n^\beta b_n^\dagger \right) |0\rangle,\tag{124}$$

where

$$\tilde{C}_n(y_\beta) = \sum_{l \neq n}^M \frac{z_l b_l^\dagger}{y_\beta^2 - z_l^2}, \quad A_n^\beta = \frac{z_n}{y_\beta^2 - z_n^2}.$$

Keeping in mind that $(b_n^\dagger)^2 = 0$, $b_n |0\rangle = 0$, we find

$$b_n |\phi(Y)\rangle = \sum_{\beta=1}^M A_n^\beta \prod_{\alpha \neq \beta}^M \tilde{C}_n(y_\alpha) |0\rangle$$

$$\begin{aligned}
&= \sum_{\beta=1}^M A_n^\beta \prod_{\alpha \neq \beta}^M (C(y_\alpha) - A_n^\alpha b_n^\dagger) |0\rangle \\
&= \sum_{\beta=1}^M A_n^\beta \prod_{\alpha \neq \beta}^M C(y_\alpha) |0\rangle - \sum_{\beta=1}^M \sum_{\alpha \neq \beta}^M A_n^\alpha A_n^\beta b_n^\dagger \prod_{\gamma \neq \alpha, \beta}^M C(y_\gamma) |0\rangle. \tag{125}
\end{aligned}$$

With the help of (125) we have that for $m \neq n$ the unnormnormalised two-point off-diagonal correlation functions are

$$\begin{aligned}
\langle \phi(Y) | b_m^\dagger b_n | \phi(Y) \rangle &= \sum_{\beta=1}^M A_n^\beta \langle \phi(Y) | b_m^\dagger \prod_{\alpha \neq \beta}^M C(y_\alpha) |0\rangle \\
&\quad - \sum_{\beta=1}^M \sum_{\alpha \neq \beta}^M A_n^\alpha A_n^\beta \langle \phi(Y) | b_m^\dagger b_n^\dagger \prod_{\gamma \neq \alpha, \beta}^M C(y_\gamma) |0\rangle \\
&= \sum_{\beta=1}^M A_n^\beta \langle \phi(Y) | b_m^\dagger \prod_{\alpha \neq \beta}^M C(y_\alpha) |0\rangle \\
&\quad - 2 \sum_{\beta=1}^M \sum_{\alpha < \beta}^M A_n^\alpha A_n^\beta \langle \phi(Y) | b_m^\dagger b_n^\dagger \prod_{\gamma \neq \alpha, \beta}^M C(y_\gamma) |0\rangle \tag{126}
\end{aligned}$$

where in the last step we use the fact that the terms in the double sum are symmetric with respect to interchange of the labels α and β . Now the two-point correlation function has been reduced to a sum of one-point form factors of b_m^\dagger and a double sum over the two-point form factors of $b_m^\dagger b_n^\dagger$. Recalling the definition (119), for the $p + ip$ model the inverse problem is easily solved as

$$b_m^\dagger = \lim_{y \rightarrow z_m} \frac{y^2 - z_m^2}{z_m} C(y).$$

Using this expression and the wavefunction scalar product formula we obtain the matrix elements of both b_m^\dagger and $b_m^\dagger b_n$. For the one-point case the result is

$$\begin{aligned}
\langle \phi(Y) | b_m^\dagger \prod_{\alpha \neq \beta}^M C(y_\alpha) |0\rangle &= \lim_{v \rightarrow z_m} \frac{v^2 - z_m^2}{z_m} \langle \phi(Y) | C(v) \prod_{\alpha \neq \beta}^M C(y_\alpha) |0\rangle \\
&= \mathcal{K}_m^\beta \det(\mathcal{T}_m^\beta)
\end{aligned}$$

where \mathcal{T}_m^β is the $M \times M$ matrix with elements

$$\begin{aligned}
(\mathcal{T}_m^\beta)_{ij} &= G_{ij}, & j \neq \beta, \\
(\mathcal{T}_m^\beta)_{i\beta} &= (\mathcal{W}_m)_{i\beta},
\end{aligned}$$

$\mathcal{K}_m^\beta = (y_\beta^2 - z_m^2)$, $G \equiv G(Y, Y)$ is given by (121), and $\mathcal{W}_m \equiv \mathcal{W}_m(Y)$ is given by (123). (To keep the notation compact, we hereafter omit the Y dependence on all such matrices.) For the two-point form factors we have

$$\begin{aligned}
&\langle \phi(Y) | b_m^\dagger b_n^\dagger \prod_{\gamma \neq \alpha, \beta}^M C(y_\gamma) |0\rangle \\
&= \lim_{u \rightarrow z_m} \lim_{v \rightarrow z_n} \frac{(u^2 - z_m^2)(v^2 - z_n^2)}{z_m z_n} \langle \phi(Y) | C(u) C(v) \prod_{\gamma \neq \alpha, \beta}^M C(y_\gamma) |0\rangle \\
&= K_{mn}^{\alpha\beta} \det(T_{mn}^{\alpha\beta}) \tag{127}
\end{aligned}$$

where $T_{mn}^{\alpha\beta}$ is the $M \times M$ matrix with the elements

$$\begin{aligned} (T_{mn}^{\alpha\beta})_{ij} &= G_{ij}, & j \neq \alpha, \beta, \\ (T_{mn}^{\alpha\beta})_{i\alpha} &= (\mathcal{W}_n)_{i\alpha}, \\ (T_{mn}^{\alpha\beta})_{i\beta} &= (\mathcal{W}_m)_{i\beta}, \end{aligned}$$

and

$$K_{mn}^{\alpha\beta} = \frac{(y_\alpha^2 - z_m^2)(y_\alpha^2 - z_n^2)(y_\beta^2 - z_m^2)(y_\beta^2 - z_n^2)}{(y_\alpha^2 - y_\beta^2)(z_m^2 - z_n^2)}.$$

This leads to

$$\langle \phi(Y) | b_m^\dagger b_n | \phi(Y) \rangle = \sum_{\beta=1}^M \mathcal{J}_{mn}^\beta \det(\mathcal{T}_m^\beta) - \sum_{\beta=1}^M \sum_{\alpha < \beta}^M \mathcal{J}_{mn}^\beta J_{mn}^{\alpha\beta} \det(T_{mn}^{\alpha\beta})$$

where

$$\begin{aligned} \mathcal{J}_{mn}^\beta &= A_n^\beta \mathcal{K}_m^\beta \\ &= \frac{z_n (y_\beta^2 - z_m^2)}{y_\beta^2 - z_n^2} \\ J_{mn}^{\alpha\beta} &= \frac{2A_n^\alpha K_{mn}^{\alpha\beta}}{\mathcal{K}_m^\beta} \\ &= \frac{2z_n (y_\alpha^2 - z_m^2)(y_\beta^2 - z_n^2)}{(y_\alpha^2 - y_\beta^2)(z_m^2 - z_n^2)}. \end{aligned}$$

We can conveniently express the determinants of \mathcal{T}_m^β and $T_{mn}^{\alpha\beta}$ in a vector notation. Defining the M -dimensional vectors \vec{G}_j , $j = 1, \dots, M$ and \vec{W}_m , $m = 1, \dots, M$ to have entries

$$\begin{aligned} (\vec{G}_j)_i &= G_{ij} \\ (\vec{W}_m)_i &= (\mathcal{W}_m)_{ij} \end{aligned}$$

we can write

$$\begin{aligned} \det(\mathcal{T}_m^\beta) &= \left| \vec{G}_1, \dots, \vec{G}_{\beta-1}, \vec{W}_m, \vec{G}_{\beta+1}, \dots, \vec{G}_M \right|, \\ \det(T_{mn}^{\alpha\beta}) &= \left| \vec{G}_1, \dots, \vec{G}_{\alpha-1}, \vec{W}_n, \vec{G}_{\alpha+1}, \dots, \vec{G}_{\beta-1}, \vec{W}_m, \vec{G}_{\beta+1}, \dots, \vec{G}_M \right|. \end{aligned}$$

Using standard properties of determinants we have

$$\begin{aligned} \det(\mathcal{T}_m^\beta) &= \left| \vec{G}_1 - \frac{J_{mn}^{1\beta}}{J_{mn}^{2\beta}} \vec{G}_2, \dots, \vec{G}_{\beta-2} - \frac{J_{mn}^{(\beta-2)\beta}}{J_{mn}^{(\beta-1)\beta}} \vec{G}_{\beta-1}, \vec{G}_{\beta-1}, \vec{W}_m, \vec{G}_{\beta+1}, \dots, \vec{G}_M \right|, \\ \sum_{\alpha < \beta}^M J_{mn}^{\alpha\beta} \det(T_{mn}^{\alpha\beta}) &= J_{mn}^{(\beta-1)\beta} \left| \vec{G}_1 - \frac{J_{mn}^{1\beta}}{J_{mn}^{2\beta}} \vec{G}_2, \dots, \vec{G}_{\beta-2} - \frac{J_{mn}^{(\beta-2)\beta}}{J_{mn}^{(\beta-1)\beta}} \vec{G}_{\beta-1}, \vec{W}_n, \vec{W}_m, \vec{G}_{\beta+1}, \dots, \vec{G}_M \right|. \end{aligned}$$

Combining these we have a single determinant expression

$$\begin{aligned} \det(\mathcal{T}_m^\beta) - \sum_{\alpha < \beta}^M J_{mn}^{\alpha\beta} \det(T_{mn}^{\alpha\beta}) &= \left| \vec{G}_1 - \frac{J_{mn}^{1\beta}}{J_{mn}^{2\beta}} \vec{G}_2, \dots, \vec{G}_{\beta-2} - \frac{J_{mn}^{(\beta-2)\beta}}{J_{mn}^{(\beta-1)\beta}} \vec{G}_{\beta-1}, \vec{G}_{\beta-1} - J_{mn}^{(\beta-1)\beta} \vec{W}_n, \vec{W}_m, \vec{G}_{\beta+1}, \dots, \vec{G}_M \right|. \end{aligned}$$

This allows us to express the off-diagonal two-point correlation functions as

$$\begin{aligned}\langle b_m^\dagger b_n \rangle &= \frac{\langle \phi(Y) | b_m^\dagger b_n | \phi(Y) \rangle}{\langle \phi(Y) | \phi(Y) \rangle} \\ &= \frac{1}{\det(G)} \sum_{\beta=1}^M \mathcal{J}_{mn}^\beta \det(\mathcal{D}_{mn}^\beta)\end{aligned}$$

where

$$\begin{aligned}(\mathcal{D}_{mn}^\beta)_{ij} &= G_{ij} - \frac{(y_{j+1}^2 - y_\beta^2)(y_j^2 - z_m^2)}{(y_j^2 - y_\beta^2)(y_{j+1}^2 - z_m^2)} G_{i(j+1)}, & j < \beta - 1, \\ (\mathcal{D}_{mn}^\beta)_{i(\beta-1)} &= G_{i(\beta-1)} - \frac{2z_n^2(y_{\beta-1}^2 - z_m^2)(y_\beta^2 - z_n^2)}{(y_{\beta-1}^2 - y_\beta^2)(z_m^2 - z_n^2)(y_i^2 - z_n^2)^2}, \\ (\mathcal{D}_{mn}^\beta)_{i\beta} &= \frac{z_m}{(y_i^2 - z_m^2)^2}, \\ (\mathcal{D}_{mn}^\beta)_{ij} &= G_{ij}, & j > \beta.\end{aligned}$$

Next we consider the computation of the diagonal two-point correlation functions. To facilitate this, we first note the commutation relation

$$[N_m, C(v)] = \frac{z_m}{v^2 - z_m^2} b_m^\dagger. \quad (128)$$

With the help of the commutation relation (128), and the fact that each N_m vanishes on the vacuum, we can write for $m \neq n$

$$\begin{aligned}\langle \phi(Y) | N_m N_n | \phi(Y) \rangle &= \langle \phi(Y) | N_m N_n \prod_{\beta=1}^M C(y_\beta) | 0 \rangle \\ &= \sum_{\beta=1}^M \frac{z_m}{y_\beta^2 - z_m^2} \langle \phi(Y) | N_n b_m^\dagger \prod_{\alpha \neq \beta}^M C(y_\alpha) | 0 \rangle \\ &= \sum_{\beta=1}^M \frac{z_m}{y_\beta^2 - z_m^2} \sum_{\alpha \neq \beta}^M \frac{z_n}{y_\alpha^2 - z_n^2} \langle \phi(Y) | b_m^\dagger b_n^\dagger \prod_{\gamma \neq \alpha, \beta}^M C(y_\gamma) | 0 \rangle \\ &= \sum_{\beta=1}^M \sum_{\alpha \neq \beta}^M \frac{z_m}{y_\beta^2 - z_m^2} \frac{z_n}{y_\alpha^2 - z_n^2} K_{mn}^{\alpha\beta} \det(T_{mn}^{\alpha\beta}) \\ &= \frac{z_m}{2} \sum_{\beta=1}^M \sum_{\alpha \neq \beta}^M J_{mn}^{\alpha\beta} \det(T_{mn}^{\alpha\beta}).\end{aligned}$$

Using similar techniques as before, we can reduce the above to a sum of M determinants. Doing this leads to the final result

$$\begin{aligned}\langle N_m N_n \rangle &= \frac{\langle \phi(Y) | N_m N_n | \phi(Y) \rangle}{\langle \phi(Y) | \phi(Y) \rangle} \\ &= \frac{z_m}{2 \det(G)} \left(\sum_{\beta=1}^{M-1} J_{mn}^{M\beta} \det(D_{mn}^\beta) + J_{mn}^{(M-1)M} \det(E_{mn}) \right)\end{aligned}$$

where

$$\begin{aligned}
(D_{mn}^\beta)_{ij} &= G_{ij} - \frac{(y_{j+1}^2 - y_\beta^2)(y_j^2 - z_m^2)}{(y_j^2 - y_\beta^2)(y_{j+1}^2 - z_m^2)} G_{i(j+1)}, & j \neq \beta - 1, \beta, M, \\
(D_{mn}^\beta)_{i(\beta-1)} &= G_{i(\beta-1)} - \frac{(y_{\beta+1}^2 - y_\beta^2)(y_{\beta-1}^2 - z_m^2)}{(y_{\beta-1}^2 - y_\beta^2)(y_{\beta+1}^2 - z_m^2)} G_{i(\beta+1)}, \\
(D_{mn}^\beta)_{i\beta} &= \frac{z_m}{(y_i^2 - z_m^2)^2}, \\
(D_{mn}^\beta)_{iM} &= \frac{z_n}{(y_i^2 - z_n^2)^2}, \\
(E_{mn})_{ij} &= G_{ij} - \frac{(y_{j+1}^2 - y_M^2)(y_j^2 - z_m^2)}{(y_j^2 - y_M^2)(y_{j+1}^2 - z_m^2)} G_{i(j+1)}, & j \neq M - 1, M, \\
(E_{mn})_{i(M-1)} &= \frac{z_n}{(y_i^2 - z_n^2)^2}, \\
(E_{mn})_{iM} &= \frac{z_m}{(y_i^2 - z_m^2)^2}.
\end{aligned}$$

References

- [1] L. Amico, A. Di Lorenzo, A. Mastellone, A. Osterloh, R. Raimondi, *Ann. Phys.* **299**, 228 (2002).
- [2] L. Amico, A. Di Lorenzo, and A. Osterloh, *Phys. Rev. Lett.* **86**, 5759 (2001).
- [3] L. Amico and A. Osterloh, *Phys. Rev. Lett.* **88**, 127003 (2002).
- [4] A. Anfossi, A. LeClair, G. Sierra, *J. Stat. Mech.: Theor. Exp.*, P05011 (2005).
- [5] J. Bardeen, L.N. Cooper, and J.R. Schrieffer, *Phys. Rev.* **108**, 1175 (1957).
- [6] M.T. Batchelor, X.-W. Guan, J.-S. He, *J. Stat. Mech.: Theor. Exp.*, P03007 (2007).
- [7] R.J. Baxter, *Phys. Rev. Lett.* **26**, 832 (1971).
- [8] R.J. Baxter *Exactly solved models in statistical mechanics* (Academic Press, London, 1982)
- [9] M.C. Cambiaggio, A.M.F. Rivas, and M. Saraceno, *Nucl. Phys. A* **624**, 157 (1997).
- [10] P.-H. Chavanis, *Phys. Rev. E* **65**, 056123 (2002).
- [11] N. R. Cooper and G. V. Shlyapnikov, *Phys. Rev. Lett.* **103**, 155302 (2009).
- [12] S. Das Sarma, C. Nayak, and S. Tewari, *Phys. Rev. B* **73**, 220502 (2006).
- [13] H.J. DeVega and N. Sanchez, *Nucl. Phys. B* **625**, 409 (2002).
- [14] J. Dukelsky, S. Pittel, and G. Sierra, *Rev. Mod. Phys.* **76**, 643 (2004).
- [15] J. Dukelsky, C. Esebbag, and P. Schuck, *Phys. Rev. Lett.* **87**, 066403 (2001).
- [16] C. Dunning and J. Links, *Nucl. Phys. B* **702**, 481 (2004).

- [17] C. Dunning, J. Links, and H.-Q. Zhou, Phys. Rev. Lett. **94**, 227002 (2005).
- [18] A. Faribault, P. Calabrese, and J.-S. Caux, Phys. Rev. B **77**, 064503 (2008).
- [19] A. Faribault, P. Calabrese, and J.-S. Caux, J. Stat. Mech.: Theor. Exp., P03018 (2009).
- [20] A. Faribault, P. Calabrese, and J.-S. Caux, J. Math. Phys. **50**, 095212 (2009).
- [21] J. Fuchs, C. Ticknor, P. Dyke, G. Veeravalli, E. Kuhnle, W. Rowlands, P. Hannaford, and C.J. Vale, Phys. Rev. A **77**, 053616 (2008).
- [22] J.P. Gaebler, J.T. Stewart, J.L. Bohn, and D.S. Jin, Phys. Rev. Lett. **98**, 200403 (2007).
- [23] M. Gaudin, *Travaux de Michel Gaudin. Modèles exactement résolus* (Les Éditions de Physique, France, 1995).
- [24] St.D. Glazek and K.G. Wilson, Phys. Rev. Lett. **89**, 230401 (2002).
- [25] St.D. Glazek and K.G. Wilson, Phys. Rev. B **69**, 094304 (2004).
- [26] C. Gómez, M. Ruiz-Altaba and G. Sierra, *Quantum groups in two-dimensional physics* (Cambridge University Press, 1996).
- [27] I.S. Gradshteyn and I.M. Ryzhik, *Table of integrals, series, and products*, A. Jeffrey and D. Zwillinger (eds.); translated from the Russian by Scripta Technica, Inc. (Academic Press, San Diego, 2000).
- [28] S.-J. Gu, *Fidelity approach to quantum phase transitions*, <http://arxiv.org/abs/0811.3127>.
- [29] V. Gurarie and L. Radzihovsky, Ann. Phys. **322**, 2 (2007).
- [30] F.D.M. Haldane, Phys. Rev. Lett. **50**, 1153 (1983).
- [31] Y.-J. Han, Y.-H. Chan, W. Yi, A. J. Daley, S. Diehl, P. Zoller, L.-M. Duan, Phys. Rev. Lett. **103**, 070404 (2009).
- [32] D. Ivanov, Phys. Rev. Lett. **86**, 268 (2001);
- [33] M. Ibañez, J. Links, G. Sierra, and S.-Y. Zhao, Phys. Rev. B **79**, 180501(R) (2009).
- [34] Y. Inada, M. Horikoshi, S. Nakajima, M. Kuwata-Gonokami, M. Ueda, and T. Mukaiyama, Phys. Rev. Lett. **101**, 100401 (2008).
- [35] J. Jang, R. Budakian, and Y. Maeno, arXiv:0908:2673
- [36] A.G. Izergin A G and V.E. Korepin, Lett. Math. Phys. **6**, 283 (1982).
- [37] M. Jimbo, Commun. Math. Phys. **102**, 537 (1986).
- [38] M. Jimbo (ed.) *Yang-Baxter equations in integrable systems* (World Scientific, Singapore, 1990)

- [39] M. Jimbo and T. Miwa, *Algebraic analysis of solvable lattice models* Regional Conference Series in Mathematics (American Mathematical Society, Providence, Rhode Island, 1995).
- [40] N. Kitanine, J.M. Maillet, V. Terras, Nucl. Phys. B **554**, 647 (1999).
- [41] V.E. Korepin, N.M. Bogoliubov, A.G. and Izergin A G, *Quantum inverse scattering method and correlation functions* (Cambridge University Press, 1993).
- [42] C. Kallin and A. J. Berlinsky, J. Phys.: Cond. Mat. **21** 164210 (2009).
- [43] J. Levinsen, N. R. Cooper, V. Gurarie, Phys. Rev. A **78**, 063616 (2008).
- [44] J. Leinaas and J. Myrheim, Nuovo Cimento B **37**, 1 (1977).
- [45] A. LeClair, J.M. Román, and G. Sierra, Phys. Rev. B **69**, 020505(R) (2004).
- [46] J. Links, H.-Q. Zhou, R.H. McKenzie, and M.D. Gould, J. Phys. A: Math. Gen. **36**, R63 (2003).
- [47] J.M. Maillet and V. Terras, Nucl. Phys. B **575** 627 (2000).
- [48] V.P. Maslov, Theor. Math. Phys. **141**, 1686 (2004).
- [49] G. Moore and N. Read, Nucl. Phys. B **360**, 362 (1991).
- [50] C. Nayak, S.H. Simon, A. Stern, M. Freedman, and S. Das Sarma, Rev. Mod. Phys. **80**, 1083 (2008).
- [51] Y. Nishida, Ann. Phys. **324**, 897 (2009).
- [52] A.A. Ovchinnikov, Nucl. Phys. B **703**, 363 (2003).
- [53] N. Read and D. Green, Phys. Rev. B **61**, 10267 (2000).
- [54] R.W. Richardson, Phys. Lett. **3**, 277 (1963).
- [55] J.M. Román, G. Sierra, and J. Dukelsky, Nucl. Phys. B **634**, 483 (2002).
- [56] R.W. Richardson, J. Math. Phys. **18**, 1802 (1977).
- [57] N.A. Slavnov, Theor. Math. Phys. **79**, 502 (1989).
- [58] E.K. Sklyanin, J. Phys. A: Math. Gen. **21**, 2375 (1988).
- [59] S. Tewari, S. Das Sarma, C. Nayak, C. Zhang and P. Zoller, Phys. Rev. Lett. **98**, 010506 (2007).
- [60] G.E. Volovik, Sov. Phys. JETP **67**, 1804 (1988).
- [61] G.E. Volovik, Lect. Notes Phys. **718**, 31 (2007) and *The universe in a helium droplet* (Clarendon, Oxford, 2003).
- [62] J. von Delft and R. Poghossian, Phys. Rev. B **66**, 134502 (2002).
- [63] J. von Delft and D.C. Ralph, Phys. Rep. **345**, 61 (2001).

- [64] F. Wilczek, Phys. Rev. Lett. **48** (1982) 1144; **49** (1982) 957 and ed. *Fractional statistics and anyon superconductivity* (World Scientific, Singapore 1990).
- [65] P. Zanardi and N. Paunkovic, Phys. Rev. E **74**, 031123 (2006).
- [66] C. Zhang, S. Tewari, R.M. Lutchyn, and S. Das Sarma, Phys. Rev. Lett. **101**, 160401 (2008).
- [67] J. Zhang, E. G. M. van Kempen, T. Bourdel, L. Khaykovich, J. Cubizolles, F. Chevy, M. Teichmann, L. Tarruell, S.J.J.M.F. Kokkelmans, and C. Salomon, Phys. Rev. A **70**, 030702 (2004).
- [68] H.-Q. Zhou and J.P. Barjaktarevic, J. Phys. A: Math. Theor. **41**, 412001 (2008).
- [69] H.-Q. Zhou, J. Links, R.H. McKenzie, and M.D. Gould, Phys. Rev. B **65**, 060502(R) (2002).